Online ISSN : 2395-602X
Print ISSN : 2395-6011
www.ijsrst.com

International e-Conference on Recent Trends in Nano-Materials and Its Applications-RTNA-2023

Organized By
Department of Physics
Sangola Taluka Shetkari Shikshan Prasarak Mandal Sangola's, Vidnyan Mahavidyalaya, Sangola
Tal-Sangola, Dist-Solapur, MH-413307, India
Collaboration with
Internal Quality Assurance Cell (IQAC)

VOLUME 10, ISSUE 9, MAY-JUNE-2023

INTERNATIONAL JOURNAL OF SCIENTIFIC RESEARCH IN SCIENCE AND TECHNOLOGY

Email : editor@ijsrst.com Website : http://ijsrst.com

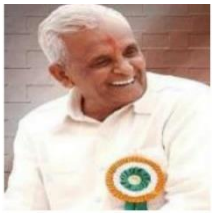

International e-Conference on Recent Trends in Nano-Materials and Its Applications (RTNA-2023)

3rd-4th May, 2023

Organised by

Department of Physics in Collaboration with Internal Quality Assurance Cell (IQAC)
Sangola Taluka Shetkari Shikshan Prasarak Mandal Sangola's
Vidnyan Mahavidyalaya, Sangola
Tal-Sangola, Dist-Solapur, MH-413307, India
Affiliated to Punyashlok Ahilyadevi Holkar Solapur University, Solapur, Maharashtra, India

In Association with

International Journal of Scientific Research in Science and Technology
Print ISSN: 2395-6011 Online ISSN : 2395-602X
Volume 10, Issue 9, May-June-2023
International Peer Reviewed, Open Access Journal
Published By
Technoscience Academy
(The International Open Access Publisher)
website: www.technoscienceacademy.com

Resource Persons

Prof. V. B. Patil. Punyashlok Ahilyadevi Holkar Solapur University, Solapur

Dr. M. P. Suryavanshi University of New South Wales, Sydney

Dr. C. D. Bathula Dongguk University, South Korea

Dr. Mahesh Shinde Twelve Benefit Corporation, California, USA

Chief Patron

Mr. Chandrakant Deshmukh (Director, STSSPM)
Mr. Vitthalrao Shinde (Secretary, STSSPM)
Mr. Ramchandra Khatkale (Director, STSSPM)
Mr. Babanrao Jankar (Director, STSSPM)
Dr. Aniket Deshmukh (Director, STSSPM)
Mr. Dipak Khatkale (Director, STSSPM)
Dr. Ashok Shinde (Director, STSSPM)
Mr. Avadhoot Kumathekar (Director, STSSPM)
Mr. Jayant Jankar (Director, STSSPM)

Organizing Committee

Prof. S. M. Mulani (Principal)
Dr. B. B. Navale (HOD, Physics)
Dr. S. S. Dhasade (Coordinator, IQAC)
Dr. J. V. Thombare (Convener, RTNA-2023)
Mr. A. M. Kamble (Treasurer)
Dr. D. K. Bandagar (Member)
Dr. S. M. Mane (Member)
Dr. V. M. More (Member)

About US

The Institution, Sangola Taluka Shetkari Shikshan Prasarak Mandal Sangola, was established in 23-Sep-1991, with the aim of giving availibility and facility of education to socially backward society, to Bahujan society including Harijan, Girijan, farmers, labours and socially deprived from progress in the region of sangola taluka since it's establishment, the sansthas has started highschool department, professional cources of +2 section and vidnyan mahavidyalay, etc . vidnyan mahavidyalay was established 23rd septmber 1991. There is the facility of B .C .S, B.C.A (degree cources), Bsc(comp) & Msc education in the college. The college has started M.A (english)cource from the year 2004 & Msc (comp science) from 2009 from 2012 since its establishment the college has been progressing ahead and has now become an importent academic center in the region of sangola taluka the college is accredited by NAAC with Grade "B" in the year 2004 Along with an intellectual & all round development of students, to develop their academic carrier, there are various departments under Arts & Science College faculities During the last year the no. of students in this college were 1600 . The big building of the college, with its large play ground, is near by S.T stand.

CONTENTS

International e-Conference on Recent Trends in Nano-Materials and Its Applications
In Association with International Journal of Scientific Research in Science and Technology
Volume 10 | Issue 9 | Print ISSN: 2395-6011 | Online ISSN: 2395-602X (www.ijsrst.com)

DC Electrical Resistivity of Aluminium Substituted Cobalt Ferrite Nanocomposites

R.A. Bugad[1], P.S. Gaikwad[2], V.B. Khandgale[2], B.G.Pawar[3]*

[1]Department of Physics, Sangola College, Sangola, Dist. Solapur (M.S.) 413307, Maharashtra, India
[2]UG Students Department of Physics, Sangola College, Sangola, Dist. Solapur, Maharashtra, India
[3]Department of Chemistry, Sangola College, Sangola, Dist. Solapur (M.S.) 413307, Maharashtra, India

ABSTRACT

Nano-particle size polycrystalline aluminum substituted cobalt ferrite samples $CoFe_{2-2y}Al_{2y}O_4$ (where y = 0.0, 0.05, 0.15 and 0.25) have been prepared by standard ceramic technique. XRD pattern of aluminum substituted cobalt ferrite reveals the single-phase cubic spinel structure. The effects of Al^{3+} on both AC and DC Electrical properties are studied. DC Electrical resistivity is found to increase with increase of aluminum content. Activation energies in ferromagnetic region are found very less than that of paramagnetic region.

Keywords: Co-Al Ferrites, Inverse cubic spinel, activation energy, resistivity, XRD, etc.

I. INTRODUCTION

Polycrystalline nanoparticles ferrites are significant class of composites having large variety of electronic, optical and magnetic properties as they possess high resistivity. Cobalt ferrite is a partially inverse spinel with formula $(Co_yFe_{2-2y})^A [\ Co_{2-2y}Fe_{2+2y}]^B O_4$ where A and B are the tetrahedral and octahedral sites respectively [1-3]. Vaingankar et.al [4] has reported that cobalt is 74% inverse spinel.

Nano ferrites material has application in making high density information storage [5], cores of audio frequency and high frequency transformer coils, magneto optical displays, electromagnetic wave absorption [6]. Nanoferrites are at present very promising material in technological applications and drug delivery [7]. Polycrystalline ferrites, which have applications ranging from microwave frequencies to radio frequencies range are very good dielectric materials. The very low conductivity of these materials is suitable for microwave applications. The dielectric properties of ferrites depend upon the preparation techniques. Knowledge of the dielectric properties is also important from the view point of applications at high frequencies. [8]. The present study is mainly concerned with experimental results of electric properties of $CoFe_{2-2y}Al_{2y}O_4$ nanoparticles. The aim of this work is to study the effect of Al -ions on the DC resistivity. In the present work; we reported the influence of composition on resistivity and structural properties of $CoFe_{2-2y}Al_{2y}O_4$ ferrite.

II. EXPERIMENTAL

2.1. Synthesis of aluminum substituted cobalt ferrite

The ferrites with general chemical formula $CoFe_{2-2y}Al_{2y}O_4$ (where y = 0.0, 0.05, 0.15 and 0.25) were prepared by the standard ceramic technique using AR grade cobalt oxide, Ferric oxide and aluminum oxide. The compositional weights of powders were mixed physically and blended in agate mortar in acetone medium. The final sintering process was carried at 1000^0C for 48 hours. The slow cooled samples were heated at rate of 80^0C per hour. The pellets were formed by using respective steel die. The pressure was applied of 10 tones / square inch by hydraulic pressure gauge.

2.2. Characterization Techniques

The XRD patterns of aluminum substituted cobalt ferrites were recorded by Philips X-Ray Diffractometer model PW 1710 using Cu Ka radiation (λ = 1.5404 A.U.). The formation of the cubic spinel structure of the samples prepared is confirmed by X- ray diffraction analysis. D.C. resistivity was measured by a four probe method on compressed and sintered pellets. Silver paste was applied on both of the flat surfaces of the pellet for good electric contacts. A low but constant voltage was applied across the sample and current through the sample was measured as a function of temperature. The activation energy was calculated from the variation in resistivity with temperature using the formula

$\rho = \rho_0 \exp(\Delta E/KT)$ ----------(1)

III. RESULTS AND DISCUSSION

3.1. XRD studies

X-ray diffraction patterns of the samples are presented in fig.1. Powder X-ray diffractometry of the ferrite samples reveals the single phase spinel structure, as well defined peaks are observed without any ambiguity. The diffraction peaks are well defined and sharp to corresponding planes (220), (311), (400), (422), (511) and (440). The calculated and observed values of inter planer distance (d) are found in good agreement with each other for all reflections.

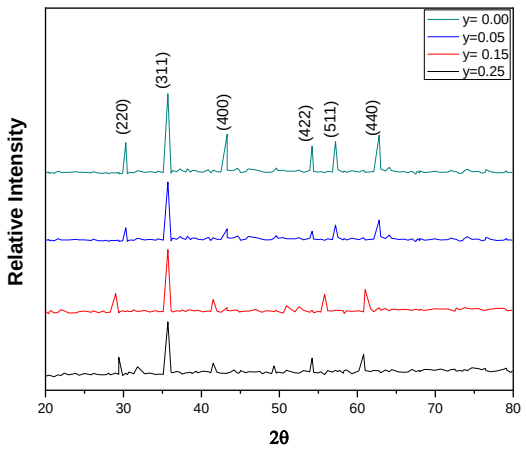

Fig.1 XRD of $CoFe_{2-2y}Al_{2y}O_4$ ferrite system

3.2 D.C electrical resistivity

D.C electrical resistivity for all the samples was measured as a function of temperature is shown in fig.2. DC electrical resistivity for all the samples was measured by four probe method.

From Fig.2 it is observed that DC electrical resistivity of all the samples show almost a linear decreasing behaviour with increasing temperature. According to [9], Ferrite structurally forms cubic close packed oxygen lattice with the cations fit into the octahedral(B) and tetrahedral (A) sites. It is observed that DC electrical resistivity increases with increasing concentration of Al^{3+} ions. Conduction in ferrite can be explained on the basis of hopping mechanism. It is well known that Al^{3+} occupy octahedral site B, while Co^{2+} and Fe^{3+} ions occupy A and B sites [10]. More, it is known that the conduction mechanism in ferrite occurs mainly through the hopping between $Fe^{2+} \leftrightarrow Fe^{3+}$ in the B- sıtes [11]. Thus , the deficient of Fe^{2+} ions with increasing Al^{3+} concentrations gives further reason for the increase of the DC electrical resistivity. The Fe^{3+} ions at the A- sites contribute little to conduction due to larger distance between them [12].

The change in slope is markedly observed in all the samples, such change is either due to Curie temperature [13] or due to change in conduction. This indicates the semiconducting nature of ferrrites. The variation in resistivity with temperature is given by using the formula (2).

$\rho = \rho_0 \exp(\Delta E/KT)$ ----------(2)

Where ΔE = Activation energy, K = Boltzmann constant & T = Absolute temperature.

For composition y = 0.0, 0.05, 0.15 and 0.25, the variation of log ρ with 1/T shows only one discontinuity in resistivity at curie temperature. The change in the slope of resistivity at Curie temperature corresponds to change in the activation energy (ΔE).

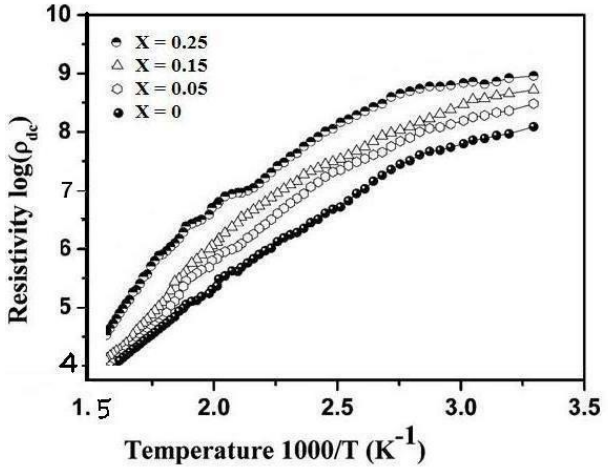

Fig. 2. Variation of DC resistivity with temperature.

Table1. Activation energy, Curie Temp. and dc resistivity of $CoFe_{2-2y}Al_{2y}O_4$ ferrite system.

Composition y	Activation Energy (eV)		Curie Temp.
	Ferri-region	Para-region	
y =0.00	0. 2694	0.4149	765
y=0.05	0.3230	0.4391	730

y=0.15	0.2570	0.4705	701
y=0.25	0.3123	0.5724	669

The activation energy was determined by slope of the graph of dc electrical resistivity as shown in Fig. 2. Activation energies were calculated using the formula (3),

$$E_a = 2.303 \times K_B \times 10^3 \times \text{slope(eV)} \text{ ---------- (3)}$$

Where, K_B = Boltxmann Constant = 8.602×10^{-5} eV/K

Komer and klisuhin have attributed the change of activation energy to magnetic transformation from ferrimagnetic to paramagnetic state [14].

The activation energies in both ferri and paramagnetic region of the composition are determined from the slope of respective lines. Activation energies in ferrimagnetic region are found very less than that of a paramagnetic region as shown in Table.1

Table 1 shows Curie temperature (Tc) obtained from dc resistivity. it was observed that, Curie temperature (T_C) reduces with Al content. This decrease in Tc has been recognized due to decrease in strength of A-B interaction as a result of change in cation distribution between A and B sites [15].The above variation is expected on replacing Fe^{3+} ions by Al^{3+}ions.

According to assumed cation distribution, the magnetic interaction between magnetic ions (Al-Fe) on B-site is decreased due to substitution of Al^{3+} content, is the reason for decrease in Curie temperature. This is in accordance to the result obtained by Mullai et al [16].

IV. CONCLUSIONS

Cobalt ferrite is partially inverse cubic spinel ferrite. All prepared ferrite samples exhibit single domain to super paramagnetic transition. The electrical properties have been studied for all samples. The resistivity variation with temperature shows typical semiconductor characteristics. The decrease in resistivity with increasing temperature could be attributed to negative temperature coefficient of resistance of $CoFe_{2-2y}Al_{2y}O_4$. The decrease in the electrical resistivity at low temperature is attributed to the impurities, which reside at the grain boundaries. It is concluded that aluminum content influences electrical conductivity of cobalt ferrite. Hence much higher DC resistivity ferrite material are used in the applications at high frequencies as microwave absorbers.

V. REFERENCES

[1]. K. Haneda and A. H. Morish, J .Appl. Phys. 63 (1988) 4285.
[2]. L. Zhavo et al ; Mat. Lett. 60 (2006) 1.
[3]. N. N. Greenwood and T. C. Gibb. Mossbauer spectroscopy.((Chapman and Hall Ltd., London.(1971) 261-66.
[4]. A. S. Vaingankar, S. A. Patil and Sahashrabudhye, Trans. Indian. Inst. metals 34, 5 (1981) 387.

[5]. R.F. Zolio, US patent 4,474(1984) 866 .
[6]. S.N. Dolia, Solid State Phenomena, 2011, 171 79-91.
[7]. Mytil Kahn and John Zhang 2001; Sousa et al 2005.
[8]. Raghavender and Jadhav 2009 ; Mater. Sci. ,. Vol. 32 .
[9]. A.Verma , O. P. Thakur, C. Prakash, T.C. Goel, R.G. Mendiratta, J. Mater.Sci. Eng.B,116 (2005).
[10]. A. A. Sattar, J.mater.Sci., 39 (2004) 451.
[11]. B.K. Bammannavar, B.K. Chougule, L.R. Naik and R.B.Pujar, J.Progress in electromagnetic research letters, vol.4, 121-129 (2008).
[12]. A.Verma , O. P. Thakur, C. Prakash, T.C. Goel, R.G. Mendiratta, J. Mater.Sci. Eng.B,116 (2005).
[13]. Ravinder, D. and B. Ravikumar, " Mater.Sci. Lett., Vol. 15, 1605 – 1608, 1996.
[14]. Komar K. P. , Kliushin V. V. , Bull. Acad. Sci. USSR, 18 (1954) 403.
[15]. B.R. Karche, B.V. Khasbarder, A.S. Vaingankar, J. Magn. Magn. Mater.168 (1997) 292-298.
[16]. R.U. Mullai, P.P. Pradeep, G. Chandrasekaran, Inter. J. Recent Trends Sci. Technol. 5(2012)78-85.

International e-Conference on Recent Trends in Nano-Materials and Its Applications
In Association with International Journal of Scientific Research in Science and Technology
Volume 10 | Issue 9 | Print ISSN: 2395-6011 | Online ISSN: 2395-602X (www.ijsrst.com)

The Role of Chromium Doping On Structural, Morphological and Optical Properties of ZnO Thin Films

V. S. Chandak[1], M. B. Kumbhar[1], P. S. Ghar[1], P. M. Kulal1[2*]

[1]Thin film and Materials Science Research Laboratory, Department of Physics, Dayanand Science College, Latur - 413512, Maharashtra, India

[2]Department of Physics, Shivaji Mahavidyalaya, Renapur, Maharashtra, India

ABSTRACT

Pure and 5% Cr-doped ZnO thin films were successfully synthesized by using a spray pyrolysis technique. Thestructural, optical, and morphological properties were examined by using an X-ray diffractometer (XRD), field emission scanning electron microscopy (FESEM),and UV-Vis spectrophotometer. The structural properties revealed polycrystalline with a hexagonal wurtzite structure. The structural parameters such as crystallite size, lattice parameters, volume, strain, u parameter, and bond length were determined from XRD patterns. The morphology of the pure films was found to be spherical grains distribute uniformly throughout the surface. With the introduction of chromium, the morphology was found to be agglomerated nanograins. The optical properties such as band gap and transmittance were determined. Band gap values were determined by using Tauc's plot and were found to be decreased for Cr-doped films. The transmittance of doped Cr-doped ZnO thin film was found to be nearly 85% which is higher than pure films. And hence the doped thin films can be suitably used in the field of optoelectronics and sensor device applications.

Keywords: Spray pyrolysis, nanostructured thin films, X-ray diffraction, optical properties, optoelectronic devices.

I. INTRODUCTION

In the last few decades, nanomaterials have received a lot of attention in both theoretical and experimental fields due to their small grain sizes, large grain boundaries, quantum size effects, and a sufficiently large surface-to-volume ratio in comparison with their bulk form[1]. However, Metal oxide semiconducting nanomaterials have been widely used in the field of solar cells, sensors, optical devices, supercapacitors, etc[2]. Among all the metal oxides, ZnO is one of the most important materials because of its chemical and electrical, and physical properties. It is a non-toxic, II-VI group semiconductor material having a wide band gap semiconductor $3.37\ eV$. Also, it exhibits large excitation binding energy $60\ MeV and$high electronmobility $\sim 400\ cm^2V^{-1}s^{-1}$[3,4]. Moreover, ZnO has Biocompatibility, chemical stability, thermal stability, and low synthesis cost material and hence ZnO has attracted much attention in the field of research[5].The properties of ZnO nanomaterials in terms of structural, electrical, optical, and morphological can be enhanced by doping

of suitable material, heat treatment, and molar concentrations of precursors solution[6,7]. In the present study, the effect of doping on structural, morphological, and optical properties has been studied. The choice of dopant depends upon the ionic radii of the dopant and host material as well as electronegativity. Such films can be synthesized by different methods including RF sputtering[8], thermal evaporation[9], successive ionic layer adsorption reaction (SILAR)[10], chemical bath deposition (CBD)[11], spray[12], etc. Among all these methods, the spray is a simple, versatile, and cost-effective method used for the synthesis of thin films. In the present work, we report the synthesis of pure and Cr-doped ZnO thin films and the structural, morphological, and optical properties and their application in the field of optoelectronics device applications.

II. METHODS AND MATERIALS

All chemicals of analytical grade were used for the synthesis of thin films. Pure and 5% Cr-doped ZnO thin films were prepared by using a precursors solution of 0.1M zinc acetate dihydrate ($Zn(CH_3COO)_2.2H_2O$), 0.1M Chromium chloride hexahydrate [$CrCl_3.6H_2O$] were purchased from Sigma Aldrich. All starting chemicals were used without further purification. Double distilled water was usedfor the preparation of the precursor solution. For the synthesis purpose spray pyrolysis technique was utilized. All the samples were synthesized on a glasssubstrate at a temperature of 400°C, flow rate of 2ml/min, and nozzle-to-substrate distance of 28 cm.

III. RESULT AND DISCUSSION

Fig. 1 shows the X-ray diffraction (XRD) patterns of pure and 5% Cr-doped ZnO thin films. XRD patterns of both films confirm the polycrystalline nature of ZnO. The observed diffraction peaks at (100), (002), (101), (102), (110), (103), (200), (112), and (201) indicate the hexagonal wurtzite structure of ZnO, which agrees with standard JCPDS card no. 79-0207. No extra peaks were observed corresponding to dopant atoms and it confirms the incorporation of the Crdopant into the ZnO host material. The average crystallite size (D) is calculated from the well-known Scherrer's formula defined as[13];

$$D = \frac{0.94\lambda}{\beta \cos\theta} \quad (1)$$

Where λ, β, θ are x-ray wavelength 1.5418 A°, the Bragg's diffraction angle and full-width half maximum (FWHM in radians) of the peak corresponding to θ value for the plane (002). The crystallite size was found to be decreased from 27.19 nm to 17.87 nm for pure and Cr-doped ZnO films. This decrease in crystallite size is due to the distortion created by the substitution of the Cr dopant into the ZnO host material.

Lattice parameters a and c were calculated using the following formula:

$$\frac{1}{d^2_{(hkl)}} = \frac{4}{3}\left(\frac{h^2+k^2+hk}{a^2}\right) + \frac{l^2}{c^2} \quad (2)$$

where h, k, l are the Miller indices and d is the interplanar spacing. The volume of the unit cell for the hexagonal structure has been estimated using the equation;

$$V = 0.866\, a^2 c \quad (3)$$

The variation of lattice parameters, c/a ratio, and unit cell volume of ZnO thin films is listed in Table 1. The decrease inthe lattice parametersand volume of the unit cell is due to the incorporation of smaller ionic radii of Cr^{3+}.

The strain in the prepared films is determined by using the relation,

$$\varepsilon = \frac{\beta \cos\theta}{4} \qquad (4)$$

With doping the crystallite size decreased and strain increased indicating that the Cr dopant slows down the growth of ZnO grains[14].

The Zn-O bond length is calculated by using the relation, $L = \sqrt{\frac{a^2}{3} + \left(\frac{1}{2} - u\right)^2 c^2}$ (5)

Where u is the internal parameter$u = \frac{a^2}{3c^2} + 0.25$

The bond length of pure ZnO is comparatively higher than that of 5% Cr-doped ZnO films leading to a structural disorder in doped films along the c-axis. Table 1 indicates structural parameters for pure and 5% Cr-doped ZnO thin films.

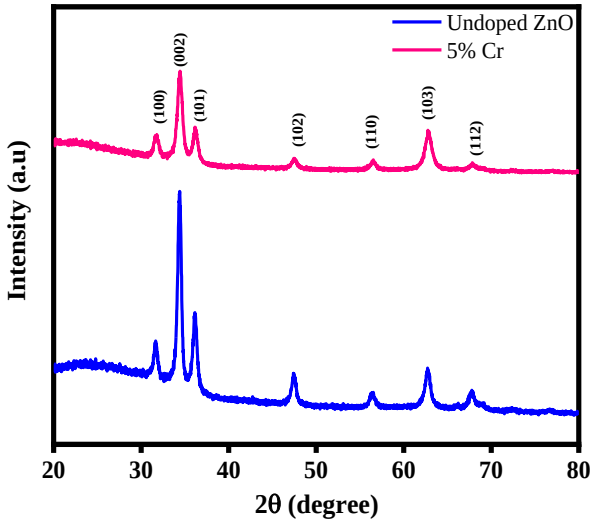

Fig. 1: XRD patterns of pure and 5% Cr-doped ZnO thin films

Table 1: Structural parameters for undoped and Cr-doped ZnO thin films

Parameters		Pure ZnO	5% Cr-ZnO
Crystallite size (D) (nm)		27.19	17.87
Lattice parameters	a (Å)	3.2576	3.2477
	c(Å)	5.2098	5.1937
The volume of the unit cell V (Å^3)		47.88	47.44
Strain (ε)		0.0014	0.0021
u-parameter		0.3803	0.3803
Bond length L (Å)		1.9814	1.9753

Morphological studies

Fig. 2 depicts the FESEM micrographs of synthesized pure and Cr-doped ZnO thin films. The well-ordered nano spherical granular was observed for pure ZnO thin films. However, the morphology has been modified withthe introduction of Cr doping. The agglomerated spherical granular-like structure was observed.

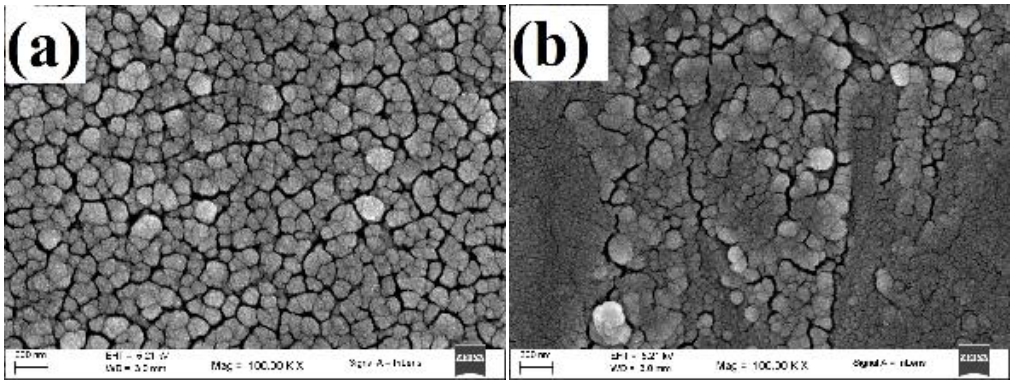

Fig.2: FESEM micrographs of (a)pure and (b)5% Cr-doped ZnO thin films

Optical properties

Fig. 3 shows Tauc's plot of pure and Cr-doped ZnO thin films.The optical band gap energy (E_g) for the prepared thin film is calculated by using Tauc's plot. using the relation;

$$\alpha h\nu = C(h\nu - E_g)^n \qquad (6)$$

where E_g is the optical band gap, C is a constant, α is the absorption coefficient $h\nu$ is a photon energy. Since ZnO is having wide direct band gap and hence (n=1/2) is used for finding out the band gap. It has been observed that the band gap is decreased from 3.28 to 3.25 eV with the 5% of Cr-doping.The decrease in band gap values was observed due to the exchange interaction. This concludes that the band gap can be tuned by doping a transition metal and used as a proper candidate in optoelectronics device applications.Fig. 3 inset depicts the transmittance spectra of pure and 5% Cr-doped ZnO thin films. The transmittance was found to be increased withthe introduction of a dopant element. This suggests that the doped samples can be suitably used in the field of transparent conducting metal oxide thin films.

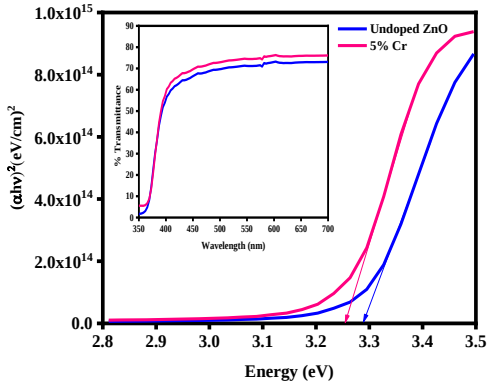

Fig. 3:Tauc's plot and inset show the % Transmittance of pure and Cr-doped ZnO thin film.

IV. CONCLUSION

Pure and Cr-doped ZnO thin films were successfully synthesized by using the spray pyrolysis technique.The synthesized films are found to be polycrystalline exhibiting a hexagonal wurtzite structure. The XRD pattern reveals thatthe synthesized samples have intense peaks along the c-axis. The impact of chromium doping on structural properties can be seen effectively. On the introduction of the dopant element, the morphology was modified to some extent. The optical properties revealed that the doped films are having nearly 85% of transmittance and can be used as transparent conducting metal oxide films. The band gap values are found to be decreased with doping suggesting that the band gap can be tuned with doping of the proper element to the ZnO host.

V. REFERENCES

[1]. R. Naji, F. Rahman, and K. M. Batoo, J. Mol. Struct. 1065–1066, 199 (2014).
[2]. A. Huang, Y. He, Y. Zhou, Y. Zhou, Y. Yang, J. Zhang, L. Luo, Q. Mao, D. Hou, and J. Yang, J. Mater. Sci. 54, 949 (2019).
[3]. P. Rong, S. Ren, and Q. Yu, Crit. Rev. Anal. Chem. 49, 336 (2019).
[4]. J. Wang, R. Chen, L. Xiang, and S. Komarneni, Ceram. Int. 44, 7357 (2018).
[5]. A. P. Rambu, L. Ursu, N. Iftimie, V. Nica, M. Dobromir, and F. Iacomi, Appl. Surf. Sci. 280, 598 (2013).
[6]. M. R. Alfaro Cruz, N. Hernandez-Como, I. Mejia, G. Ortega-Zarzosa, G. A. Martínez-Castañón, and M. A. Quevedo-Lopez, J. Sol-Gel Sci. Technol. 79, 184 (2016).
[7]. O. Gürbüz and M. Okutan, Appl. Surf. Sci. (2016).
[8]. M. Shaheera, K. G. Girija, M. Kaur, V. Geetha, A. K. Debnath, R. K. Vatsa, K. P. Muthe, and S. C. Gadkari, Opt. Mater. (Amst). 101, 109723 (2020).
[9]. N. H. Sheeba, S. C. Vattappalam, G. S. Okram, V. Sharma, P. V. Sreenivasan, S. Mathew, and R. ReenaPhilip, Mater. Res. Bull. 93, 130 (2017).
[10]. K. R. Devi, G. Selvan, M. Karunakaran, K. Kasirajan, L. B. Chandrasekar, M. Shkir, and S. AlFaify, J. Mater. Sci. Mater. Electron. 31, 10186 (2020).
[11]. A. F. Abdulrahman, S. M. Ahmed, S. M. Hamad, and A. A. Barzinjy, J. Electron. Mater. 50, 1482 (2021).
[12]. K. Ravichandran, A. J. Santhosam, O. M. Aldossary, and M. Ubaidullah, Phys. Sci. 96, 125825 (2021).
[13]. A. H. Shah, J. Mater. Sci. Mater. Electron. (2020).
[14]. G. A. Ali, M. Emam-Ismail, M. El-Hagary, E. R. Shaaban, S. H. Moustafa, M. I. Amer, and H. Shaban, Opt. Mater. (Amst). 119, 111312 (2021).

International e-Conference on Recent Trends in Nano-Materials and Its Applications
In Association with International Journal of Scientific Research in Science and Technology
Volume 10 | Issue 9 | Print ISSN: 2395-6011 | Online ISSN: 2395-602X (www.ijsrst.com)

Development and Validation of RP-HPLC Method for the Estimation of Mesalamine in Bulk and Formulation

Vanita Choukhande*[1], Dr.Varsha Tegeli[1], Ankush Pawar[1], Dr. Yogesh Thorat[1], Dr.Meenakshi Menerikar[2]

[1]D. S. T. S Mandal's College of Pharmacy, Solapur 413004, Maharashtra, India

[2]Manjushree Research Institute of Ayurved Science, Near GGS, Piplej, Pethapur- Mahudi Road, Gandhinagar, Gujarat, India

ABSTRACT

A rapid, sensitive and specific RP-HPLC method involving UV detection was developed and validated for quantification of mesalamine. Chromatography was carried out on a pre-packed Phenomenex Luna C8(2) column (150 ×4.6 mm, 5 µm) with Phenomenex security guard cartridge C8 as stationary phase and mobile phase methanol: water (30:70% v/v) at the flow rate 1 mL/min. Mesalamine was detected at 232nm. The developed method is validated as per ICH Q2 (R1).

The method showed good linearity (R^2 = 0.9989) in the range of 5 to 25 µg/mLand average recovery of 99%. The method isprecise (%RSD 1.64). Mesalamine, eluted at 2.1 min.

Keywords: Methanol, Water,Mesalamine, 5-Amionsalicylicacid, (5ASA), Mesalazine ,Mesalamine 400mg, HPLC Younglin Autochro3000,RP-HPLC.

- **Graphical Abstract**

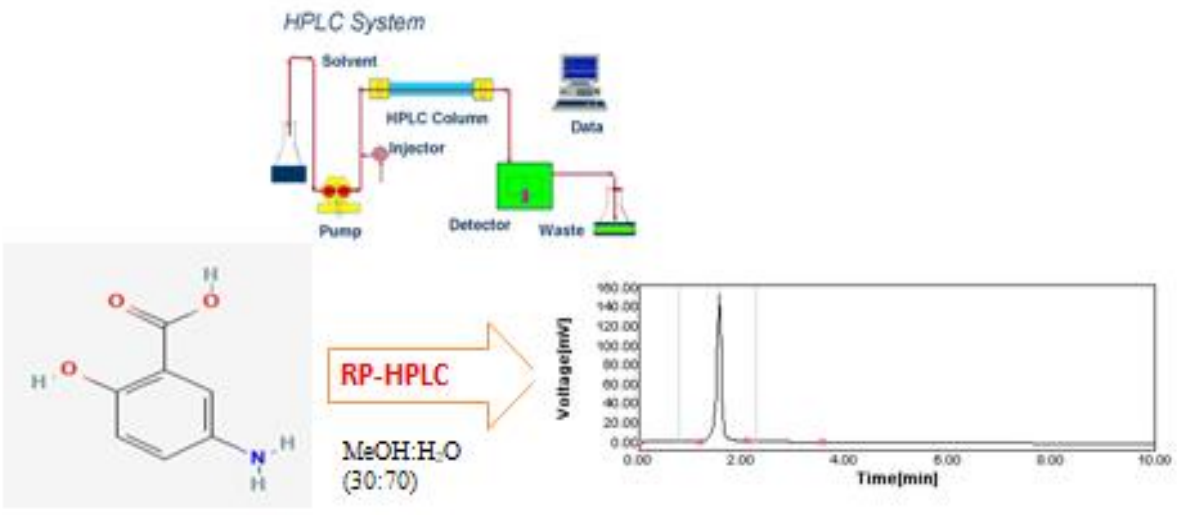

I. INTRODUCTION

High-Performance Liquid Chromatography (HPLC) is a technique in analytical chemistry commonly used to separate, identify, and quantify each component in a mixture. Analytical method development is the process of selecting an accurate assay procedure for the determination of composition of formulation. The analytical method must be developed using the protocol and acceptance criteria set out in International Council for Harmonization (ICH) guidelines Q2(R1). An analytical procedure is developed to test a defining characteristic of a drug substance or drug product against the predetermined acceptance criteria for that characteristic. Analytical method development and validation can be best understood as the process of showing that the analytical procedures are adequate for assessing the drugs, particularly the Active Pharmaceutical Product (API). Analytical test method validation provides a documented process, demonstrating that the analytical procedure employed for a specific test is suitable for its intended purpose, provides evidence of method's performance and ensures quality and reliability of results[1].

The chemical name of mesalamine is 5-amino-2-hydroxybenzoic acid Its molecular formula $C_7H_7NO_3$and Its molecular weight is 153.14g/mol[2,3].

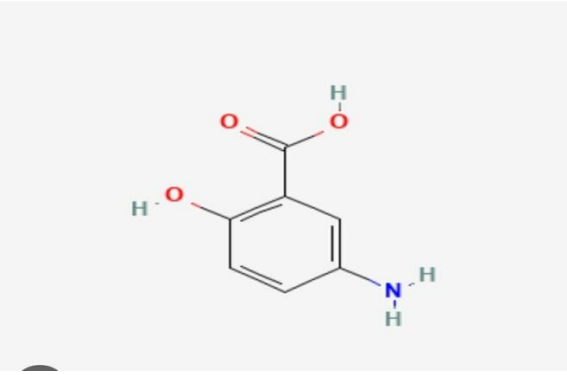

Fig. 1 Structure of Mesalamine

Mesalamine is also as mesalazine or 5-amino salicylic acid (5-ASA) ,is an anti-inflammatory drug used to treat in inflammatory bowel disease ,such as ulcerative colitis and mild to-moderate Crohn's[4]Mesalamine is a bowel –specific amino salicylate that acts locally in the gut and has its predominant actions there having few systemic side effects. As a derivative of salicylic acid mesalamine is also thought to be an antioxidant that traps free radicals, which are potentially damaging byproducts of metabolisum.[5]Mesalamine is considered the Active moiety of sulfalazine, which is metabolized to Sulfapyridine and mesalamine. [6]some common side effects include headache, nausea, abdominal pain and fever.[7]

Side effects of mesalamineinclude:

1) Most serious side effect comes like that , Pericarditis ,liver problems , kidney problem , pregnancy ,breastfeeding ,sulfa allergy etc.,[7,8]
2) It effects are primary gastrointestinal but may also include ;GI effects include nausea , diarrhea and abdominal pain ,
3) Myelosuppression (leukopenia , neutropenia ,agranulocytosis ,aplastic anaemia, and thrombocytopenia) as well as hair loss ,peripheral neuropathy , pancreatitis , liver problems, myocarditis ,

4) Lupus erythematosus-including urticarial),drug fever ,interstitial nephritis and nephrotic , syndrome colitis ,Stevens Johnson syndrome and erythema multiforme.[9]

Mesalamine cause muscle or joint pain, aching tightness of stiffness, back pain, heartburn, burping, constipation, etc. it is used to treat and prevent flare ups of mild to moderately active ulcerative colitis (an inflammatory bowel disease).

Exact mechanism of mesalamineunknown but is speculated that mesalamine decreases synthesis of prostaglandin and leukotriene, modulating the inflammatory response derived from the cyclooxygenase and lipooxygenase pathway. It appears to act locally on colonic mucosa .[10]

In the literature survey, it was found that few RP-HPLC[11]and UV-[12]is Spectrophotometric methods were reported for the determination of Mesalamine the formulation. HPLC,[13] UPLC[14], LC-MS[15] either in singal or in combined forms . The objective of this work is to establish the ideal chromatographic conditions for estimating mesalamine in bulk and a formulation using the RP-HPLC method and to validate the results following ICH guidelines.

II. MATERIAL AND METHODS

Chemicals and reagents:

Mesalamine was obtained as gift sample from Sun pharma Vapi, Gujarat. India. . Mesalamine400mg tablet was purchased local market.

Instrumentation:

Younglin Acme 9000 with UV detector (UV730D), Software (Autochro-3000),Ultras onicator(Oscar Microclean 103), RC membrane 0.45µm, 25mmSyringe filters of Phenomenex and, Ultipor® N_{66}® Nylon 6,6 membrane 0.45µm, 47mm(Pall Life Sciences Pvt. Ltd, Mumbai) filters were used, electronic balance (Shimadzu AY220).

Preparation of standard solution:

The Mesalamine (10 mg)was transferred to 10 ml volumetric flask and dissolved in Water, then volume was made up to the mark with Water. 1ml of solution was diluted to 10ml with Water to obtain 100 µg/mL solutions.

Preparation of tablet sample:

Ten tablets were weighed and powdered. Powder equivalent to 400mg of Mesalamine was transferred to 10mL volumetric flask, dissolved and volume was made up to mark with Water .Then filtered through Whatman filter paper.

Determination of absorption maxima:

The mesalaminesolution (10µg/mL) was scanned in the range of 200-800 nm in the UV-VIS spectrophotometer(Shimadzu1800). The lamb damax was obtained from the UV spectrum.

Method development:

The solution of mesalamine(10µg/mL) was prepared in Water and filtered through syringe filter, then injected into HPLC system. The trials of different compositions of mobile phase tried on Phenomenex Luna

C8 column (150 ×4.6 mm, 5 µm) to get the peak having acceptable limits for symmetry, theoretical plates, tailing factor.

Chromatographic conditions:

Younglin Acme 9000 with UV detector (UV730D)carried out using Autochro 3000 software.Phenomenex Luna C8 column (150 ×4.6 mm, 5 µm) as stationary phase and mobile phase Methanol: water (30:70V/V). At flow rate of 1 mL/min with 20µL injection volumeat 232nm.was used for development and validation of this RP-HPLC method

Method validation:

The developed method was validated as per ICHQ2 (R1)guidelines. Specificity, linearity, accuracy, precision parameters are studied.

Specificity:

Specificity refers the ability to assess unequivocally the analyte in the presence of components which may be expected to present.Blank, standard solution (15µg/mL) and solution of the tablet were filtered through syringe filter and injected into HPLC system. The chromatogram was recorded.

Linearity:

The mesalamine solution of 5, 10, 15, 20, 25 µg/mL were prepared from standard solution.The solutions were filtered through syringe filter and injected into HPLC system. Peak areas were recorded. The calibration curve was prepared by plotting peak area against concentration and correlation coefficient was determined.

Range:

The range of analytical method was decided from the interval between upper and lower level of calibration curve. The range of analytical method was 5 to 25µg/mL.

Precision:

Precision study was done in two ways: repeatability and intermediate precision. Precision was expressed as relative standard deviation (%RSD).

Repeatability:

The six replicates of 15 µg/mL of mesalamine were filtered through syringe filter and injected into HPLC system. Peak area was recorded and %RSD was calculated.

Intermediate precision:

The six replicates of 15µg/mL of mesalaminewere filtered through syringe filter and injected into HPLC system on next day. Peak area was recorded and %RSD was calculated.

Accuracy:

Accuracy was evaluated by standard addition method at three levels 80% 100% 120%.The tablet powder equivalent 1267µg of Mesalamine was transferred to four different 10mL volumetric flasks (mesalamine as 0, 80%,100%, 120%) separately and 0, 0.8, 1, 1.2mL of 50µg/mL standard solution was added respectively and the volume made up to the mark with Water.The solutions were filtered through syringe filter and injected into HPLC system. Peak area was recorded. Accuracy was reported as % recovery.

Robustness:

Robustness refers to is its ability to remain unaffected by small but deliberate changes that are made in method parameters. The wavelength (±1nm i.e., 232nm, 233nm, 231nm) and flow rate (±0.1mL/min i.e., 0.9mL/min, 1.0 mL/min, 1.1mL/min) were changed to study robustness.

The standard solution of 16µg/mLwas filtered through syringe filter and injected into HPLC system. Peak area was recorded and %RSD was calculated for these variations.

Systems suitability:

System suitability testing is an integral part of many analytical procedures. The tests are based on the concept that equipment, electronics, analytical operations, and sample to be analysed constitute an integral system that can be evaluated as such.System suitability was performed by injecting standard solution of 16 µg/mL of mesalamine and chromatogram was recorded to check parameters like retention time, theoretical plates, tailing factor and resolution.

Assay of Tablet:

The tablet solution was filtered through syringe filter and injected into HPLC system. The chromatogram was recorded at 232nm and mesalaminecontent in the tablet was calculated.

III. RESULTS AND DISCUSSION

The mesalamine shows absorption maxima at 232nm. This wavelength was used for detection. During initial trials of new analytical method development priority is to provide simple, economical and, precise HPLC method for determination of mesalamine.

The method development was initiated using Methanol and Water mobile solvents on Phenomenex C8 (150 X 4.6 mm, 5µm). The trial of methanol and Water in the combination of 30:70 showed better peak of good symmetry having tailing factor(0.81), theoretical plates (2584) and eluted at 2.1 min (Fig. 2).

Specificity:

Overlayof chromatograph of Blank,Standard,and, sample are as shown in the fig 3, It is observed that drug in both solutions eluted at the same retention time. This indicates there is no interference of excipients in drug analysis and method is specific.

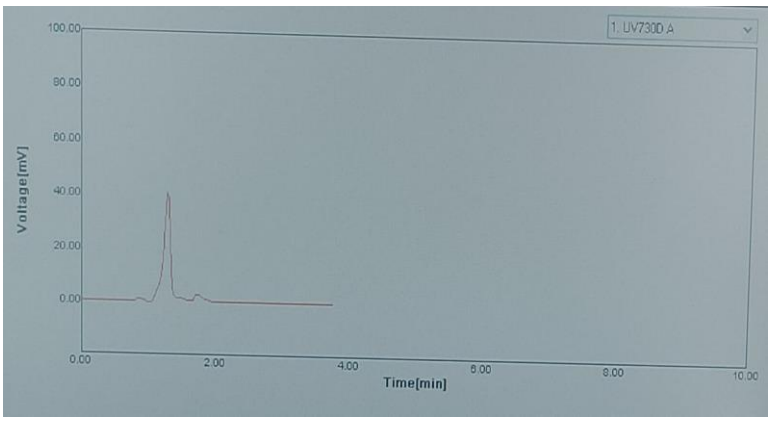

Fig 1: Specificity

Linearity :

The response of area of different concentration is present in table1 the graph was found to be Peak Area V/S Concentration (fig 3) the calibration curve showed good linearity in the range 5-25mg/ml, for Mesalamine for Mesalamine API with correlation coefficient (r2) of 0.9989 (fig3;table1) in that refers to ability within the range to obtain test result which are directly proportional to the concentration analyte in thesimple way. A typical calibration curve has the regression equation of y = 202.09 x =3009.1 for Mesalamine.

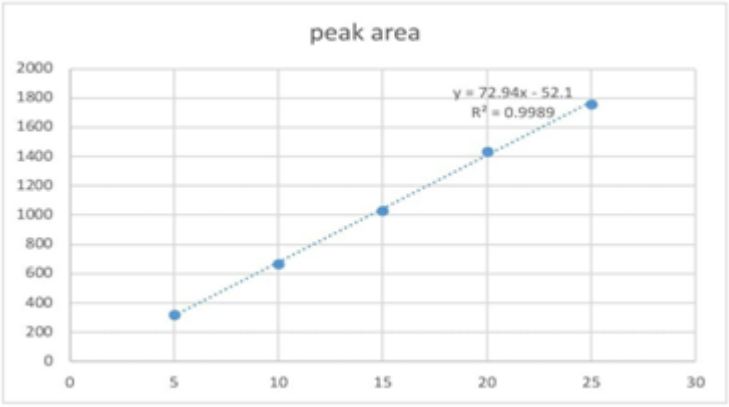

Fig 2: Calibration curve of Mesalamine .peak area v/s concentration (API)

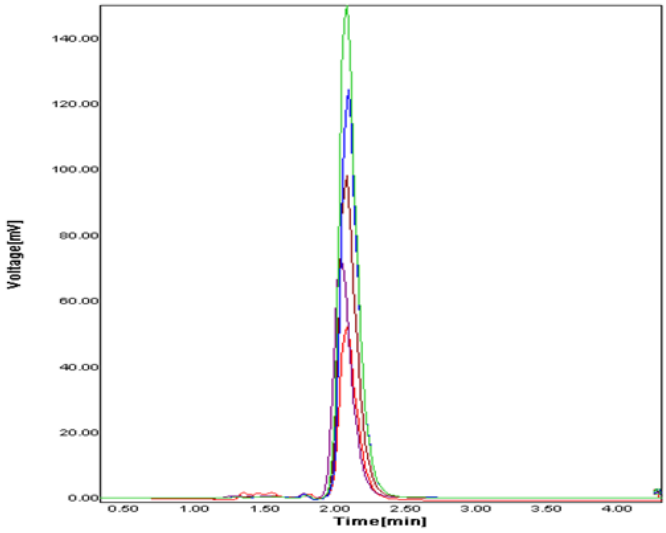

Fig 4 : Overlay of chromatographic 5-25µg/ml of Mesalamine

Table : 1 Result of linearity

Sr. No.	Concentration(µg/mL)	Peak Area
1	5	321
2	10	665
3	15	1029
4	20	1436
5	25	1759

Precision

The intra and inter day variation of the method was carried out and high values of mean assay and low values standard deviation and %RSD (% RSD < 2 %) within a day and day to day variations for Mesalamine revealed that the proposed method is precise. It is Repeatability and intermediate precision have been expressed by % RSD .

Table : 2 Result of Precision

Injection	Peak Area		
Coc(15)	Repeatability	Intermediate precision	
		Day-1	Day-2
1	1029	1021	883
2	1075	1040	865
3	972	1057	878
4	1025	1040	880
5	989	1055	887
6	1009	1020	882
SD	35.89847	17.4547	7.574079
%RSD	0.358985	0.174547	0.008615

Accuracy the recovery of method ,determined by adding a previously analyzed test solution with additional drug standard solution , in that known amount of concentration in sample at 80 % ,100% , 120 % . added concentration was compared recovered concentration to determine % recovery.% recovery of Mesalamine 100 to 102.% the values recover % .(%RSD)listed in table 3 indicate the method is accurate .

Table : 3 Results of Accuracy

Sr. no.	Recovery level in %	Concentration (µg/mL)	Amount recovered (µg/mL)	% Recovery
1	80	8.186	1262	102
2	100	19.88	1398	100
3	120	22.12	1562	102.4

Assay :

The developed method was applied for estimation of Mesalamine in tablet. The result of the assay is shown table 4 Mesalamine tablet contain 98.3% of stated amount of Mesalamine.

Table : 4 Results of Assay.

Tablet form	Amount taken	Amount found	% Content
Mesalamine 400	16 µg/mL	9.83 µg/mL	98.3

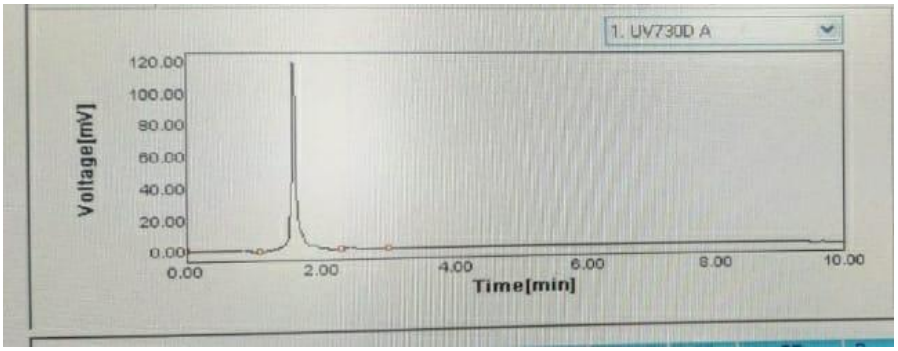

Fig : 5Assay of Mesalamine

Robustness : In that robustness influence of small changes in chromatographic conditions such as change in flow rate (+- 0.1min/ml), Temperature , wavelength detection and mobile phase concentration also favor . the development of RP-HPLC .

Table :5 Robustness

Parameters	**Area**
Wavelength of UV detector	
233	1021
231	1040
Mean	1030.5
SD	13.43503
% RSD	0.13435
Flow Rate	
0.9 mL/min	1057
1.1 mL/min	998
Mean SD	1027 41.7193
% RSD	0.417193

System Suitability : it perform 16 µg/ml of Mesalamine was injected in the HPLC , The System suitability parameters- retention time ,tailing factor , theoretical plates and resolution factor, were determined and their limit.

Table 6 System Suitability

Sr. No.	Parameters	Observed Value	Criteria
1.	Retention Time	1.6	-
2.	Theoretical Plates	2236	>2000
3.	Tailing Factor	1.5	<2.0
4.	Resolution	2.5	>2.0

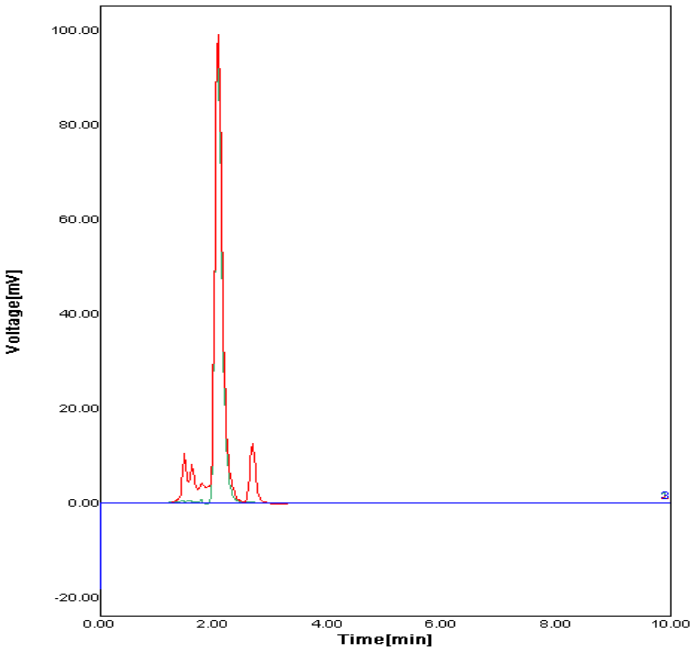

Fig :6Overlay of 15µg/ml Standard Solution

- Chromatogram (Red),20µg/ml of sample solution
- Chromatogram (Blue) is blank and (Green)

Limit of Detection and Limit of Quantification : The Developed method was highly sensitive with LOD of **2.52µg/ml** and LOQ **7.65µg/ml.**

IV. CONCLUSION

A sensitive and selective stability indicating RP-HPLC method has been developed and validated for the analysis of Mesalamine based on peak purity results ,obtained from the analysis of Mesalamine .force degradation samples using described method ,it can be conducted that the absence of co-eluting peak along with the main peak of Mesalamine indicated that the developed method is specific for the estimation of Mesalamine in presence of degradation products. Further the proposed RP-HPLC method has excellent sensitivity,precision and reproducibility.

V. ACKNOWLEDGMENT

The authors are thankful to the Sun Pharma vapi , Gujarat. Providing gift sample of Mesalamine .we are also thankful to principal and management of D.S.T.S.Mandal's college of pharmacy,Solapur for providing all facilities to complete this work successfully.

VI. REFERENCES

[1]. Saroj H. Gatkal , Priti R. Mhatrte , Vitthai V. Chopade , Prvin D. Choudhari, Development and Validation of Stability Indicating HPLC Assay Method for Determination of Mesalamine in Bulk Drug and Tablet Formulation, Int J. Pharm Sci Rev. Res .,20(1) ,May –Jun 2013 n0 34,200-204.Accepted no: 14-03-2013 . Finalized NO: 30-04-2013.

[2]. ShrishailGhaurghure ,KuldeepkumarSawant and Savita S Deokar ; UV Spectrophotometric Method Development and Validation of Mesalazine in Bulk and Solid Dosage from. ,;International Journal of Pharmacy and Biological Sciences .-IJPBS (2021)11(1):131-135 ISSN-2230-7605, Print ISSN-2321-3272.

[3]. NaliniKantaSahoo, MadhusmitaSahu, PodilapuSirnivasaRao , GoutamGhosh ,;Validation of Stability indicating RP-HPLC method for the estimation of mesalamine in bulk and tablet dosage form ,[ELSEVIR], Pharmaceutical Methods 4(2013)56-61 , Recived 27 October 2013, Accepted 10 December 2013 ,;Available online 10 January 2014.

[4]. The Merck index,14thed, White House Station , NJ ,USA : Merck Research Lab-Oratories , Merck and Co.; 2006:613.

[5]. Tripathi KD, Drugs for Constipation and Diarrhoea .new Delhi,5th ed.2003:621.

[6]. Stretch GL,Campbell BJ, Dwarakanth AD, etal, 5-amino Salicylic acid ab-sorption and metabolisum in ulcerative colitis patients receiving maintenance Sulphasalazine ,Osalazine or Mesalazine ,Aliment PharmacolTher ,1996;10:941-947.

[7]. Mesalamine Monograph for Professionals Drugs .com. American Society of Health System Pharmacsist.

[8]. British national nationalformulary :BNF 76(76ed.)Pharmaceutical Press .2018 pp.39-41 ISBN 9780857113382.

[9]. Assaol 400mg MR Tablets –Summary of product Characteristics (Spmc)(emc) .14 April 2016 ,Retrieved 30 December.2019.

[10]. Meher, C., Vani, M.; Simple UV spectrometric method for estimation of mesalamine in bulk and its formulation; International Research Journal of Pharmacy, (2013); 4(8): 231–233

[11]. K.HanumanthRao, A. LakshmanaRao, And KB .Chandra Sekhar, Validation RP-HPLC Method For The Estimation of Mesalamine in Bulk And Tablet dosage form ,International Journal of Research in pharmacy And Chemistry (IJRPC) ISSN:2231-2781.IJPRC2013,3(2).

[12]. SrinivasaRaoNarala and K, Saraswathi , Development and validation of Spectrophotometric method for the Estimation, of Mesalamine in Pharmaceutical Prearations, J.Chem, Pharm Res .,2011,3 (1):784-787.ISSN No:0975-7384.CODE (USA):JCPRc5.

[13]. Venugopal D, Arvind BK., Appal, Raju S, Arshad MD, Ashok LG, Development and Validation of HPLC method for determination mesalamine in tablet dosage forms, Pharm Sci, Monitor ,2012;3:74-81.

[14]. Trivedi RK, Patel MC, Kharkar AR, Determination of mesalamine related impurities form drug product reversed phase validated UPLC method , j Chem, 2011;8:131-148.

[15]. Pastorini E, Locatelli M, Simoni P, Roda , G Roda, E Roda, Development and validation of a HPLC-ESI-MS/MS method for the determination of 5-aminosalicylic acid, and its major metabolite N-acetyl-5-amino salicylic acid in human plasma . JChromatogr B AnalytTechnol Biomed Life Sci 2008;872:99-106.

International e-Conference on Recent Trends in Nano-Materials and Its Applications
In Association with International Journal of Scientific Research in Science and Technology
Volume 10 | Issue 9 | Print ISSN: 2395-6011 | Online ISSN: 2395-602X (www.ijsrst.com)

Antimicrobial Activity of Flaxseed Marketed Oil on Different Microbes

Aishwarya Dongare*, Utkarsha Shivasharan, A. H. Hosmani
Department of Pharmaceutical Quality Assurance, DSTS Mandals College of Pharmacy, Solapur-413004, Maharashtra, India

ABSTRACT

Flaxseed has antibacterial, antifungal, anti-inflammatory, and antimicrobial activity. The purpose of this study is to check the activity of two different marketed cold-pressed flaxseed oils. In that study, the two different oils are taken and their activity was checked against different gram-positive and gram-negative bacteria (*Escherichia coli, Staphylococcus aureus)* pathogenic fungus (*candida Albicans, and aspergillus Niger),* and periodontal bacteria (*streptococcus mutans and porphyromonas gingivalis).* The agar well diffusion technique was utilized against these six microbicides. The wells of 6 mm diameter were bored and oil was applied to two different wells. The zone of inhibition of it was measured in millimeters after 48,72 hours of incubation at 38°C.No inhibitory effect was noticed against *S mutans*, low effect against *S aureus* and *E Coli, p gingivalis*and good inhibition against *candida Albicans* and *Aspergillus Niger.* In conclusion, flaxseed oil is a good alternative medication and it can be used for the treatment of wound infections caused by bacteria andas an antifungal agent.

KEYWORDS: marketed flaxseed oil*, E Coli, S aureus, candida Albicans, A Niger, S mutants, P gingivalis.*

I. INTRODUCTION

The scientific name for flaxseeds is *Linumusitatissimum L*, which translates to "most helpful" in Latin. It is a multifaceted crop that can be planted for fiber or oil production (El-Beltagi, Salama, & El-Hariri, 2007; Diederichsen & Richards, 2003; Vaisey-Genser & Morris, 2003; Tour'e & Xueming, 2010)[1]. Flax comes in yellow and brown variants. Depending on how the seeds will be used, end consumers in the food business typically have a preference for one colour kind over the other. If the flax is crushed for oil, the colour kind is less significant. Some types, which may sell for more money, were created with higher quantities of omega-3 fatty acids.[2]

Linseed oil is commonly marketed as a food under the name flaxseed oil. It is obtained from the dried ripe seeds of the flax plant, *Linum usitatissimum*, and consists of the glycerides of linolenic, linoleic, oleic, stearic, palmitic, and myristic acids (Merck 2015) [3]. flaxseed oil is an edible oil obtained from the flax plant. It is high in α-linoleic acid and has hydrophobic properties that help it to reduce moisture and seal porous surfaces. These properties are believed to be responsible for the effective reduction of microorganisms and fungal infections.[4] In earlier studies, the *L. usitatissimum* fixed oil has been reported to exhibit significant anti-

inflammatory [5], antiarthritic [6], antiulcer [7], and antidiabetic [8] properties. The antimicrobial property of *L. usitatissimum* oil and its therapeutic effectiveness in bovine mastitis [9], an inflammatory disorder caused by microbial infection has been reported recently [10]. Flaxseed oil was used as a diuretic during the Middle Ages to treat renal diseases (Moghaddasi 2011) [11]. Flaxseed oil is mostly found in cotyledons (75%) and less in seed coats and endosperms (22%). The main constituents of the oil are triglycerides of α-linolenic (52%), less in seed coat and endosperm. According to another study, flaxseed lignans extract showed considerable antifungalactivityagainst*Aspergillusflavus*and*AspergillusNiger*at2.5to3.0mg/ml,rangingfrom70%to 90%. (Barbary et al., 2010) [12]. By preventing tiredness and slowing down the ageing process, flaxseed oil is said to increase both mental and physical endurance[13]. *L usitatissimum* fixed oil showed good antibacterial activity against a number of microbial strains, including *Streptococcusagalactiae* (NCIM 2401), *Micrococcusluteus* (ATCC 10240, ITCC9341), *Staphylococcusaureus* (ITCC8531,ATCC29737), *Bacillus pumilus* (ATCC 14884), *Enteric* (ATCC 8739) [14] By preventing tiredness and slowing down the ageing process, flaxseed oil is said to increase both mental and physical endurance. Flaxseed is stated to have properties like Vranahrit (wound healing), and is beneficial for Vata (Misra 1963).[15]The antibacterial activity of flaxseed against periodontal pathogens was carried out in a study that demonstrated that flaxseed extract is efficacious against *P gingivalis*.[16].The current research presents an evaluation of the antimicrobial activity of flaxseed oil against six different organisms.

II. MATERIALS AND METHODS

Flaxseed oil was obtained from the local market and used for this study. Microorganisms obtained from V G Shivdare institute of biotechnology,Solapur.

MICROORGANISM:

The following microorganisms were used for antimicrobial activity. *Escherichia coli, Staphylococcus aureus, candida Albicans,aspergillus Niger,streptococcus mutans and porphyromonas gingivalis.* All the microorganisms were maintained at 4° C on nutrient agar slants.

Antibacterial Susceptibility Test:

The well diffusion method on Muller Hinton Agar (MHA) medium was used to screen the antibacterial activity[17] The MHA plates were prepared by pouring media into sterile Petri plates and bacterial culture inoculated by spread plate technique. Wells of 6 mm diameter were bored and oils were applied to wells of the plates were incubated at 37°C for 48 and 72 hr. The diameter of inhibition zones was measured.

Antifungal Susceptibility Test:

From the well diffusion method, it is observed that marketed flaxseed oil shows a zone of inhibition in the range of 14-21mm.*S mutants*do not show any zone of inhibition(fig.A), *S aureus* shows the zone of inhibition

of 16mm,*E coli* shows 15 mm of zone of inhibitionwhile *p gingivalis* shows 14mm of zone and *C albicans* and *aspergillus Niger* shows 20-21 mm of the zone of inhibition respectively.

III. RESULT AND DISCUSSION

zone of inhibition of two marketed flaxseed oils was found to be_

Table 1. zone of inhibition of flaxseed marketed oils

Test organisms	Zone of inhibition	
	F. oil 1(brown oil)	F. oil 2(yellow oil)
S mutants	-	-
S aureus	-	16mm
E coli	15 mm	-
C. albicans	20mm	-
A. Niger	21mm	-
P. gingivalis	14mm	-

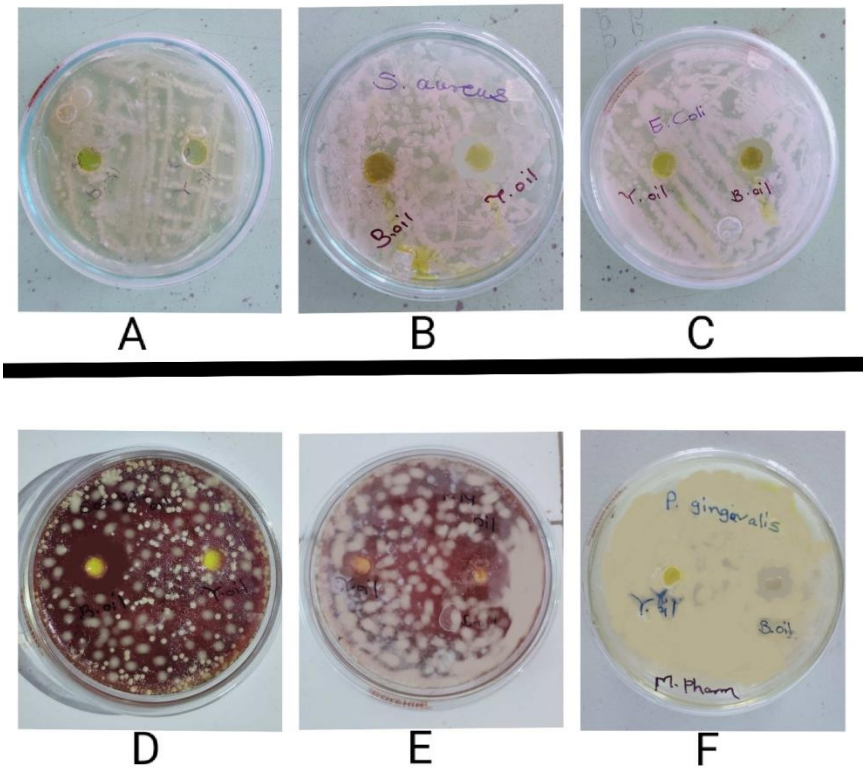

Fig.1 zone inhibition of flaxseed marketed oils against

A. *Streptococcus mutans*, B. *staphylococcus aureus*, C. *Escherichia coli*, D. *Candida albicans*, E. *Aspergillus Niger*, F. *Porphyromonas gingivalis*.

From well diffusion method, it is observed that flaxseed oils exhibited higher antifungal activity against *Candida albicans* and *Aspergillus Niger* than other bacteria(fig.1).

IV. CONCLUSION

The study provides useful knowledge about the activity of flaxseed-marketed oils on different microbes. The oil shows antifungal properties against tested fungi (Table 1) and also shows an effect against some bacteria (Fig. 1).

V. REFERENCES

[1]. El-Beltagi, Salama, & El-Hariri, 2007; Diederichsen & Richards, 2003; Vaisey-Genser & Morris, 2003; Tour'e & Xueming, 2010.
[2]. Laux M (2011) http://www.agmrc.org/commodities__products/grains__ oilseeds/flax _profile .cfm Last accessed 13–03–2012
[3]. Merck 2015. The Merck Index Online. 2015. Cambridge, UK: Royal Society of Chemistry,
[4]. Brian P. Baker and Jennifer A. Grant Linseed Oil Profile Active Ingredient Eligible for Minimum Risk Pesticide Use. New York State Integrated Pest Management, Cornell University, Geneva NY
[5]. Kaithwas G., Mukherjee A., Chaurasia K., and Majumdar D.K. 2011. Anti-inflammatory, analgesic, and antipyretic activities of inflammation L. usitatissimum (flaxseed/linseed) fixed oil. Indian Journal of Experimental Biology, 49(12): 932-938.
[6]. Kaithwas G. and Majumdar D.K. 2010. The therapeutic effect of Linum usitatissimum (flaxseed/linseed) fixed oil on acute and chronic arthritic models in albino rats. Inflammopharmacology, 18(3): 127-136.
[7]. Kaithwas G. and Majumdar D.K. 2010.Evaluation of the antiulcer and antisecretory potential of Linum usitatissimum fixed oil and possible mechanism of action. Inflammopharmacology, 18(3): 137-145.
[8]. Kaithwas G. and Majumdar D.K. 2012.In vitro antioxidant and in vivo antidiabetic, antihyperlipidemic activity of linseed oil against streptozotocin-induced toxicity in albino rats. European Journal of Lipid Science and Technology, 144: 1237-1245.
[9]. Kaithwas G. and Mukerjee A., Kumar P., Mujumdar D.K. 2011.Linum Usitatissimum (linseed/flaxseed) fixed oil: antimicrobial activity and efficacy in bovine mastitis. Inflammopharmacology, 199(1): 45-52.
[10]. Amber Hanif Palla, Anwar-UI-Hassan Gilani, Samra Bashir2022.Multiple Mechanisms of Flaxseed: Effectiveness in Inflammatory Bowel Disease.
[11]. Moghaddasi MS. Linseed and usages in Humanlife. Adv Environ Biol. 2011;5(6):1380–1392. [Google Scholar] [Ref list]*

[12]. Barbary OM, El-Sohaimy SA, El-Saadani MA, Zeitoun AMA (2010). Antioxidant, antimicrobial, and anti-HCVactivities oflignanextracted from flaxseed. Res JAgric Biol Sci, 6(3):247-256.

[13]. AbdelillahA,HoucineB,HalimaD,MeriemCS,ImaneZ,EddineSDetal.(2013).Evaluationofthe antifungalactivityoffreefattyacidsmethylestersfractionisolatedfromAlgerianLinumusitatissimumL.seedsa gainsttoxigenicaspergillus. AsianPac J Trop Biomed,3(6):443-448.

[14]. Kaithwas G, Mukerjee A, Kumar P, Majumdar DK (2011). Linum usitatissimum (linseed/ flaxseed) fixed oil: antimicrobial activity and efficacy in bovine mastitis. Inflammopharmacology, 19(1): 45-52.

[15]. Misra B. "Tailavarga" in Bhavaprakashanighantu. Part I. In: Misra B, Vaisya R, editors. The Kashi Sanskrit series. Varanasi: Chaukhumba Bharati Academy; 1963. p. 779

[16]. Apoorva B Badiger, Triveni M Gowda, Rajarajeshwari S, Satish Saswat 2019.Antimicrobial effect of flaxseed (Linum usitatissimum) on periodontal pathogens: An in vitro study.International Journal of Herbal Medicine 2019; 7(3): 16-19.

[17]. Bauer R, Kirby W, Sherris MK, and Turck M: Antibiotic susceptibility testing by standard single disc diffusion method, Am. J. Clin. Pathol. 1966; 45: 493-496.

International e-Conference on Recent Trends in Nano-Materials and Its Applications
In Association with International Journal of Scientific Research in Science and Technology
Volume 10 | Issue 9 | Print ISSN: 2395-6011 | Online ISSN: 2395-602X (www.ijsrst.com)

Formulation and Evaluation of Herbal Lipstick from Beetroot Powder

Sandhyarani Gajare[1]*, Utkarsha Shivsharan[1], Dr. A. H. Hosmani[2]
[1]D.S.T.S. Mandal's College of Pharmacy, Solapur 413004, Maharashtra, India
[2]Government College of Pharmacy, Karad, Maharashtra, India

ABSTRACT

The aim of present study to create the herbal lipstick from the natural colorants. In order to prepare herbal lipstick from the beet root powder and evaluate the prepared lipstick. Lipstick are formulations commonly used to improve the gorgeousness of lips and add glamorous touch to the makeup. Herbal lipstick is a cosmetic formulation containing pigments, perfumes, waxes, preservatives, anti-oxidants, oils, colors. The advantage of herbal lipstick is safe, cost effective, non-toxic, and pigments used from easily available plants and vegetables. The aim of the present study which includes the formulation and evaluation of herbal lipstick using color pigments from natural sources such as beetroot.

Due to lot of side effects of available synthetic formulation in the market the prepared herbal lipstick evaluated on parameters such as color, pH parameter, skin irritation test, perfume stability, solubility study, surface anomalies, aging stability. The present study concluded that the use of natural colorants in lipstick formulation having less or no side effects. It has potential to increase consumer acceptance because of use of different natural ingredients and harmless colorant used.

KEYWORDS: Beet root, Natural colorant, Herbal lipstick formulation, *Betavulgaris,*color cosmetic, skin testing.

I. INTRODUCTION

Cosmetics is a word comes from the Greek word **"Kosmtikos"** it means the organization, power and skill in beautifying[1].Cosmetics are the formulations that are used to improve the appearance of the human beauty[2,3]. Cosmetic substances include lipstick, skin care creams, lotions, perfumes, powders, hair colors, nail polish, gels, baby products and other so many products are in huge demand in developing and developed countries[4]. Herbal cosmetic products have increasing demand in the world market and they are precious gift from the nature. There is broad choice of herbal cosmetic products to convince our beauty regime[5]. Herbal lipsticks are produced from natural color from frequently available vegetables and plants. Commonly used colored pigments are beet root, rose, papaya, tomato, carrot, henna, alkanet root, indigo and it is easy to produce blends for our need. The commonly used ingredients for the preparation of lipstick are oil, emollients, waxes and pigments. Such ingredients mainly used for protection of lips, texture and color[6].Herbal lipstick contains many natural nutrients are present which are safer to use and it is free from hazardous chemicals and it is safe

to consume, therefore herbal lipstick prepared from the natural ingredients from beet root powder, rose water, bees wax. Herbal lipstick contains natural ingredients that are non-toxic as compare to the synthetic agents [7].

Beet root is usually known in Canada and the USA as a beet and it is a taproot part of a beet plant. The vegetable is stated to as a beetroot in British English, it is also known as red beet, garden beet, table beet, golden beet or dinner beet. It is one of numerous cultured diversities of *Betavulgaris*sub, specious *vulgaris* Conditiva Group [8]. *Beta vulgaris* (Beet root) is a plant from Chenopodiaceae family that is concluded in Amaranthaceaefamily[9]. Red purple color of beets due to the variety of betanin pigments and is commonly used industrially as a red feed coloring and coloring agent in lipstick [10].

IDEAL CHARATERISTICS OF HERBAL LIPSTICK:

1. Herbal lipsticks are smooth and are easy to apply.
2. It is non-toxic and non-irritant.
3. It has different color, odour, texture and packing and specific plasticity.
4. It is free from contamination.
5. It is free from gritty particles.
6. It does not melt or hard within a variation of climatic temperature.
7. It should be stable in shelf-time and it is free from bloom and sweating during storage condition of lipstick.
8. It should have a good degree of indelibility.
9. It should be non-drying.
10. It should not lose its shiny appearance during storage.
11. It should remain free from the bloom or sweating during storage.
12. It should be a long lasting [11,12].

BENEFITS OF HERBAL LIPSTICK:

1. It is safe to use.
2. It is natural in nature.
3. It is cost-effective and non-expensive.
4. It has no side effects.
5. It is free from hazardous chemicals.
6. It is kinder to the environment.
7. It is not tested on animals [13].

ADVANTAGES OF HERBAL LIPSTICK:

1. Natural ingredients used in herbal lipstick hence it is safe to use.
2. It contains natural nutrient that keep lips healthy.
3. Different shades and combination should be obtained from these natural pigments.

4. Natural colorants have different natural shades of color such as ruby red, beetroot purple, pale red, deep violet, dark purple.
5. It hydrates the lips.
6. Non -irritation to the skin of lips.
7. Stable physically and chemically.
8. Shiny and smooth appearance.
9. Wide range of shades of color to choose form[14].

II. MATERIALS AND METHODS

Materials:

Bees wax, paraffin wax, castor oil, beet root powder, lemon juice, vanilla essence, rose water. These are the various ingredients which are used for the preparation of herbal lipstick.

Vanilla essence and rose water purchased from the local market of Solapur. Lemon juice was squeezed from the lemons practically. Bees wax, paraffin wax and castor oil were used from laboratory.

Selection of herbs:

The selection of herb used in the formulation of herbal lipstick based on the literature survey.

1. Collection of plant material:

Beetroot was purchased from the local market of Solapur.

2. Extraction method:

Beetroot was purchased from the local market of Solapur. Beetroot was washed and peeled, cut into small-uniform size pieces. These small-uniformed pieces spread over the butter paper and It cover with fine mesh and kept it for shade dry for a day. If there is any moisture content left then it dry in oven. Then take a dried beetroot and make fine powder by using grinder. These fine powder pass through the fine sieve. Check the powder for the grainy particles and again sieve if it is required. Weigh the amount of powder and packed it [15].

Ingredients of herbal lipstick:

Table. I :

Ingredients	Use
Castor oil	Blending agent
Paraffin wax	Glossy and hardness
Bees wax	Glossy and hardness
Beet root powder	Coloring agent
Rose water	Flavouring agent
Lemon juice	Antioxidant
Vanilla essence	Preservatives

III. METHOD OF PREPARATION OF HERBAL LIPSTICK

The herbal lipstick was prepared by general method of lipstick formulation. Bees wax and paraffin wax were melted in china dish on water bath till becomes hot liquid. Beet root powder mixed with required quantity of castor oil and heated. Then add the first preparation into the second preparation. Now add required quantity of lemon juice and heat properly. After that add required quantity of vanilla essence and rose water. Then final formulation is kept in the mould and cool it by keeping in ice for 30 mins. After 30 min remove and the store prepared lipstick in refrigerator [16]

Table.II Formulation Table of herbal Lipstick:

S. No.	Ingredients	Use	F1	F2	F3	F4	F5	F6
1	Castor oil	Blending agent	4ml	4ml	4ml	4ml	4ml	4ml
2	Paraffin wax	Glossy and hardness	1gm	1.5gm	2gm	2.5gm	3gm	3.5gm
3	Bees wax	Glossy and hardness	2gm	2.5gm	3gm	3.5gm	4gm	4.5gm
4	Beetroot powder	Coloring agent	1.5gm	2gm	2.5gm	3gm	3.5gm	4gm
5	Rose water	Flavouring agent	1ml	1ml	1ml	1ml	1ml	1ml
6	Lemon juice	Antioxidant	0.5ml	0.5ml	0.5ml	0.5ml	0.5ml	0.5ml
7	Vanilla essence	Preservative, Q.S.	q. s.	q. s.	q. s.	q. s.	q. s.	q. s.

IV. EVALUATION OF HERBAL LIPSTICK:

The formulated herbal lipstick was evaluated for different evaluation tests such as melting point, skin irritation, perfume stability, surface abnormalities, aging stability, solubility test, pH.

1. Organoleptic properties:

The formulated lipstick was evaluated for organoleptic properties such as color, odor, and texture[17].

2. Solubility test

The prepared herbal lipstick was dissolved in many solvents like acetone, hexane, petroleum ether, water, alcohol etc. and determine the solubility[18].

3. Melting point:

Melting point is determined to indicate the limit of safe storage. The melting point of prepared herbal lipstick was determined by capillary tube method. The melting point of lipstick was done by taking melted sample in a capillary tube and then capillary tube is subjected to the ice for 2 hrs for cooling then capillary tube is tied to a thermometer. Then capillary tube was dipped into the beaker containing water which was subjected to continuous stirring. A temperature at which the sample start to increase along with capillary tube it is considered as melting point[19,20].

4. Skin Irritation test:

The prepared herbal lipstick formulations were studied for the skin irritation test. The skin irritation test done by applying the formulated herbal lipstick on the skin for 15 minutes and observe results.

5. Determination of pH:

The pH of the prepared of herbal lipstick was determined by using pH meter.1 gram of lipstick was dissolved in 100 ml of distilled water and measure the pH .

6. Perfume stability:

Perfume stability test done by storing the prepared lipstick at 40°c and periodically comparing ,after bringing the temperature down ;with the fresh lipstick.

7. Surface abnormalities:

Surface abnormalities studied by the surface defects such as formation of crystals on surface, contamination by moulds, fungi etc . Formation of wrinkles, exudation of liquid substances and of solid fatty substances.

8. Aging stability:

Aging stability test was done by product was stored in 40°c. And periodically observe of oil bleed , crystallization of wax on the surface[21].

V. RESULT

The formulated herbal lipstick was evaluated and it was found that, F4 was the best among the six batches. From the present study it was concluded that the formulated herbal lipstick has better option to the women because of the minimal side effects.

The aim of the present study formulation and evaluation of lipstick containing herbal ingredients which has minimum side effects and cost effect over the synthetic formulation.

Table no.III

Evaluation Parameters	F1	F2	F3	F4	F5	F6
Color	Light pink	Light pink	Pink	Dark pink	Dark pink	Wine
Texture	Smooth	Smooth	Smooth	Smooth	Smooth	Smooth
Melting point	55	54	58	60	62	65
Ph	6.20	6.32	6.50	6.66	6.80	6.82
Skin irritation	No	No	No	No	No	No
Perfume stability	Good	Good	Good	Good	Good	Good
Surface anamolies	No defect	No defect	No defect	No defect	No defect	No defect

VI. DISCUSSION

Cosmetics with the natural ingredients are safer than the synthetic means the chemical-based cosmetics. Cosmetics prepared with the natural ingredients have ability to protect the skin. The present work formulation and evaluation of herbal lipsticks were carried out to formulate a herbal lipstick using natural ingredients which has minimum side effects compared synthetic ones. The present formulation of herbal lipsticks formulated by using different natural ingredients , such as Bees wax, castor oil, paraffin wax, beet

root powder, rose water, vanilla essence, lemon juice. Beet root used as a natural coloring agent it better option as compared to the synthetic color which have hazardous side effects.

The formulation table of herbal lipstick containing (F1-F6) were prepared and evaluated tests were performed. From the six formulation all formulations showed promising results.

VII. ACKNOWLEDGEMENT

The authors are thankful to the D.S.T.S. Mandal's college of pharmacy Solapur for support, co-operation, encouragement and providing all necessary facilities, which enabled to complete this work successfully.

I express my sincere thanks to our respected Principal, Dr. R.Y. Patil. D. S. T. S. Mandal's college of pharmacy, Solapur for his cooperation and for providing all facilities.

VIII. REFERENCES

[1]. Yogesh S Mali, Ganesh Newad, Azam Z Shaikh. Review on Herbal Lipstick. Research Journal of Pharmacognosy and Phytochemistry. 2022; 14(2):113-8. doi: 10.52711/0975-4385.2022.00021

[2]. Talpekar P, Borikar M. Formulation, development and comparative study of facial scrub using synethetic and natural exfoliant. Research J. Topical and Cosmetic Sci. 2016, 7(1), 01-08.

[3]. Gavarkar P, Adnaik R, Chavan D, Bagkar A, Bandgar R. Physicochemical Investigation of Some Marketed Herbal Hair Oil. Research J. Topical and Cosmetic Sci. 2016, 7(2), 70-72.

[4]. Rautela Sunil, Tailor Chandra Shekhar, Badola Ashutosh.Formulation and Evaluation of a Herbal Lipstick : A New Approach. International Journal of Pharmaceutical Erudition.May 2013, 3(1), 26-30.

[5]. G. Sudha Rani , G. Pooja , V. Harshvardhan , B. Vamshi Madhav , B.Pallavi Formulation and Evaluation of Herbal Lipstick from Beetroot (Beta vulgaris)Extract. Research Journal of Pharmacognosy and Phytochemistry.2019;11(3):197-201. doi:10.5958/0975-4385.2019.00034.7

[6]. Devika R. Kotekar1, RakshataDesai , Nagesh C., Suma N. , Pratiksha Patil and Aishwarya Patil. Formulation And Evaluation Of Herbal Lipstick Using Natural Colorants. World Journal of Pharmaceutical Research: Volume 11, Issue 4, 1335-1344.

[7]. D. A. Bhagwat, N. D. Patil, G. S. Patel, S. G. Killedar, H. N. More. Formulation and Evaluation of Herbal Lipstick using Lycopene Extracted from Solanum lycopersicum L. Research J. Pharm. and Tech. 2017; 10(4): 1060-1064. doi: 10.5958/0974-360X.2017.00192.5

[8]. Sainath M, Kumar KS, Babu KA. Formulation and evaluation of herbal lipstick. International Journal of Advanced Research In Medical & Pharmaceutical Sciences (IJARMPS), 2016; 1(1).

[9]. Jamdade K, Kostha A, Jain N, Dwivedi S, Malviya S, Kharia A. Formulation and Evaluation of Herbal Lipstick Using Beta Vulgaris and PunicaGranatum Extract. International Journal of Pharmacy & Life Sciences, 2020; 1: 11(4).

[10]. Akilandeswari K, Shanthini N, Formulation and Evaluation of Herbal lipsticks, 2018; 1(1): 1-10.

[11]. Pandit Deepika, Gujrati Aditi, Rathore K S, "Formulation and Evaluation of Herbal Lipstick from the Extract of Papaya", International Journal of Pharmaceutical Science, July-August 2020; 63(1): 107-110.

[12]. AboliBornare, TejasviTribhuwan, ShrutikaMagare, Aishwarya Shinde, Swati Tarkase, "Formulation an Evaluation of Herbal Lipstick", International Journal of Creative Research Thoughts, September 2020; 8: 2390- 2397.

[13]. Shayesta Khan, uzma s, Abdul Sameeeh ,Juveria M, S M Shahidulla .Formulation and Evaluation of Beta Vulgaris Herbal Lipstick . International Journal of Innovative Research in Technology. May 2022Volume 8: Issue12.

[14]. Swetha Kruthika V, S Sai Ram, Shaik Azhar Ahmed, Shaik Sadiq, Sraddha Deb Mallick, and T Ramya Sree, "Formulation and Evaluation of Natural Lipsticks from coloured pigments of Beta Vulgaris Taproot", Journal of Pharmacy and Pharmaceutical Sciences, July-September 2014; 3: 65-68.

[15]. Anilkumar V., Kalyani R., Sangeeta Kumari L. Design, Development And Evaluation of Herbal Lipstick from Natural Colour Pigment. International journal of pharmacy and pharmaceutical Research. May 2020; volume-18: issue 2.

[16]. Sanket Jain, Shraddha Jain, Sujit Pillai, Rampal Singh Mandloi, Nidhi Namdev. Formulation and Evaluation of Herbal Lipstick by using Beet root extract. Research Journal of Pharmacognosy and Phytochemistry. 2022; 14(1):23-5. doi: 10.52711/0975-4385.2022.00005.

[17]. Neeraj Bainsal, Simranjeetkaur,SudhanshuMallan. Pharmacognostical Physiochemical and Phytochemical studies of different varieties of Beet root grown in Punjab. Research J. Pharm. And Tech. 2021:10(3):1689-1692.doi:10.5958/0974-360X.2017.00192.5

[18]. Nuha Rasheed, Syed Abdul Rahman, Samreen Hafsa. Formulation and Evaluation of Herbal Lipsticks. Research J. Pharm. and Tech. 2020; 13(4): 1693-1700.17.

[19]. Kawarkhe PR, Deshmane SV, Biyani K. Formulation and Evaluation of Antioxidant Face Cream Containing Raspberry Fruit and Grape Seeds Extract. Research J. Topical and Cosmetic Sci. 2016, 7(2), 73-78.

[20]. Elumalai A, Chinna M, Nikhitha M. Formulation and Evaluation of a Herbal Lipstick from Punica granatum Fruit Peel. Res. J. Topical and Cosmetic Sci. 3(1), 2012, 20-22.

[21]. Nutan Gawande, Sanika Kate, Karishma Waghmare. Formulation and Evaluation of some Cosmetic preparations using novel natural colorant from Ixora coccinea. Asian J. Res. Pharm. Sci. 2021; 11(1):22-28. doi: 10.5958/2231-5659.2021.00004.7

International e-Conference on Recent Trends in Nano-Materials and Its Applications
In Association with International Journal of Scientific Research in Science and Technology
Volume 10 | Issue 9 | Print ISSN: 2395-6011 | Online ISSN: 2395-602X (www.ijsrst.com)

Improvement of Gas Sensing Performance of SnO_2 Sensors for NO_2 Gas by Annealing Environment Fabricated by Thermal Evaporation

S. M. Ingole[1], V. B. Patil[2]*

[1]Arts, Commerce and Science College Onde, Vikramgad, Palghar- 401605, (MS), Maharashtra, India

[2]Functional Materials Research Laboratory, School of Physical Sciences, Solapur University, Solapur, M.S. 413255, Maharashtra, India

ABSTRACT

Post-deposition annealing was carried out in argon ambient to investigate the corresponding effects onto gas sensing performance of SnO_2 nanostructured film synthesized by thermal evaporation and further characterization with x-ray diffraction, scanning electron microscopy and EDAX analysis for confirming its structure, morphology, and composition. The chemo-resistive gas sensing properties of SnO_2 nanostructures for various oxidizing and reducing gases was investigated. Experimental results show that the SnO_2 nanostructured sensing film has high sensitivity and selectivity for NO_2 gas compared to other test gases. The gas sensing study of the SnO_2 film prepared with thermal evaporation after annealing in Argon atmosphere at 700°C showed an excellent sensing towards NO_2 gas at 200°C operating temperature with highest sensing response of 443% for 100 ppm NO_2 gas with very fast response and recovery time. The SnO_2 nanostructured sensor manifests remarkably enhanced sensing performance, including good response and recovery time suggestive of the promising application of the SnO_2 in the gas sensing.

Keywords: Thermal evaporation; Argon Atmosphere, Metal Oxide; XRD; SEM; EDAX; NO_2 Sensor.

I. INTRODUCTION

Environmental safety policy of many countries is directed towards the monitoring, measurement, and control of CO, H_2S, O_3, H_2, NH_3, and other pollutants in the air. Today, air pollution caused by nitrogen oxides (NO_x), especially NO and NO_2, has becomes an important environmental problem. In fact, NO_2 can interact with other pollutants such as volatile organic compounds (VOCs) to form ozone in the lower atmosphere [1], create smog in cities, and chemical reactions of NO_2 gas with water vapor can cause acid rain [2]. Hence development of NO_2 gas sensors for environmental monitoring becomes a necessary task [3]. Nanostructured metal oxides are extremely chosen for gas sensing applications because of their reversible interaction with many gases. The ZnO, SnO_2, CuO, TiO_2, WO_3, V_2O_5 etc. are several metal oxides that have been extensively studied for gas sensing application [4]. Between them, SnO_2 is the mainly used for sensing applications due to its inherent oxygen vacancies and wide band gap of 3.6 eV [5]. Gas Sensors based on semiconductor tin oxide (SnO_2) have attracted attention for over four decades because of their physicochemical properties and their

ability to detect various gases (oxidizing and reducing gases) with high response [6]. So far, thermal evaporation [7], sol–gel [8], spray pyrolysis [9], radio frequency (RF), magnetron sputtering [10], and chemical vapor deposition (CVD) [11] methods have been used to prepare the SnO_2 nanostructured thin film. Among these methods, the thermal evaporation method has been widely studied because of it has many advantages of easy processing, less power consumption, high yield, high crystallinity, and controllable shape [12].

In present work, SnO_2 nanostructures thin film were prepared on glass substrate following a route of thermal evaporation and then, annealing in Argon atmosphere promotes a progressive oxidation of the fabricated Sn film, transforming the amorphous long-range disordered as-deposited tin oxide into ordered structures for enhance gas sensing performance. In this following section, details of the experimental procedure, characterization of the samples and gas sensing properties will be presented.

II. EXPERIMENTAL DETAIL

Tin oxide (SnO_2) nanostructure were fabricated in high vacuum thermal coating unit (IHVU). High purity 99.99% Aldrich made Sn powder was used as the source material for SnO_2 synthesis. The Sn powder was stored in molebodium boat. Place the boat in vacuum chamber connected with high voltage. The precleaned glass substrates were attached to substrate holder. The chamber pressure is maintained from 10^{-5} to 10^{-6} mbar. The required current was increased to evaporate Sn powder. During this process, a distance of 15 cm is left between the source and substrate. The coated film was annealed for 20 minutes at 700^{o}C in an argon atmosphere in the tubular zone furnace. After cooling to room temperature in a tubular furnace, the film was used for further analysis.

The morphology and crystalline structure of SnO_2 film was examined by scanning electron microscopy (SEM Model: JEOL-6300F), an x-ray diffractometer (Rigaku, Ultima IV, Cu kb/40 kV/40 mA, k = 1.5406 Å) with scan range 10–80. Gas sensing tests of SnO_2 film was performed on custom fabricated high temperature gas sensing measurement unit described elsewhere [12]. The known amount of gas is injected into the test chamber of volume 250cc by a syringe. 1mm wide and 1 cm apart like two silver electrode was drawn on sensor film as contacts for resistance measurement. To measure the gas response, resistance change of sensor film was measured in presence of fresh air and in NO_2 gas atmosphere. Resistance measurement is carried out by using Keithley 6514 System Electrometer. This electrometer is controlled by a computer and is measure the change in resistance of sensor film. To calculate gas response of sensor the formula is given as,

Response (S)= (Rair – Rgas)/ Rair * 100……..1

Where, Rair and Rgas represented the resistance of sensor in presence fresh air and NO2 gas respectively.

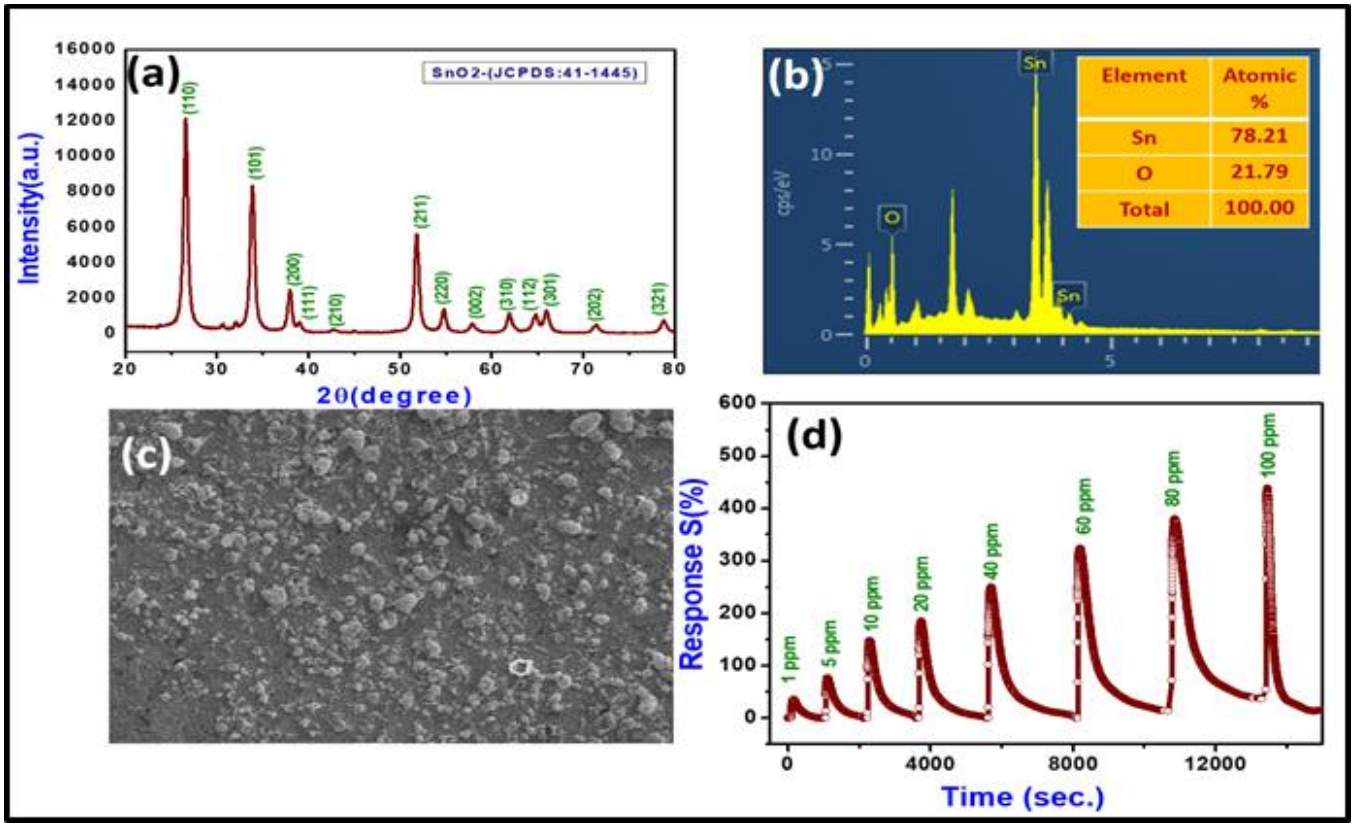

Fig.1(a) XRD, (b)EDAX, (c)SEM & (d) Dynamic response curve of SnO_2 sensor for NO_2 gas

III. RESULT AND DISCUSSION

3.1. Structural and morphological Analysis

The characteristic X-ray diffraction patterns of Tin oxide (SnO_2) grown at 700^{0}C are shown in figure 1(a). All well-defined diffraction peaks are indexed to the tetragonal rutile structure of SnO_2 phase, which is reliable for standard JCPDS No.41-1445 data for SnO2 [13]. Here no other peaks are not observed in given XRD pattern, this reveals that no other phases and impurities cannot be found in the final product. The SnO_2 was oriented along the (110) direction because peak intensity of (110) reflection is maximum as compare with other reflection peaks. The chemical composition of the SnO_2 nanostructure was checked with the EDAX spectra shown in figure 1(b). The element content and weight percentages are shown in appendices of the figure. The characteristic peaks of Sn and O from the corresponding line are shown. The results showed the existence of elements, Sn and O from SnO_2. However, the nonappearance of any other peak except those due to Sn and O evidence of the growth of SnO_2 nanostructure and chemical quality of the grown films without any elemental impurities. The Scanning electron micrograph of the prepared SnO_2 sensing film is shown in figure.1(c). Micrograph shows a cluster of small globular particle like structure with rough in surface. This surface roughness may be due to the intensification in surface volume of the sensing film due to annealing [14]. The increase in the surface area of the film can increase the adsorption of gas molecules, providing more surface-active sites [15].

3.2. Gas Sensing Study

For the gas sensing study, the selectivity is the ability of the sensing film to respond to a specific gas in the existence of other gases. The gas sensing ability of the SnO2 sensing film prepared with thermal evaporation was analysed in the presence of various gas analytes such as oxidizing gases (NO_2 and Cl_2) and reducing gases (H_2S, NH_3, and CH_3OH) for 100 ppm concentration at 200°C operating temperature. The SnO_2 film shows a maximum response to NO_2 gas compared to other gases. The high sensitivity of the sensing film for NO_2 declares that the film is selective to NO_2 gas, due to much faster reaction rate between the surface of SnO_2 nanoparticles and NO_2 gas molecule and the film is further tested for different concentrations of NO_2 to find the variation in the sensor response with respect to gas concentration. The operating temperature of sensor is a very significant task, which employs the adsorption / desorption process of oxygen ions on the top surface of the sensing film, to optimize operating temperature of tin oxide sensing film the gas detection measurement was carried out at different temperature ranges from 100^{0}C to 300^{0}C. In the present study SnO_2 sensing film shows highest response of 439% for 100 ppm concentration of NO_2 gas at temperature 200^{0}C compared to other operating temperature. So further gas sensing study carried out at 200^{0}C operating temperature.

Figure 7(b) shows dynamic response curve of SnO_2 sensor in the concentration range of 1ppm to 100 ppm of NO_2 gas as a function of time at 200^{0}C. From figure it is clearly observed that response increased with increased in gas concentration. The response tests were carried out for known concentration of NO_2 gas injected into the chamber via syringe. After interaction of gas molecules with sensor the change in resistance due to adsorption of gas molecules on sensor and then come back to its original resistance due to desorption of gas molecules by sensor. The response of sensor is calculated using Eq. (1). From figure it is observed that, the response of SnO_2 sensor was about 38, 80, 151, 186, 253, 328,384 and 443% to 1,5, 10, 20, 40, 60, 80 and 100 ppm of NO_2 gas respectively with very fast response and recovery time. In the previous study as, prepared film was annealed in ambient air and the sensing film shows response of 23% and 403% to 1 and 100 pmm of NO2 gas respectively [12]. In the present report response of SnO2 sensors enhanced this is may be due to the presence of a greater number of oxygen ions on the surface of the film [16]. Sensing film were annealing in Argon atmosphere promotes a progressive oxidation. Response of sensor will increases may be explained based on surface area of the sensor and the number of active sites of the sensor film.

IV. CONCLUSION

We investigate the effects of annealing atmosphere on gas sensing performance, we have reported the fabrication of SnO_2 thin films by thermal evaporation on glass substrates followed by annealing in Argon atmosphere. The XRD analysis revealed that formation of tetragonal rutile nanostructured SnO_2. The gas sensing performance of SnO_2 film at optimized temperature of 200^{0}C was carried out towards host of gases such as NO_2, Cl_2, H_2S, CH_3OH, and NH_3. Our SnO_2 sensor films are selective to NO_2 and exhibit maximum response of 443% with fast response time and recovery time. It is confirmed that sensing film annealing in argon environment shows maximum response compare to annealing in air. Annealing atmosphere are also

important for the properties of the gas sensor. The results obtained in this paper may be helpful to the fabrications and further application of SnO_2 gas sensors.

V. REFERENCES

[1]. B. T. Marquis, J. F. Vetelino, "A semiconducting metal oxide sensor array for the detection of NOx and NH3", Sens. Actuators B 77 (2001) 100–110.

[2]. J. Brunet, V.P. Gracia, A. Pauly, C. Varenne, B. Lauron, "An optimised gas sensor microsystem for accurate and real-time measurement of nitrogen dioxide at ppb level", Sens. Actuators B 134 (2008) 632–639.

[3]. Anjali Sharmaa, Monika Tomar b, Vinay Guptaa, "SnO2 thin film sensor with enhanced response for NO2 gas at lower temperatures" Sensors and Actuators B: Chemical 156 (2011)743-752.

[4]. A.K. Prasad, S. Amirthapandian, S. Dhara, S. Dash, N. Murali, A.K. Tyagi, "Novel single phase vanadium dioxide nanostructured films for methane sensing near room temperature", Sens. Actuators, B: Chem. 191 (2014) 252–256.

[5]. A. Cabot, A. Vilá, J.R. Morante, "Analysis of the catalytic activity and electrical characteristics of different modified SnO2 layers for gas sensors", Sens. Actuators, B: Chem. 84 (2002) 12–20.

[6]. A. Chowdhuri, V. Gupta, K. Sreenivas, "Fast response H2S gas sensing characteristics with ultra-thin Cu islands on sputtered SnO2", Sens. Actuators B 93 (2003) 572–579.

[7]. V.R. Katti, A.K. Debnath, K.P. Muthe, M. Kaur, A.K. Dua, S.C. Gadkari, V.C. Sahni, "Mechanism of drifts in H2S sensing properties of SnO2: CuO composite thin film sensors prepared by thermal evaporation. Sens. Actuators B 96 (2003) 5981–5986.

[8]. J. Jeng, "The influence of annealing atmosphere on the material properties of sol-gel derived SnO2: Sb films before and after annealing", Appl. Surf. Sci. 258(2012)5981–5986.

[9]. S. Chacko, M.J. Bushiri, V.K. Vaidyan, "Photoluminescence studies of spray pyrolytically grown nanostructured tin oxide semiconductor thin films on glass substrates", J. Phys. D- Appl. Phys. 39 (2006) 4540–4543.

[10]. M.A. Gubbins, V. Casey, S.B. Newcomb, "nanostructural characterisation of SnO2 thin films prepared by reactive RF magnetron sputtering of tin", Thin Solid Films 405(2002) 270–275.

[11]. Y. Liu, E. Koep, M. Liu, A highly sensitive and fast-responding SnO2 sensor fabricated by combustion chemical vapor deposition. Chem. Mater. 17(15), 3997–4000 (2005).

[12]. S.M. Ingole, S.T. Navale, Y.H. Navale, D.K. Bandgar , F.J. Stadler , R.S. Mane , N.S. Ramgir, ,S.K. Gupta, D.K. Aswal, V.B. Patil, "Nanostructured tin oxide films: Physical synthesis, characterization, and gas sensing properties", Colloid and Interface Science 493 (2017) 162–170.

[13]. Davender Singh, VirenderSingh Kundu , A.S. Maan, " Structural, morphological and gas sensing sudy of palladium doped tin oxide nanoparticles synthesized via hydrothermal technique" J. Molecular Structure 1100(2015)562-569.

[14]. S.S. Lekshmy, I.J. Berlin, L.V. Maneeshya, Anitha, K. Joy, "Structural and optical characterisation of tin dioxide thin films by sol-gel dip coating technique", IOP Conf. Ser.: Mater. Sci. Eng. 73(2015)012018.

[15]. S. Ponmudi, R. Sivakumar, C. Sanjeeviraja, C. Gopalakrishnan, K. Jeyadheepan", Appl. Surf. Sci. 483(2019) 601-615.

[16]. R. Chandra, M. Nath, "Facile synthesis of ZnO-SnO2 anchored ZIF-8 nanocomposite: a potential photocatalyst ", Environ. Sci. Pollut. Res. 27(2020)25103-25115.

International e-Conference on Recent Trends in Nano-Materials and Its Applications
In Association with International Journal of Scientific Research in Science and Technology
Volume 10 | Issue 9 | Print ISSN: 2395-6011 | Online ISSN: 2395-602X (www.ijsrst.com)

Review On Recent Issues of Microplastics: Understanding The Minute Crisis with Big Consequences

Akanksha K. Kadam, Dr. Mahendra Suhas Kavale*

Physics Research Laboratory, Department of Physics, Sangameshwar College, Autonomous Solapur – 413001, Maharashtra, India

ABSTRACT

Plastic is the dark side of revolution started from 20th century. This is becoming a big headache to the modern world. Its degradation also is a critical issue. Now it has reached in the food chain. This review focuses on the entrance of microplastics in daily life. Microparticles and hence Microplastics have become a major environmental issue in recent years due to their persistent presence in the environment. This literature review seeks to examine the sources, composition, and impacts of microplastics on the ecosystems. The results of this research will help to inform better management strategies to reduce the presence of microplastics in ecosystems.

Keywords: Microplastics, hazardous particles,

I. INTRODUCTION

Microplastics are one of the most pervasive environmental pollutants of our time, affecting the environment and human health. The term microplastic was first time defined by Thompson in 2004 [1]. According to him these are the small sized plastic particles in the ocean. These tiny plastic particles, which are less than five millimetres in size, are increasingly being found in soil, water, and air around the world. Their size is below human perception. While microplastics have been found in many different places, their sources are still largely unknown. In this article, we will discuss what microplastics are, the potential sources of these pollutants, and the potential impacts on the environment and human health.

It is an increasingly concerning issue, with their presence in the environment and food chain posing potential risks to human health. It shall explore how they enter the environment, how they can affect humans and other organisms, and what measures are being taken to address the problem. Plastics are man-made organic polymers derived from the extraction of oil or gas [2–3].

Ecological plastic debris is defined by their physical state viz., solid-state, solubility, chemical composition, shape, size, colour, and origin. The classification of plastics is available. Microplastic consists of primary microplastics manufactured in microscopic size for particular purposes (micro beads) and secondary microplastics derived from huge plastic debris degraded and split by long-term chemical, physical, and biological environmental effects [4–5].

Their study involved both fieldwork and laboratory analysis of samples collected from various freshwater and marine environments. The data collected was used to determine the origin, composition, and concentrations of microplastics in different aquatic ecosystems, as well as the potential impacts of these particles on aquatic organisms and the environment.

II. METHODOLOGY

We searched the scientific literature using key search terms to obtain relevant publications.

2.1. Classification: Plastics were categorized as nano (1000 nm), micro (1000 mm), meso (10 mm), and macro (1cm) [6].

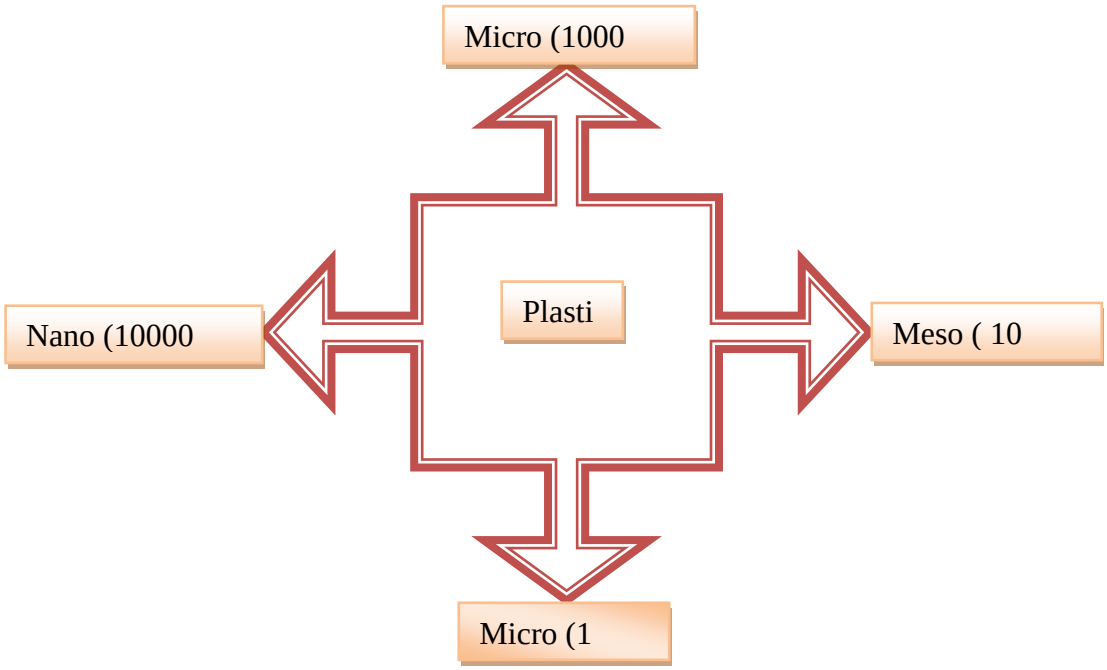

Figure: 1. Classification of plastics based on size

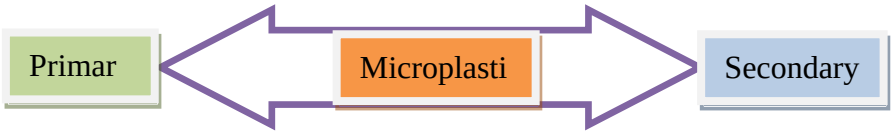

Figure: 2. Classification of plastics based on manufacturing

2.2. Sources of microplastics in the ecosystem: The main sources of solid waste microplastics are food waste, sludge, and landfill debris. These waste streams may contain microplastics that are linked to different micropollutants that can harm ecosystem health as they go up the food chain [7].

2.3 Microplastics in the ecosystem: Microplastics originate from waste products or by products from both commercial product development and the breakdown of larger plastics. When they are dumped to soil or sea results as a pollutant, microplastics can be harmful to the environment and animal health. Microplastics are viewed as a global problem because of their damaging impacts on humans and fish. Fish is the main source of human protein, which is crucial for body growth.

Microplastics have been found in lettuce, broccoli, pears, apples, and carrots. Radishes, turnips, and other root crops could potentially be infected. Prior research has shown microplastics in a variety of meats, including chicken, tinned fish, shellfish, and meat from other marine animals [8].

2.3.1. Effects of dissolution of Microplastics in water: According to Reuters, Microplastics have been discovered in a wide range of foods, including seafood, fruits, vegetables, beer honey, and sea salt, as a result of the pervasive use of plastics in the production and processing of food. Microplastics can also be released into the environment as a result of improper handling of food waste. Microplastics found in the sea can be ingested by marine animals. The plastic then accumulates and can end up in humans through the food chain [9].

2.3.2. Microplastics in food chain: Researchers have proposed that oxidative stress, DNA damage, and inflammation, among other health issues, could result from human exposure to microplastics. Seafood and land – based foods are important entry points for microplastics into the human food chain, which leads to food waste via wasted food [10].

III. IMPACT OF MICROPLASTICS ON HUMAN BODY

Water stored in the plastics bottles for longer duration results into shift in the neutral to acidic nature of water. The pH of water becomes acidic. This acid causes many effects of human body including increase in the stones in the body, permanent changes in the DNA, increase in the reproductive problems in humans, rise of the acidity of the blood hence causing cancer and blockages on the arteries and veins ultimately damage of function of heart [11].

3.1 microplastic ingestion: Researchers were found the microplastics everywhere; consequently, they estimated that globally on average, humans may ingest 0.1–5 g of microplastics weekly through various exposure ways [12].

IV. CONCLUSIONS

From the above studies it is to be concluded that the overuse plastics and overexploiting the branches of chemical sciences we all are at potential risk on human life. To have a better life for next generations we should ban the use of all types of plastics.

V. ACKNOWLEDGEMENTS

One of the authors, Akanskha K. Kadam is highly thankful to Government of India, Ministry of Science and Technology, DST for award of scholarship under INSPIRE – SHE scheme.

VI. REFERENCES

[1]. Thompson RC. (2004). Lost at Sea: Where Is All the Plastic? Science, 304(5672), 838–838. https://doi:10.1126/science.1094559

[2]. Derraik, J.G.B., 2002. The pollution of the marine environment by plastic debris: a review. Marine Pollution Bulletin 44, 842–852., Rios, L.M., Moore, C., Jones, P.R., 2007. Persistent organic pollutants carried by synthetic polymers in the ocean environment. Marine Pollution Bulletin 54, 1230–1237.

[3]. Thompson, R.C., 2006. Plastic debris in the marine environment: consequences and solutions. In: Krause, J.C., Nordheim, H., Bräger, S. (Eds.), Marine Nature Conservation in Europe. Federal Agency for Nature Conservation, Stralsund, Germany, pp. 107–115.

[4]. Besseling E, Foekema EM, van den Heuvel-Greve MJ, Koelmans AA. (2017). The Effect of Microplastic on the Uptake of Chemicals by the Lugworm Arenicola marina (L.) under Environmentally Relevant Exposure Conditions. Environ Sci Technol. 51(15), 8795– 8804. https://doi:10.1021/acs.est.7b02286

[5]. Cole M, Lindeque P, Halsband C, Galloway TS. (2011). Microplastics as contaminants in the marine environment: A review. Mar Pollut Bull. 62(12), 2588–2597. https://doi.org/10.1016/j.marpolbul.2011.09.025.

[6]. Hartmann N, Huffer T, Thompson RC, Hassellov M, Verschoor A, Daugaard AE, Wagner M. (2019). Recommendations for a definition and categorization framework for plastic debris. Environ Sci Technol. 53(3):1039-1047 https://doi:10.1021/acs.est.8b05297.

[7]. https://www.reuters.com/business/environment/plastic-entering-oceans-could-nearly-triple-by-2040-if-left-unchecked-research-2023-03-08.

[8]. https://www.reuters.com/graphics/ENVIRONMENTPLASTIC/0100B4TF2MQ/index.html

[9]. A Review of Human Exposure to Microplastics and Insights Into Microplastics as Obesogens, Kurunthachalam Kannan and Krishnamoorthi Vimalkumar; Front Endocrinol (Lausanne). 2021;12:724989., doi: 10.3389/fendo.2021.724989

[10]. Mishra et al., 2019, Alharbi et al., 2018, Volschenk et al., 2019, Pal and Maiti, 2019, Ribeiro et al., 2019.

[11]. Review of microplastics in the indoor environment: Distribution, human exposure and potential health impacts; M Dewika, et al, Chemosphere, 2023 May; 324:138270. PMID: 36878370, doi: 10.1016/j.chemosphere.2023.138270.

[12]. Kala Senathirajah, Simon Attwood, et al Journal of Hazardous Materials Volume 404, Part B, 15 February 2021, 124004; https://doi.org/10.1016/j.jhazmat.2020.124004.

International e-Conference on Recent Trends in Nano-Materials and Its Applications
In Association with International Journal of Scientific Research in Science and Technology
Volume 10 | Issue 9 | Print ISSN: 2395-6011 | Online ISSN: 2395-602X (www.ijsrst.com)

Lattice Constants of Aluminium Substituted Nanoparticle Copper Cobalt Ferrite

S.S. Karande, M.S. Kavale
Department of Physics, Sangameshwar College (Autonomous), Solapur (M.S.), Maharashtra, India

ABSTRACT

Nano-particle size polycrystalline aluminum substituted copper cobalt ferrite samples $Cu_xCo_{1-x}Fe_{2-2y}Al_{2y}O_4$ (where x= 0.0, 0.2 0.4, 0.6, 0.8, 1.0; y = 0.05, 0.15 and 0.25) have been prepared by standard ceramic technique. The effects of aluminium and copper on structural properties of cobalt ferrite are studied. A universal testing machine as well as Archimedes's method was applied for determining the physical properties of the samples. Phase formation is investigated using X-ray diffraction, Infrared absorption technique and Scanning electron microscope technique. The Lattice constant 'a' of samples goes on increasing with Al^{3+} and copper content. The ratio c/a is found increasing when addition of copper content and decreases with aluminium content. It means that Al^{3+} and copper acquire the tetragonal prolate type distortions on B site and hence (c/a) ratio increases and automatically crystal lattice turned from tetragonal spinel to cubic spinel.

Keywords: Polycrystaline, nanoparticle size, standard ceramic technique and Inverse cubic spinel

I. INTRODUCTION

Cobalt ferrite is a partially inverse spinel with formula $[Cu_xFe_{1-x}]^A$ $[Cu_{1-x}$ $Fe_{1+x}]^B$ O_4 where A and B are the tetrahedral and octahedral sites respectively [1-3]. Vaingankar et.al (4) has reported that cobalt is 74% inverse spinel. Degree of inversion is found to vary with heat treatment and quenching [5]. The cation distribution may also differ at surface and nonsurface atoms [6]. Copper cobalt ferrite is having high coercive force field. Mechanical hardness and chemical stability is magnetic recording, magneto-optical recording and electronic devices [7]. Magnetic properties of nanoparticles find wide technological applications such as high density recording, magnetic refrigeration, Ferro-fluids, spintronics and drug delivery etc.[8]. Several researchers have reported on Cd, Cr, Mn, Ti, Zn, Gd, and Nd. Substituted cobalt ferrite [9-11]. Raghavendraet. al. [12] have synthesized aluminium doped cobalt ferrite by the sol-gel method and reported the results on particle size.The estimated values of the porosity of the samples lie between 4.5% and 16.2% in Magnetoelectric composites with composition (x) $Ni_{0.2}Co_{0.8}Fe_2O_4$ (ferrite) + (1–x)$PbZr_{0.8}Ti_{0.2}O_3$[13]. In this present work we report the standard ceramic synthesis, structural properties of Al^{3+}substituted coppercobalt spinel ferrite nanoparticles.

II. EXPERIMENTAL

Materials:

High purity starting materials are used as Cobalt Oxide (CoO):- 74.9326 gm, Copper Oxide (CuO):- 74.5454 gm, Ferric oxide(Fe_2O_3):- 159.6922 gm, Aluminum Oxide (Al_2O_3):- 101.9612 gm

Preparation of ferrite:

Nano crystalline powder samples of $Cu_xCo_{1-x}Fe_{2-2y}Al_{2y}O_4$ (where x= 0.0, 0.2, 0.4, 0.6, 0.8, 1.0; y = 0.05, 0.15 and 0.25) were prepared by the standard ceramic technique. Starting materials CuO, CoO, Fe_2O_3 and Al_2O_3 of AR grade obtained from Sigma – Aldrich, India were used. These samples were heated at ramping rate of 80 ^{0}C hr $^{-1}$ at 1000^{0}C for 48 hours. XRD and IR analysis revealed the cubic spinel structure of the synthesized samples and functional groups in the samples respectively. The absence of any extra line confirms the formation of single phase ferrite. The average particle size 'D' was determined from line broadening (311) reflection using the Debye Scherer formula discussed elsewhere [14]. Calculations of lattice constant, physical density, X-ray density, porosity, site radii and ionic bond lengths on both sites were calculated by using formulae discussed elsewhere [15] and graphically shown in fig.4. Infrared absorption spectra of powdered samples were recorded in the range 350-800 cm^{-1} using Perkin-Elmer FTIR spectrum and spectrometer by KBr pellet technique. The scanning electron microscopes are shown in fig.3

III. RESULTS AND DISCUSSION

The X-ray diffraction patterns of the samples are presented in (fig.1). Powder X-ray diffractometer of the ferrite samples reveals the single phase spinel structure, as well defined reflection is observed without any ambiguity. The diffraction peaks are corresponding to (200), (311), (400), (422), (333/511), (440) and (533) planes. The lattice constants ‘a’ and ‘c’ for all prepared samples are calculated by using prominent (311) XRD peak. The calculated and observed values of inter planer distance (d) are found in good agreement with each other for all reflections. (shown in fig. 4)

From the calculations of lattice constants ‘a’ and ‘c’ for all the prepared ferrites it is observed that c >a and tetragonality ratio (c/a) is found in the range of 1.03 to 1.07. This result is in good agreement with previous report [16-17].In this present report tetragonality ratio for copper ferrite is 1.06. It means 70% copper resides on B site and it exhibits prorate type distortions in the crystal lattice. The previous report [18] well supports the present results reported this communication. Both Fe^{3+} and Cu^{2+} are John-Teller ion which produces prolate type distortions on (B) site and hence c >a and (c/a) = 1.06. Therefore copper ferrite exhibits tetragonal spinel structure in host crystal lattice of cobalt ferrite. In addition of copper content in tetragonality ratio is found increasing but due to addition of aluminium tetragonality ratio deceases. It means that Al^{3+} and copper suppress the tetragonal prolate type.

The crystallite sizes (t) of all the prepared samples were computed by Scherer rule utilizing the peak width at one-half intensity of the maximum intensity peak (311).

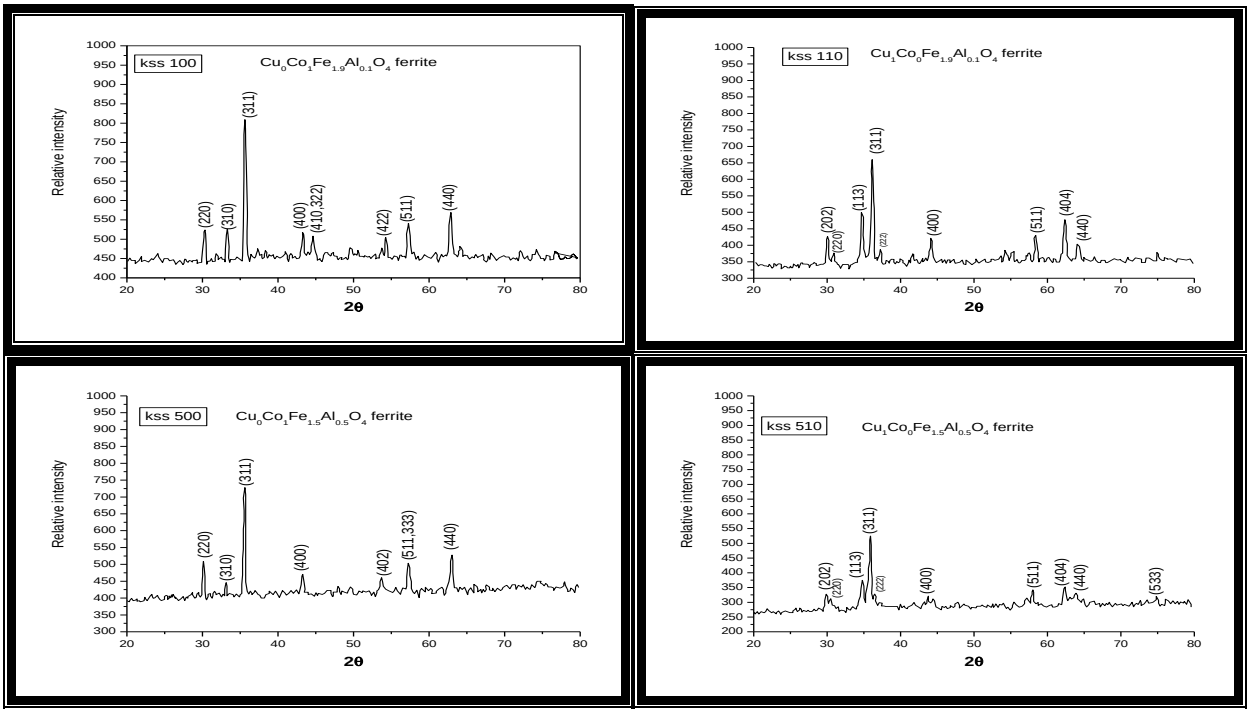

Fig: 1 XRD patterns of system $Cu_xCo_{1-x}Fe_{2-2y}Al_{2y}O_4$

The Al (y = 0.05-0.25) doped copper cobalt ferrite samples show a higher grain growth and the crystallite size (t) lies in the extent of 52.53-94.4 nm. The mean particle size calculated from diffractograms is in the range of 50 to 100 nm. That suggest the particles in the ferrites samples are fine and there is continuous grain growth in all compositions. It gives the confirmation of suitable microstructure formation in all compositions. The width of the reflection peak (311) for all the compositions is approximately the same due to the nearly equal particle size.

The infrared absorption spectra are showing two distinct absorption bands ν_1 due to tetrahedral (A) site interstitial voids near 600 cm^{-1} and other ν_2 due to octahedral (B) site interstitials voids near 400 cm^{-1}. Our results in this present communication are well supported by previous reports [19, 20].

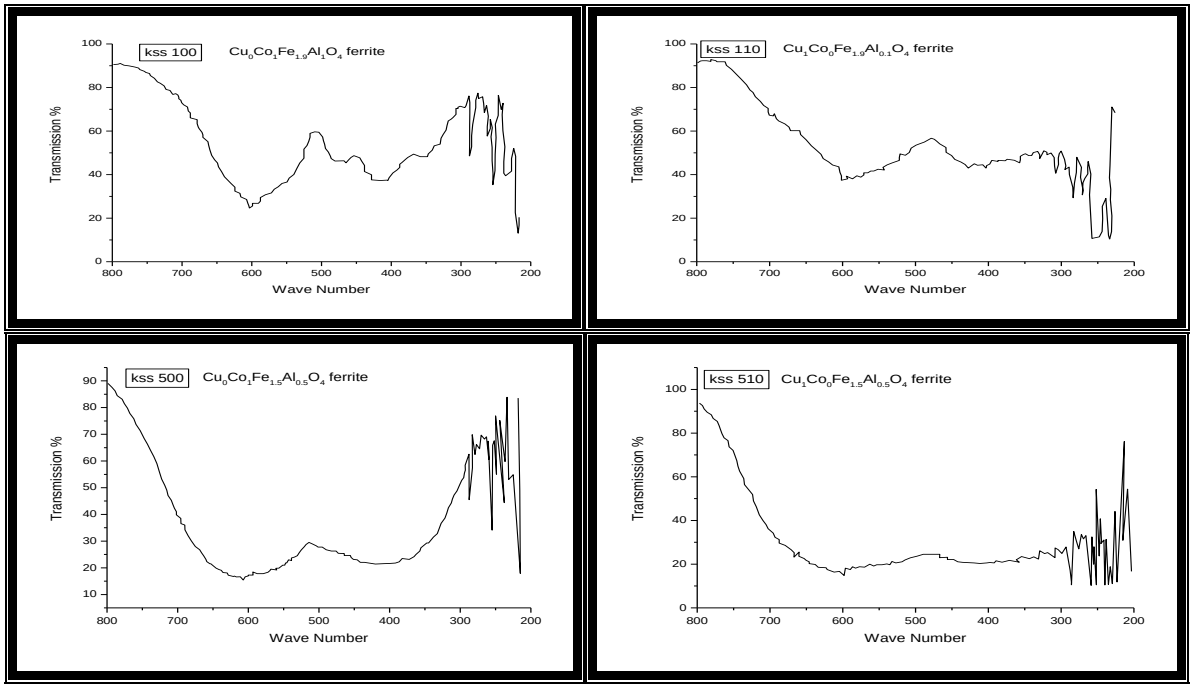

Figure 2: Absorption spectra for system $Cu_xCo_{1-x}Fe_{2-2y}Al_{2y}O_4$

The close inspection of all micrographs revealed that there is continuous grain growth with well – defined grain boundaries formed. The present system shows multi domain behavior. No exaggerated grain growth is observed in any composition. The average grain size is found to decrease with increase in Al content in copper cobalt ferrite. However in the present system the grain growth shows generally a decreasing trend with aluminum content, which is rather expected because of multi-domain behavior of these compositions in copper cobalt ferrite. Grain growth is almost accompanied with grain size, which is increasing with copper and aluminum content. So it appears that copper and aluminum content favors the grain growth. The scanning electron micrographs shown below

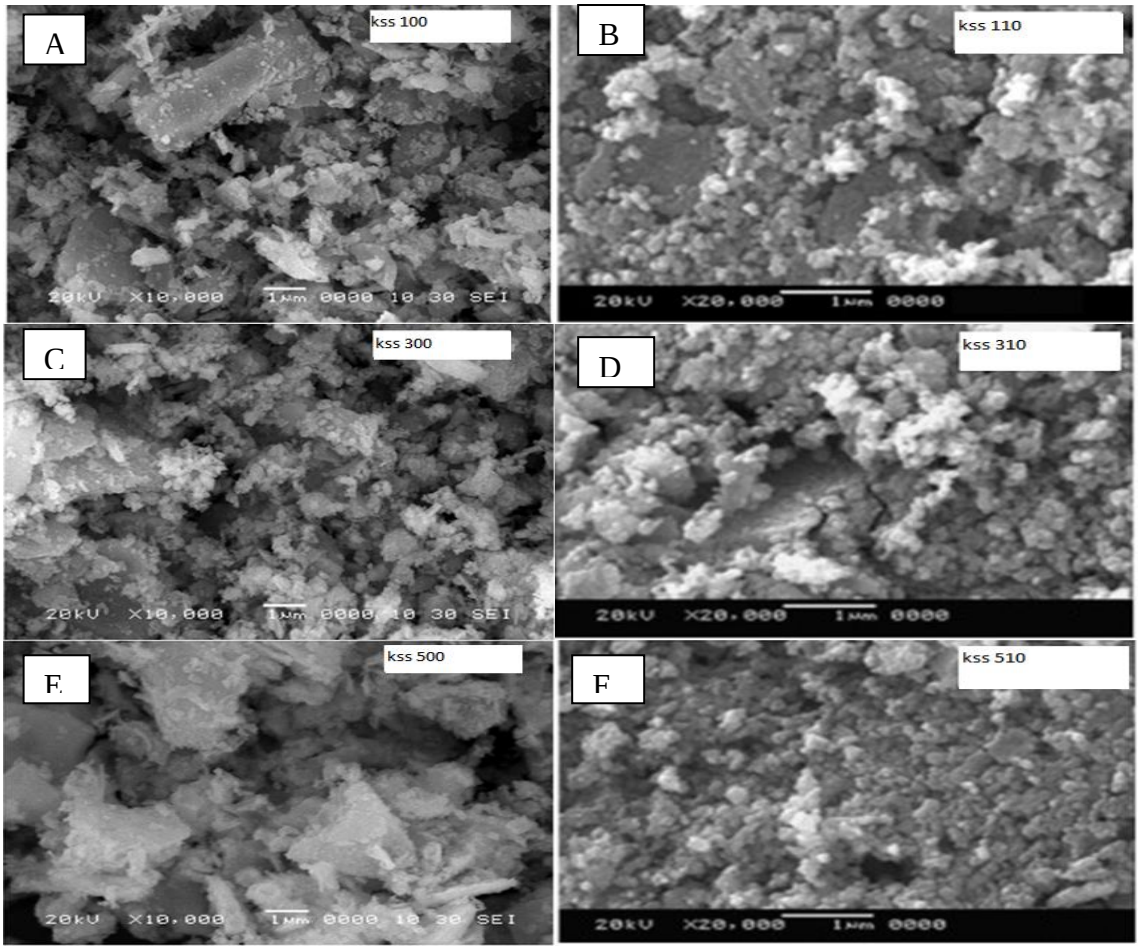

Fig: 3 (A) to (F) scanning electron microscopes of $Cu_xCo_{1-x}Fe_{2-2y}Al_{2y}O_4$:
(A) KSS 100-$Cu_0Co_1Fe_{1.9}Al_{0.1}O_4$, (B) KSS 110- $Cu_1Co_0Fe_{1.9}Al_{0.1}O_4$,
(C) KSS 300- $Cu_0Co_1Fe_{1.7}Al_{0.3}O_4$, (D) KSS 310- $Cu_1Co_0Fe_{1.7}Al_{0.3}O_4$,
(E) KSS 500- $Cu_0Co_1Fe_{1.5}Al_{0.5}O_4$ & (F) KSS 510- $Cu_1Co_0Fe_{1.5}Al_{0.5}O_4$

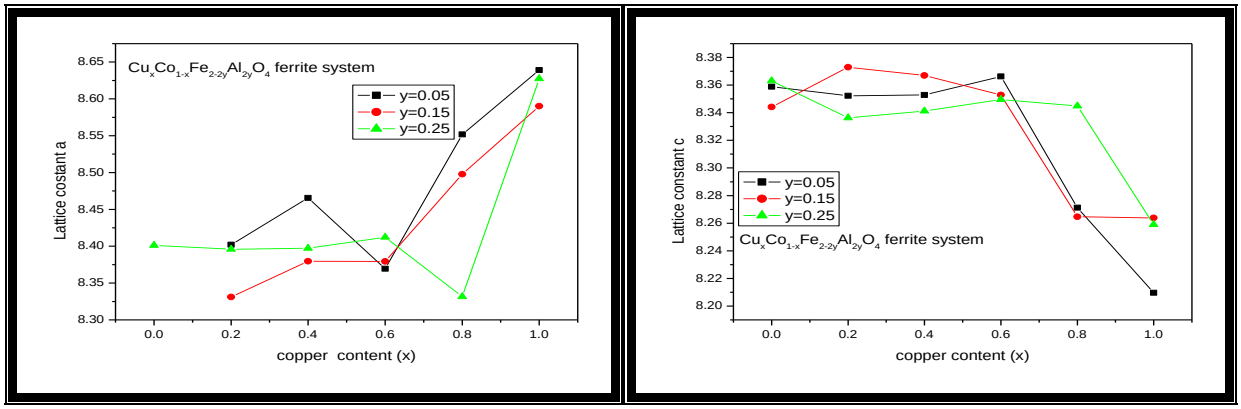

Fig:4: Variation of lattice constant a, lattice constant c, with copper content and aluminium content.

IV. CONCLUSION

Copper cobalt ferrite is partially inverse cubic spinel ferrite. Addition of Al^{3+} ions replaces Fe^{3+} on (B) site resulting in increase of lattice constant. The lattice constant obtained from XRD data shows non-linear behaviour. The infrared absorption spectra showing two distinct absorption bandν_1 due to tetrahedral (A) site interstitial voids near 600 cm^{-1} and other ν_2 due to octahedral (B)site interstitials voids near 400 cm^{-1} It can be seen from the micrographs that the average grain size decreases with increasing substitution of doping concentration of Al^{3+} in copper cobalt ferrite which decrease in porosity.

V. REFERENCES

[1]. K. Haneda and A. H. Morish, J .Appl. Phys. 63 (1988) 4285.
[2]. L. Zhavo et al ; Mat. Lett.60 (2006) 1.
[3]. N. N. Greenwood and T. C. Gibb. Mossbauer spectroscopy.((Chapman and Hall Ltd., London.(1971)261-66.
[4]. A. S. Vaingankar, S. A Patil and Sahashrabudhye, Trans. Indian. Inst. metals 34, 5 (1981) 387.
[5]. Ohbayashik and Iida S. J., Phy. Soc. Japan 23 (1967) 776.
[6]. E. J. Choi et.al., J.Magn.Mater.262 (2003) L118.
[7]. Y. W. Ju, J.-H.Park, H.-R.Jung, S.-J Choa and W. -J .Lee, Mater.Sci. Eng. B 147 (2008) 7.
[8]. P. C. Rajesh Varmaet.al,J. Alloys.comp.453 (2008) 29.
[9]. M. L. Khan, Z. Jhon Zhang, Appl.Phys.Lett.78 (2001) 3651.
[10]. P. M. Vasambekar, C. B. Kolekar and A.S.Vaingankar; Mat.Chem.Phys.60 (1999)282.
[11]. J. F. Hochepied, M. P.Pileni, J.Phys.87 (2000) 2472.
[12]. A. T. Raghvendra, R. G. Kulkarni and K.M. Jadhav; Chinese J. of Phys.vol.48 No.4 (2010) 512-522.
[13]. B.K. Bammannavar, G.N. Chavan, L.R. Naik, B.K. Chougule; Materials Chemistry and Physics;Vol.117 (2009) ;P.46–50
[14]. H. P. Klug, L. E. Alexander, X-ray diffraction procedure for polycrystalline and amorphousmaterials,(Willey N.Y 1997)637.
[15]. A. B. Gadkari, T. J. Shinde, P. N. Vasambekar, J. Mater Sci: Mater Electron 21 (2010) 96-103.
[16]. Sagal K., Tabellen F. Rontegenstrukturanalyse, Springer, Berlin, 1958.
[17]. Borisenko A., Toropov N. A; Z. Prikl Chem, 1950, 23, 1165.
[18]. Goodenough J.B and Loeb A. L ,Phys. Rev., 1955, 98, 391.
[19]. Waldron R.D, Phy. Rev, 1955, 99(6), 1727.
[20]. K. V. S. Badarinath, Phys. Stat. Solidi (a) 1985, 91, 19-23.

International e-Conference on Recent Trends in Nano-Materials and Its Applications
In Association with International Journal of Scientific Research in Science and Technology
Volume 10 | Issue 9 | Print ISSN: 2395-6011 | Online ISSN: 2395-602X (www.ijsrst.com)

Consequence of Co – Precursor On Interfacial Tensions Concerning Water and Silica Coatings

Mahendra S. Kavale*, Subhash S. Karande

Physics Research Laboratory, Department of Physics, Sangameshwar College, Autonomous, Solapur – 413 004, Maharashtra, India

ABSTRACT

We made a successful attempt on the synthesis of transparent silica coatings on glass. We also studied the effect of co – precursor on solid liquid interfacial tensions in terms of contact angle hysteresis of liquids on the silica coatings. Double distilled water was used as probe liquid with liquid to vapour surface tension 0.072 N/M. We observed the harmonious nature of the wettability theories and our experimental work done. The wettability of the surface, presence of projections on the surface, non – polar groups present on the groups all these are the essential parameters in the behaviour of the surface water drop contact angle hysteresis.

Keywords: sol-gel process, contact angle hysteresis, wettability, transparent coatings.

I. INTRODUCTION

The study of contact angle is an important thermodynamic parameter in the quantification of wettability of surface. It is the common measure of the hydrophobicity of the solid surface. The literature survey [1–4] it is well recognized that the significant contact angle measurements can be used in the determinations of solid – liquid surface tensions. Many techniques [5] have been used to measure contact angle which was motivated by the thought of using the first equation obtained by Thomas Young in 1805 [6–9]. This Young's equation rules the equilibrium of the three interfacial tensions and the Young contact angle θ_Y of a liquid drop on a solid as per the equation,

$$\gamma_{LV} COS\theta_Y = \gamma_{SV} - \gamma_{SL} \quad (1)$$

Where, γ_{LV} is the liquid-vapour surface tension, γ_{SV} the solid – vapour surface tension, γ_{SL} the solid – liquid surface tension, and θ_Y is the Young contact angle. Young assumes that the solid surface is smooth, homogeneous and rigid; it should also be chemically and physically inert with respect to the liquids to be employed.

Basically, all solid surfaces exhibit contact angle hysteresis and because of this hysteresis, the contact angle interpretation in terms of the equation (1) is continuous. All the experimentally calculated or observed contact angles are trustworthy and proper. These extensive studies have directed contact angle hysteresis to

surface roughness [10–15] and surface heterogeneity, as well as metastable energy states [16–18]. Some observed that hysteresis decreases with increase in molecular volume of the liquid on monolayers [19–20]. Also from the literature, contact angle hysteresis was found to be related to molecular mobility and packing of the surface, liquid penetration and surface swelling [21–22]. Studies have been shown that the contact angle hysteresis strongly depends on the liquid molecular size and solid/liquid contact time [23–24]. These extensive conclusions lead to the belief that liquid sorption and liquid retention are causes of contact angle hysteresis. Hence, the current research work is based on the observations of the determining the true contact angle with water droplets on the silica coatings. These coatings were prepared by two stage sol–gel process and dip coating by using different hydrophobic precursors in order to interpret the correct contact angles on silica coatings.

II. MATERIALS AND METHODS

The synthesis of silica thin coatings was done by using the chemicals methyltriethoxysilane (MTES AR Grade), Iso-butyltrimethoxysilane (ISO-BTMS AR Grade) (Sigma-Aldrich Chemie, Germany), as precursor and co - precursor and ethanol (S.D. fine Chem. Ltd, Mumbai, India) as a solvent, ammonium fluoride (NH_4OH) (Thomas Baker, Mumbai, India) as catalyst. The glass substrates were cleaned by the procedure described earlier [25].

III. RESULTS AND DISCUSSION

3.1: FOURIER TRANSFORM INFRARED SPECTROSCOPY

From the FTIR spectra several characteristic deeps were confirmed in the range of 500 to 4000 cm^{-1} signifying the presence of non-polar methyl groups in the silica coatings.

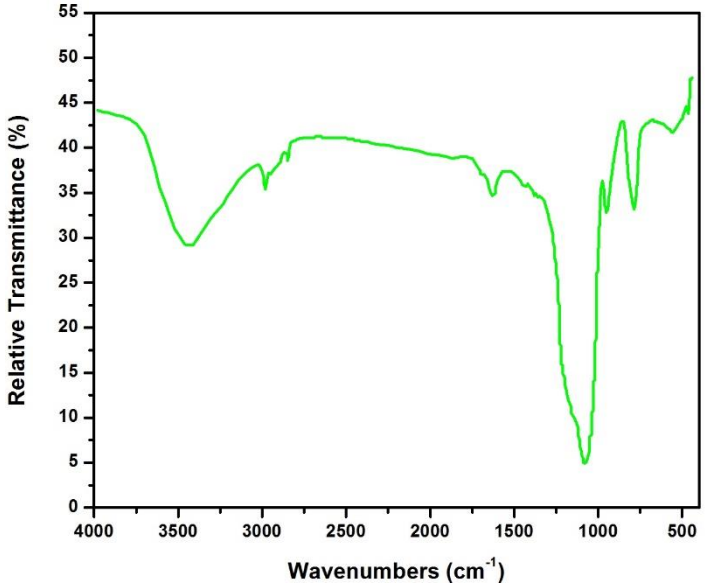

FIGURE 1: FT–IR SPECTRA OF THE SILICA COATINGS

Figure 1, is the FT–IR spectra of the silica coatings. The FT – IR spectrum signifies different functional groups of the methyltriethoxysilane (MTES) precursor. In the MTES based silica thin coatings the non-hydrolysable (–CH_3) groups are responsible for the hydrophobic property of the coatings. FTIR spectrum consists of the C–H, Si–C bonds at 2900 cm^{-1}, 1250 cm^{-1} respectively and which reveal the extent of hydrophobicity. The absorption deeps of the C–H, Si–C are also visible. The FT–IR spectra contains the deeps observed at the around 1000, 800, and 500 cm^{-1} are due to the asymmetric, symmetric and bending modes of the silicon dioxide respectively [26].

3.2: CONTACT ANGLE HYSTERESIS

The wettability of the silica coatings was quantified with the water droplet of 10 µL volume using the Rame-Hart goniometer. Surface hydrophobicity is usually determined by measuring the contact angle (CA) of water droplet on a surface to be tested. In this method the volume of the water droplet can affect the contact angle. There is usually a difference between the angles produced as the volume of the drop is increased as (the advancing angle) and that when it is decreased (the receding angle). This difference, termed as the contact-angle hysteresis, gives a measure of the surface 'stickiness'. The greater this difference (larger hysteresis) the more water drops will stick to the surface. Usually low hysteresis is desired when dealing with superhydrophobicity of the surfaces. This means water droplets will roll off extremely easily. Theoretical equilibrium angles lie between the advancing and receding angles, sometimes being determined by vibrating the drop. Figure 2 A, is the CA image of the Iso-BTMS modified MTES based silica coatings which has shown the CA as high as 147°.

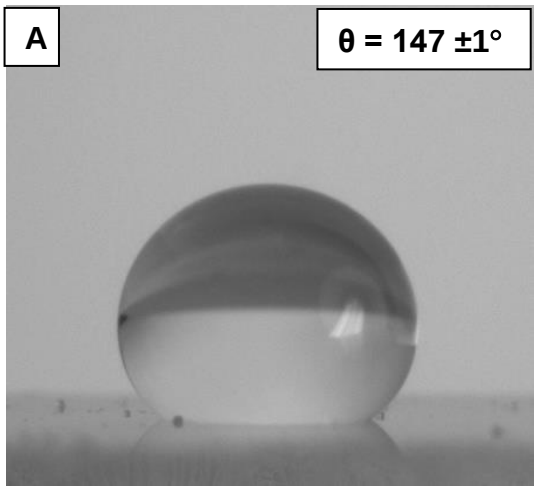

FIGURE 2 (A): CA IMAGES ON THE SILICA COATINGS

Sr. No.	silica coatings	Static Contact angle (θ = ±1°)	Advancing Angle (θ = ±1°)	Receding angle (θ = ±1°)	CA Hysteresis (θ = ±1°)
1	MTES	129	124	112	12
2	Iso-BTMS	147	146	143	3

TABLE 1: CONTACT ANGLE HYSTERESIS OF ON THE SILICA COATINGS

From the table it is clear that the CA hysteresis for the silica films is very low and which is well analogues with the literature survey.

IV. CONCLUSIONS

The contact angle hysteresis i.e. the deviation from the true contact angle between the solid and the liquid plays a significant role in quantifying the behaviour of non-wettability of the hydrophobic surfaces. The current research work has been demonstrated that the non-wettability characteristic in the silica coatings can be easily obtained from the hydrophobic precursors by using sol-gel route. If the solid surface energy is high it will attract the water molecules via van der Waals forces of attractions and it is called as the hydrophilic surfaces which gets wet easily. Generally, for the superhydrophobic surfaces the contact angle hysteresis was found to be very low and the same demonstrated here.

V. REFERENCES

[1]. W.A. Zisman. (1964) Contact angle, wettability and adhesion, in: Advances in Chemistry Series, vol. 43, American Chemical Society, Washington, DC,
[2]. D. Li, A.W. Neumann. (1992) J. Colloid Interface Sci. 148: 190.
[3]. D. Li, A.W. Neumann. (1992) Adv. Colloid Interface Sci. 39: 299.
[4]. D.Y. Kwok, A.W. Neumann. (1999) Adv. Colloid Interface Sci. 81: 167
[5]. F.M. Fowkes. (1964) Ind. Eng. Chem. 12 : 40.
[6]. O. Driedger, A.W. Neumann, P.J. Sell, Kolloid-Z. (1965) Polym. 201:52.
[7]. A.W. Neumann, R.J. Good, C.J. Hope, M.J. Sejpal. (1974) J. Colloid Interface Sci. 49 : 291
[8]. J.K. Spelt, D. Li. (1996). A.W. Neumann, J.K. Spelt (Eds., Applied Surface Thermodynamics, Marcel Dekker Inc, New York, pp. 239-292.
[9]. C.J. van Oss, M.K. Chaudhury, R.J. Good. (1988) Chem. Rev. 88 : 927
[10]. F.E. Bartell, J.W. Shepard. (1953) J. Phys. Chem. 57 : 211.
[11]. R.E. Johnson Jr., R.H. Dettre. (1964) Adv. Chem. Ser. 43 : 112.
[12]. J.D. Eick, R.J. Good, A.W. Neumann. (1975). J. Colloid Interface Sci. 53: 235.
[13]. J. F. Oliver, C. Huh, S.G. Mason. (1977). J. Adhes. 8: 223.
[14]. J. F. Oliver, C. Huh, S.G. Mason. (1980.) Colloids Surf. 1: 79.
[15]. J. F. Oliver, S.G. Mason. (1980) J. Mater. Sci. 15 : 431.
[16]. A. W. Neumann, R.J. Good. (1972) J. Colloid Interface Sci. 38 : 341.
[17]. L. W. Schwartz, S. Garoff. (1985) Langmuir 1 : 219.
[18]. A. Marmur. (1994). J. Colloid Interface Sci. 168 : 40.
[19]. C.O. Timmons, W.A. Zisman. (1966) J. Colloid Interface Sci. 22:165.
[20]. A.Y. Fadeev, T.J. McCarthy. (1999) Langmuir,15 : 7238.
[21]. R.V. Sedev, J.G. Petrov, A.W. Neumann. (1996) J. Colloid Interface Sci. 180: 36.

[22]. R.V. Sedev, C.J. Budziak, J.G. Petrov, A.W. Neumann. (1993) J. Colloid Interface Sci. 159 : 392.
[23]. C.N.C. Lam, N. Kim, D. Hui, D.Y. Kwok, M.L. Hair, A.W. Neumann (2001) Colloids and Surfaces A, 189 : 265.
[24]. C.N.C. Lam, L.H.Y. Ko, L.M.Y. Yu, A. Ng, D. Li, M.L. Hair, A.W. Neumann, (2001) J. Colloid Interface Science, 243: 208.
[25]. Mahendra S. Kavale , D.B. Mahadik, V.G. Parale, P.B.Wagh, Satish C. Gupta, A. V.Rao, Harish C. Barshilia, Applied Surface Science. (2011) 258: 158-162.
[26]. B.E. Yoldas, J. of non crystalline solids. (1984) 63: 145.
[27]. N.D. Hegde, A.V. Rao, (2007). J of Material science, 42 : 6965-6971.

International e-Conference on Recent Trends in Nano-Materials and Its Applications
In Association with International Journal of Scientific Research in Science and Technology
Volume 10 | Issue 9 | Print ISSN: 2395-6011 | Online ISSN: 2395-602X (www.ijsrst.com)

Synthesis and Characterization of Pure and Co-Doped NiO Nanoparticles Using Co-Precipitation Method

P.M. Kulal[1,2*], V.S. Chandak[1], P.S. Ghar[1], M.B. Kumbhar[1*]

[1]Thin Films and Materials Science Research Laboratory, Department of Physics, Dayanand Science College, Latur 413 512, Maharashtra, India

[2]Department of Physics, Shivaji Mahavidyalaya Renapur, Latur (M.S.), Maharashtra, India

ABSTRACT

NiO nanoparticles doped with cobalt (Co) and undoped particles were synthesized via the co-precipitation method, using nickel (II) nitrate hexahydrate ($Ni(NO_3)_2{\cdot}6H_2O$) as the precursor agent and cobalt acetate hexahydrate ($(CH_3COO)_2Co{\cdot}4H_2O$) as the doping agent. Finally, the samples were calcinated at 300°C. The synthesized samples underwent various characterization techniques, including UV-Visible spectroscopy, X-ray diffraction (XRD) and scanning electron microscopy (SEM). The XRD pattern was used to determine the crystalline size and structure of the NiO nanoparticles, while SEM was utilized to analyze the morphology and particle size. The UV-Visible absorption spectra were used to calculate the SPR absorption peak and band gap value.

Keywords: Pure NiO, Co doped NiO, XRD, SEM, UV-Visible.

I. INTRODUCTION

NiO is one of the most commonly used transition metal oxides in a variety of applications. It is a semiconductor made up of an antiferromagnetic oxide of the NaCl type. Its wide band gap makes it an ideal semiconductor with p-type conductivity sheets [1]. Due to its unique optical, electronic, magnetic, thermal, and mechanical properties, and its potential applications in catalysis, battery electrodes, gas sensors, electrochromic films, photoelectronic devices, magnetic materials, etc., NiO nanoparticles of uniform size and well-dispersed have attracted the attention of numerous researchers [2-7]. It is still essential in these applications to synthesize high quality and ultra-fine powders with the required size, shape, optical properties, and magnetic properties and so on. Synthesizing high-quality and ultra-fine powders with the required size, shape, optical and magnetic properties, and so on is still crucial in these applications. The preparation processes are directly related to particle structural properties such as particle size, distribution, and morphology. Different methods have been explored and developed for creating nanoscale crystalline oxide powders, many of which aim to reduce the cost of chemical synthesis and produce materials for technological applications. Researchers have used various techniques to produce NiO nanoparticles, including evaporation

[8-9], magnetron sputtering [10-12], sol-gel [13-14], surfactant-mediated synthesis [15], thermal decomposition [16], solvothermal [17], polymer-matrix-assisted synthesis [18], and so on.

II. EXPERIMENTAL

2.1. Materials

All chemicals used in this work were analytical grade reagents and used without further purification. nickel (II) nitrate hexahydrate Ni(NO3)2.6H2O as precursor agent and cobalt acetate hexahydrate (CH3COO)2CO.4H2O and sodium hydroxide (NaOH) were purchased were purchased from Sigma-Aldrich and ethanol and methanol (99.998%) were used as the solvents without further purification. The water utilised in this work was deionized.

2.2. Preparation of Pure and Cobalt Doped Nickel Oxide Nanoparticles

The pure NiO nanoparticles (NPs) were prepared by separately dissolving stoichiometric amounts of nickel (II) nitrate hexahydrate Ni(NO3)2.6H2O and NaOH in 100 ml distilled water. The obtained NaOH solution was added dropwise to the prepared nickel (II) nitrate hexahydrate in distilled water and then stirred continuously at room temperature for 2 h. The obtained precipitate was separated from the solution by filtration, washed several times with distilled water and ethanol then dried in air at 100 ºC to obtain NiO nanocrystals. The obtained samples were annealed at 300 ºC for 12 h. For the synthesis of the 2% and 4% Co-doped NiO samples the same procedure was used.

2.3. Characterizations

The samples were characterized by using Ultima IV, Rigaku Corporation, Japan X-ray diffractometer (XRD) with Cu Kα radiation source of wavelength 1.5406 Å, recorded at room temperature over the 2θ range of 20° to 80° to understand the crystallinity and phase orientation of the pure and Co doped NiO nanoparticles. The surface morphology, size distribution and the composition of the elements of the prepared samples were determined with scanning electron microscope (SEM JSM-IT200) using image analyser. The optical absorption/ transmission spectra of NiO and Co doped NiO nanoparticles were recorded using a JASCO V770 Model name V-770 spectrophotometer.

III. RESULTS AND DISCUSSION

3.1. Structural Analysis

As seen in Fig.1, chemically synthesized Pure NiO and cobalt-doped NiO NPs exhibit different diffraction patterns. All of the samples include cubic nickel oxide (ICDD:78-0643), which belongs to the Fm3m space group, according to the XRD results. The energy from the heat can improve the vibration and diffusion of the lattice atoms for crystallization, increasing the intensity of chemically produced NiO NPs.

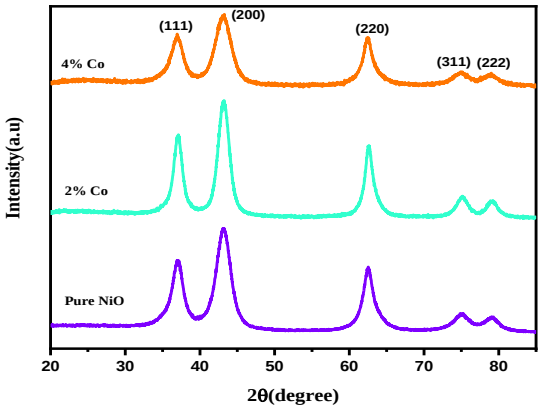

Fig.1 XRD patterns

The calcinated sample's XRD patterns showed Sharpened reflection peaks that show an increase in the size of the crystallites in NiO NPs. It is simple to identify the crystal planes of the bulk NiO at the sites of the peaks appearing at 2θ = 37.14, 43.22, 62.54, 75.16, and 78.94, respectively. A face-centered cubic (fcc) NiO phase with a lattice constant (a) of 4.176 (space group Fm3hm [225]) can be used to index all reflections [15]. The relationship can be used to obtain the cubic NiO lattice constants "a" is,

$$\frac{1}{d^2} = \left(\frac{h^2+k^2+l^2}{a}\right) \quad \text{.....} \quad (1)$$

The formula v=a^3 is used to get the unit cell volume. Table 1 displays the computed lattice constant value and unit cell volume.

The crystalline size of pure NiO and cobalt doped NiO NPs are calculated by using Debye-Scherrer's relation [16].

$$D = \frac{k\lambda}{\beta \cos\theta} \text{----------} \quad (2)$$

Where β is the full width half- maximum value of the high intensity peak, k is the shape factor and λ is the wavelength of the X – ray source used in the XRD. The obtained D values are in the range of 97.08 nm, 59.94 nm and 50.95 nm for pure NiO, 2% and 4% Co doped NiO NPs respectively. Figure.1 displays the XRD patterns of nominally composed (2% and 4%) Co substituted NiO NPs. The intensity-corresponding diffraction peaks to the plane include (111), (200), (220), (311) and (222). Moreover, it has been noted that the XRD peak broadening increases with rising Co concentrations when Co is doped up to 2%. There were no longer any cobalt metal peaks, oxides, or other contaminant phases. Using the FWHM for the (2 0 0) peak, the crystalline size and dislocation density of the NPs were estimated. Also, the dislocation density (d) was computed using the following formula to provide additional details on the quantity of faults in the films [20,21].

$$\delta = \frac{1}{D^2} \text{.....} \quad (3)$$

It is clear that the crystalline size of the samples decreases with increasing dopant concentration of cobalt. Also it is clear that the particle agglomerates due to van der wall's forces and they are responsible for ultrafine cobalt nanoparticles. The dislocation density values 1.0644 X 1014 cm-2, 1.0645 X 1014 cm-2 and 1.0647 X 1014 cm-2 increases with doping concentration. The improved crystallization is shown by lower dislocation

densities and larger crystalline size. The following relationships were used to determine micro strain in addition,[22]

$\varepsilon = \frac{\beta \cos \theta}{4}$ ..... (4)

In the case of chemically synthesized Pure NiO and 2% & 4% Co doped NiO NPs, the micro-strain increases. It is clear that the increase in strain causes an increase in the lattice constant values, a reduction in particle size, and the broadening and small shifts in the XRD peaks (refer to Table 2). The standard and measured d values, (hkl) miller indices, and diffraction angle (2θ) of the NPs were shown in Table 1 for pure NiO, 2%, 4% co doped NiO NPs. Also calculated microstructural properties such as Crystalline size (D), Dislocation density (δ) and Microstrain (ε) relation shown in fig 2. Also Crystalline size (D), Dislocation density (δ) and Microstrain (ε), Lattice Parameter (a), Volume (a3) for all the NPs were evaluated by XRD patterns and presented in table 2.

Table 1: The standard and measured d values, (hkl) miller indices, and diffraction angle (2θ) of the pure NiO, 2%, 4% co doped NiO NPs.

hkl	Standard d (A^0)	Pure NiO		2% Co: NiO		4% Co : NiO	
		2θ	d (A^0)	2θ	d (A^0)	2θ	d (A^0)
(111)	2.41	37.1	2.41	37.08	2.423	36.8	2.44
(200)	2.08	43.2	2.09	43.2	2.093	43.06	2.09
(220)	1.47	62.5	1.48	62.48	1.486	62.32	1.489
(311)	1.25	75.1	1.26	75.14	1.264	74.96	1.266
(222)	1.20	78.9	1.21	78.72	1.215	78.72	1.215

Table 2: Crystalline size (D), Dislocation density (δ), Microstrain (ε), Lattice Parameter (a), Volume (a3) values of NPs for the (2 0 0) plane.

Microstructural Properties	Pure NiO	2% Co: NiO	4%Co: NiO
Crystalline Size (D) nm	97.08	59.94	50.95
Dislocation Density (δ) X 10^14 cm-2	1.0644	1.0645	1.0647
Microstrain (ε)	3.221E-05	5.229E-05	6.148E-05
Lattice Parameter (a)	4.183152643	4.184996596	4.19795351
Volume (a3)	73.20000939	73.29685277	73.9797527

3.2. Surface morphology studies

SEM images of the pure NiO nanoparticles and those doped with 2% and 4% cobalt, taken at various magnifications, are presented in Figure 3 (a, b, c) respectively. The morphological features of all samples were nearly identical, indicating that the addition of cobalt did not affect the crystal structure, thus confirming the

incorporation of cobalt into the Ni lattice site. However, increasing the doping concentration resulted in a significant reduction in particle size and aggregation.

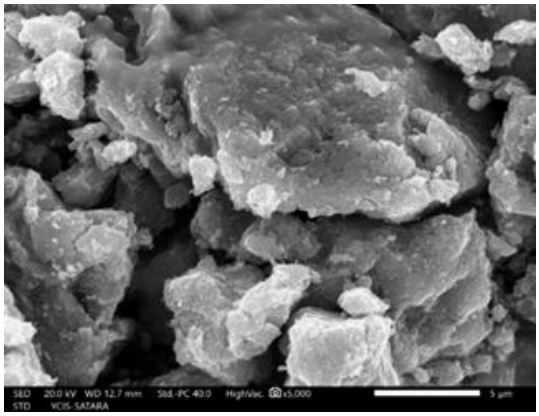

a) Pure NiO

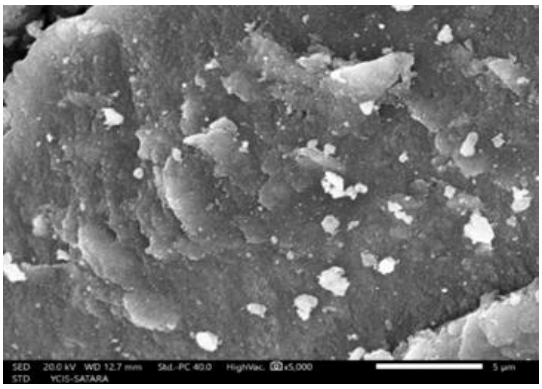

b) 2% Co- NiO

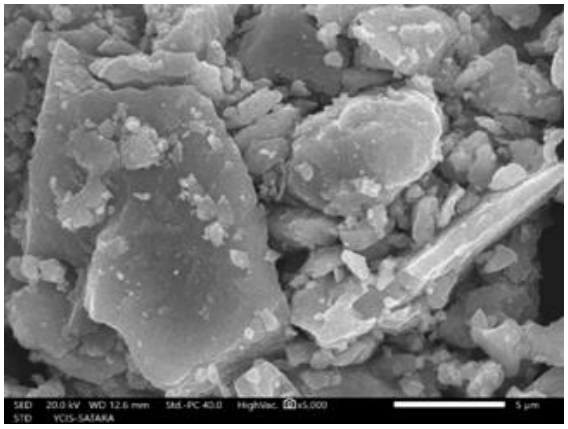

c) 4% Co- NiO

Fig.3 (a,b,c) SEM images

3.4. Optical Analysis The UV-visible absorption spectra of pure and cobalt-doped nickel oxide nanoparticles at 2% and 4% are shown in Fig. 5. The band gap and absorbance of each nanoparticle were examined in the 200–800 nm range in order to examine the impact of Co doping concentration on the optical characteristics.

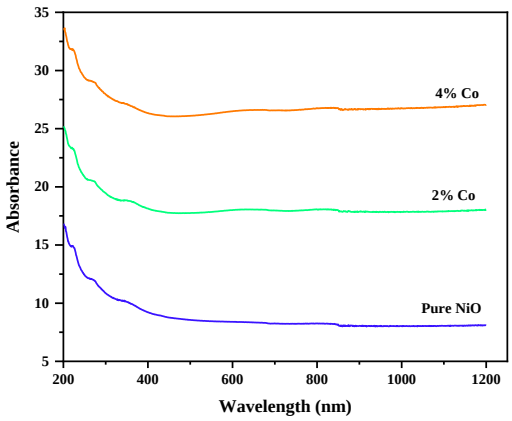

Fig. 5 UV-VIS. absorption spectra

The UV-visible absorption spectra of pure and cobalt-doped nickel oxide nanoparticles at 2% and 4% are shown in Fig. 5. The band gap and absorbance of each nanoparticle were examined in the 200–800 nm range in order to examine the impact of Co doping concentration on the optical characteristics [23]. XRD and SEM studies also supported the rise in crystallite and grain sizes. By using the Tauc relationship, the optical band gap of NiO NPs has been assessed [22]. A number of variables, including oxygen deficiency, band gap, impurity centres, particle size, lattice strain, and surface roughness, affect absorbance in general [21].

$\alpha h\nu = A (h\nu - Eg)^n$ ------- (5)

where α is absorption coefficient, and n= ½ for direct band gap semiconductor. An extrapolation of linear region of plot of hν vs (αhν)2 gives the value of band gap Eg as shown in Fig. 6

The direct band gap of pure NiO NPs was calculated to be 3.90 eV. The optical band gap of Co-doped NiO NPs decreased with the increase in Co doping. The Eg values were found to be 3.60 and 3.50 eV for samples that were doped with 2% and 4% of cobalt, respectively. It was found that the optical band gap was gradually decreased with Co doping. The decrease in the optical band gap of NiO with the increase in Co-doping may arise due to the replacement of substituted ions in the NiO lattice. Such Co ions introduce some additional energy levels in the NiO band gap near the valence band edge thereby decreasing the energy of direct transition [23]. The band gap of cobalt oxide (about Eg=1.6 eV) is smaller than that of NiO (3.05 for the present work), therefore, band gap of Co-doped NiO should be smaller than the band gap of pure NiO as suggested by the obtained results [24].

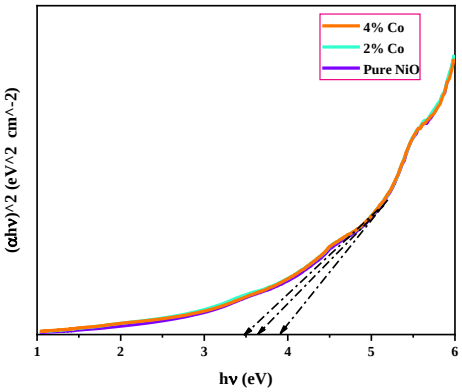

Fig. 6 Bandgap spectra

IV. CONCLUSION

The nanoparticles of Pure and Co-Doped NiO Nanoparticles have been successfully synthesized by a simple precipitation method at room temperature. XRD analysis shows the sample prepared are in a cubical phase. The broad peak of XRD pattern indicates nanocrystalline behavior of the particles. The morphological characteristics of all the samples were almost indistinguishable, suggesting that the introduction of cobalt had no impact on the crystal structure. This finding confirms that cobalt was successfully integrated into the Ni lattice site. The UV-Vis shows an increasing absorption at the edge of UV – region and decreasing in the visible region for both pure and cobalt-doped NiO nanoparticles. The estimated band gap of pure NiO nanoparticles is 3.9 eV. However, as the concentration of Co doping increases, the band gap value decreases to 3.6 eV and 3.5 eV for Co concentrations of 2% and 4%, respectively.

Conflict of interests

Authors declare that they have no conflicts of interests.

V. REFERENCES

[1]. Sato H., Minami T., Takata S. and Yamada T., Transparent conducting p-type NiO thin films prepared by magnetron sputtering, Thin solid films, 1993, 236, 27-31.

[2]. Alcantara R., Lavela P., Tirado J.L., Stoyanova R. and Zhecheva E., Recent advances in the study of layered lithium transition metal oxides and their application as intercalation electrodes, J. Solid. State. Electrochem., 1998, 3(3), 121-134.

[3]. Gabr R.M., El-Naimi A.N. and Al-Thani M.G., Preparation of nanometer NiO by the citrate gel process, Thermochim. Acta., 1992, 197, 307-318.

[4]. Miller E.L. and Rocheleau R.E., Electrochemical behaviour of reactively sputtered iron-doped NiO, J. Electrochim. Soc., 1997, 144(9), 3072-3077.

[5]. Moon Y.T., Park H.K., Kim D.K., Seog I.S. and Kim C.H., Preparation of monodispersed and spherical zirconia powders by heating of Alcohol-aqueous salt solution, J. Am. Ceram. Soc., 1995, 78(10), 2690-2694.

[6]. Wu Y., Wu B. and Wu T., Influence of the preparation method on the performance of nanostructured Zr-Ni-O catalysts, J. Chem. Mater. Sci., 2008, 95(1), 29-37.

[7]. Yoshio M, Todorov Y, Yamayo K., Nogochi H., Itoh J., Okada M. and Mouri T., Preparation of LiyNi1-xMnxO2 as a cathode for Lithium-ion battery, J. Power. Sources, 1998, 74(1), 46-53.

[8]. Wang C.B., Gau G.Y., Gau S.J., Tang C,W. and Bi J.L., Preparation and characterization of Nanosized NiO, Catal. Lett., 2005, 101,241.

[9]. The-Long L., Youn-Yuen S., Gim-Lin H., Chia-Chan L. and Chen-Bin W., Microwave-assisted nd liquid oxidation combination techniques for the preparation of NiO nanoparticles, J. Alloys. Compounds, 2008, 450, 318-322.

[10]. Wang Y. and Ke J.J., Preparation of NiO powder by decomposition of basic nickel carbonate in microwave field with NiO seed as a microwave absorbing additive, Mater. Res. Bull., 1996, 31, 55.
[11]. Wang Y.D., Ma C.L. and Li X.D., Preparation of nanocrystalline metal oxide powders with the surfactant-meditated method, Inorg. Chem. Commun., 2002, 5(10), 751-755.
[12]. Wu Y., He Y., Wu T., Chen T., Weng W. and wan H., Influence on some parameters on the synthesis of nanosized NiO material by modified sol-gel method, J. Mater. Lett., 2007, 61, 3174-3178.
[13]. Ying W., Yiming H., Tinghua W., Weizheng W. and Huilin W., Effect of synthesis method on the physical and catalytic property of nanosized NiO, J. Mater. Lett., 2007, 62, 2679-2682.
[14]. Schiffrin D.J., Capped nanoparticles as potential electronic components with nanoscale dimension, MRS. Bull., 2001, 26, 1015-1019.
[15]. Y.D. Wang, C.L. Ma, X.D. Sun, H.D. Li, Preparation of nanocrystalline metal oxide powders with the surfactant-meditated method, Inorg. Chem. Commun., 2002, 5, 751-755.
[16]. Xiang L., Deng X.Y. and Jin Y., Experimental study on synthesis of NiO nanoparticles, Scripta. Mater., 2002, 47, 219-224.
[17]. M.A. Yıldırım, A. Ates, Opt. Commun. 283 (2010) 1370–1377.
[18]. W.D. Callister, Materials Science and Engineering an Introduction, John Wiley and Sons, New York, 1997.
[19]. Spector DL, Goldman RD, Leinwand LA (1998) Culture and biochemical analysis of cells. Cell Lab Man 1:341–349
[20]. S. Agrawal, A. Parveen, A. Azam, Structural, electrical, and optomagnetic tweaking of Zn doped CoFe2–xZnxO4–δ nanoparticles, J. Magn. Magn. Mater. 414 (2016) 144–152. doi:10.1016/j.jmmm.2016.04.059.
[21]. T. Taşköprü, F. Bayansal, B. Şahin, M. Zor, Structural and optical properties of Co-doped NiO films prepared by SILAR method, Philos. Mag. 95 (2014) 32–40. doi:10.1080/14786435.2014.984788.
[22]. J. Tauc, Optical Properties of Amorphous Semiconductors, in: J. Tauc (Ed.), Amorph. Liq. Semicond. SE - 4, Springer US, 1974: pp. 159–220. doi:10.1007/978-1-4615-8705-7_4.
[23]. J. Chen, X. Wu, A. Selloni, Electronic structure and bonding properties of cobalt oxide in the spinel structure, Phys. Rev. B. 83 (2011) 245204. doi:10.1103/PhysRevB.83.245204.
[24]. B. Sahin, F. Bayansal, M. Yüksel, H.A. Çetinkara, Influence of annealing to the properties of un-doped and Co-doped CdO films, Mater. Sci. Semicond. Process. 18 (2014) 135–140. doi:10.1016/j.mssp.2013.11.014.
[25]. Y. Akaltun, M.A. Yıldırım, A. Ates, M. Yıldırım, Opt. Commun. 284 (2011) 2307–2311.
[26]. A. Ates, M.A. Yıldırım, M. Kundakçı, A. Astam, Mater. Sci. Semicond. Process. 10 (2007) 281–286.
[27]. L. Hannachi, N. Bouarissa, Physica B 404 (2009) 3650–3654.

International e-Conference on Recent Trends in Nano-Materials and Its Applications
In Association with International Journal of Scientific Research in Science and Technology
Volume 10 | Issue 9 | Print ISSN: 2395-6011 | Online ISSN: 2395-602X (www.ijsrst.com)

Tungsten Oxide Thin Film Synthesized by Electrodeposition for Electrochromic Applications

B. K. Mandlekar, A. L. Jadhav, S. L. Jadhav, A. V. Kadam*

Lab of Electrochemical Studies, The Institute of Science, Dr. Homi Bhabha State University, 15, Madam Cama Road, Fort, Mumbai- 400032, Maharashtra, India

ABSTRACT

Electrodeposited tungsten oxide (WO3) thin films have shown better performance in electrochromic applications due to the formation of finer particles on the substrate surface and improved contact between the substrate surface and film. In the present work, we have synthesized WO3 thin films on FTO at ambient conditions and checked the electrochromic performance in lithium percolate electrolyte solution. In addition, various physical properties of the films were studied. The XRD reveals the amorphous nature of the WO3 thin film materials. In the morphological structure evaluation, the crack structures of WO3 nanomaterials were observed. FTIR optical studies confirmed the W-O materials' stretching vibration nature. The 0.3M of WO3 nanomaterials exhibit a higher coloration efficiency of 192.20 mC cm-2 at 630 nm, fast switching time (coloration time = 1.29s, bleaching time = 1.22 s,). The present report suggests that the anodic electrodeposition of WO3 thin film is highly efficient for electrochromic applications.

Keywords: WO3 thin films, Electrochromic Property, Coloration Efficiency, Cracks Morphology, Nanoparticles.

I. INTRODUCTION

Some materials exhibit reversible changes in color under the influence of light, and heat. These phenomena are respectively called photochromism and thermochromism [1]. Some materials show reversible changes in color under the influence of an electric field. This phenomenon is called Electrochromism. Materials showing Electrochromism are called Electrochromic materials [2] This phenomenon occurs due to electrochemical oxidation and reduction reactions of the electrochromic material caused by an applied electrical current or potential [3]. Electrochromic materials broadly can be categorized into 1) Inorganic and 2) Organic Materials. Inorganic electrochromic materials (EC materials) are mainly oxides of transition elements [4].

In transition metal Electrochromic materials, Tungsten(W) shows a remarkable change of coloration and decoloration upon applying an Electric field. Tungsten Oxide is the most reviewed Electrochromic material due to its Electrochromic properties. Tungsten trioxide powder is found to be yellow to greenish-yellow in color. Berzelius had reported in the year 1815 that the color of tungsten trioxide changes when hydrogen was

passed over gently warmed tungsten trioxide [5]. Tungsten trioxide (WO_3) can be colored deeply by light irradiation of appropriate energy. This phenomenon is called photochromism [6]. So WO_3 is a photochromic as well Electrochromic material. In this article, we have deposited WO_3 on FTO glass by an electrodeposition method. The precursor solution used in this article is Tungstic acid. In this article concentration of the precursor solution is changed and the electrochromic behavior of the WO_3 film was studied.

II. SYNTHESIS AND CHARACTERIZATION

The AR grade Tungstic oxide H_2WO_4 powder was dissolved in double distilled water. The solution was kept for magnetic stirring with RPM near 400 for 15 minutes. While stirring, the Ammonia was then dropwise added to the Solution. The addition of the Ammonia was restricted till we get a pH equal to 12. After 15 minutes of stirring the solution was filtered with filter paper. We get a clear solution. This solution was then used for Electrodeposition. Meanwhile, FTO glass (of size 1x3 cm^2) was washed and cleaned with Acetone. The FTO glass was further cleaned by keeping it in a sonicator for 15 minutes. The electrodeposition was done by a three-electrode system. The FTO glass was used as the working electrode. Platinum was used as the counter electrode. Electrodeposition time was set for 900 seconds. The dried films were then tested for Electrochromism by taking Cyclic Voltammetry using a 608E CHI instrument. UV spectrum and XRD, SEM of the films were taken for further analysis and characterization.

III. RESULT AND DISCUSSION

X-Ray Diffraction Analysis

The X-Ray Diffraction (XRD) of WO_3 deposited on FTO was analyzed for its crystallographic studies as shown in Fig. 1. The XRD analysis of deposited WO_3 does not show any sharp or intense peak. XRD reveals that the prepared WO_3 nanomaterials are of a semi-crystalline nature. The observed WO_3 peaks are well matched with the JCPDS card 01-072-1465 at 2Θ values is 17.46, 26.43, 31.21, and 38.80, and the miller indices are (020), (111), (031), and (211) respectively [7]. The observed peaks on FTO, show the peaks (*) at 2Θ values are 33.8°, 37.59°, 51.75°, 54.64°, 61.39°, 65.2°, 78.65° [8]. The rest of the part in the graph shows the amorphous nature of the films of WO_3 on substrates of FTO.

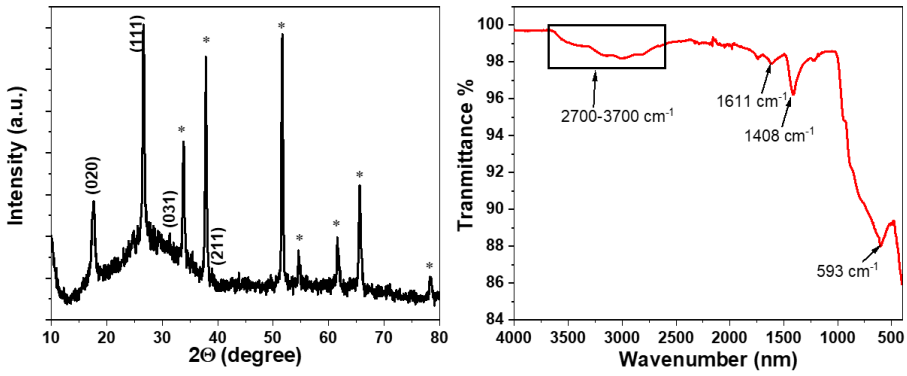

Fig. 1 (a) X- Ray Diffraction plots of WO_3 films, (b) FTIR spectra of WO_3 films.

FTIR Analysis

The FTIR spectra of the prepared WO_3 samples produced at 0.3M are carried at 4000 cm^{-1} to 400 cm^{-1} wavenumber as shown in fig. 2. The pure WO_3 samples have a sharp and intensive FTIR peak near 593 cm^{-1}, assigned to the W–O–W bridging vibration bond at the corner-sharing of the octahedron in the WO_3 crystal [9]. The broadband in the 2700–3700 cm^{-1} region and 944 indicates that the hydroxide (–OH) group is present in samples. The sharp peaks observed at around 1409 cm^{-1} indicate the presence of the NH^+ complex and water molecules in WO_3. In addition, the peak at 841 cm^{-1} was observed which corresponds to the O–O vibrational bond with W–O–W bridging bond [9].

SEM Analysis

Fig. 3 (a & b) shows the SEM morphological images of tungsten oxide (WO_3) deposited on the FTO substrates at ambient conditions. The WO_3 deposited on FTO depicts the cracked morphological structures with sizes 100-200 nm including the existence of dense interconnected granular morphological structures. The FTO indicate the uniform growth of WO_3 grains with cracks on their entire surface. The observed cracks are more suitable for the discussion of the electrolyte ion intercalation-deintercalation process which is investigated in further electrochromic studies.

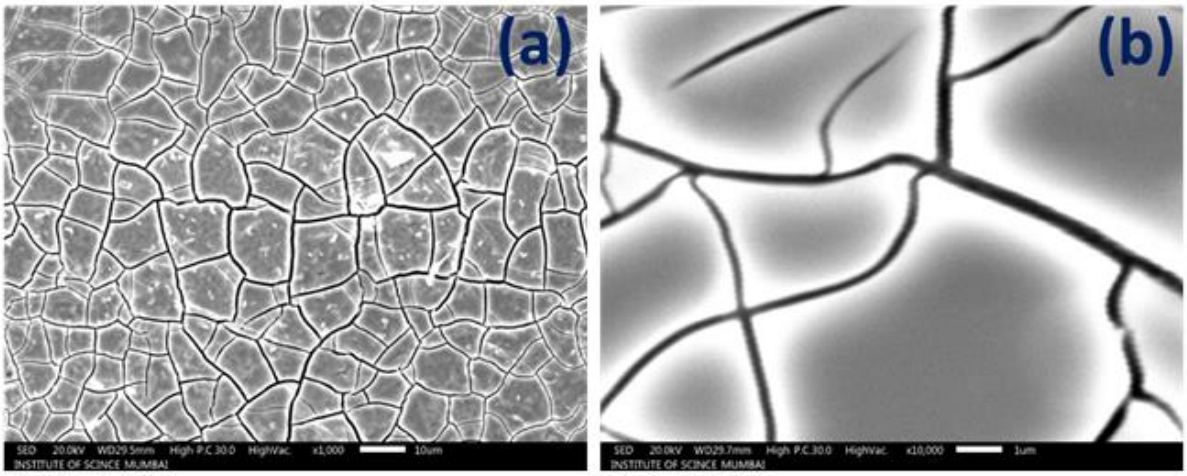

Fig. 3 SEM images of WO_3 films on FTO thin film at higher and lower magnifications.

Electrochromic Analysis

Fig. 4 (a) shows the CVs of WO_3 materials analyzed using a scan rate of 100 mVs^{-1} in 0.5M $LiClO_4$ + PC electrolyte. Fig. 4 (a) demonstrates that the current density of WO_3 deposited on FTO is a larger current density, which promotes higher diffusion. Therefore, FTO has been considered in further EC studies. Also, in WO_3 nanomaterials +0.15 V anodic bleaching starts while cathodic coloration starts at –0.36 V. This shows a slight quasi-reversible behavior of WO_3 nanomaterials Strong reversibility of WO_3 deposited on FTO indicates that the films continue to operate as effective intercalation/deintercalation hosts, indicating remarkable endurance. The redox couple is shown below in the coloration and de-coloration states [9].

$WO_3 + xLi^+ + xe^- \rightarrow Li_xWO_3$

(Bleaching state) (Blue coloring state)

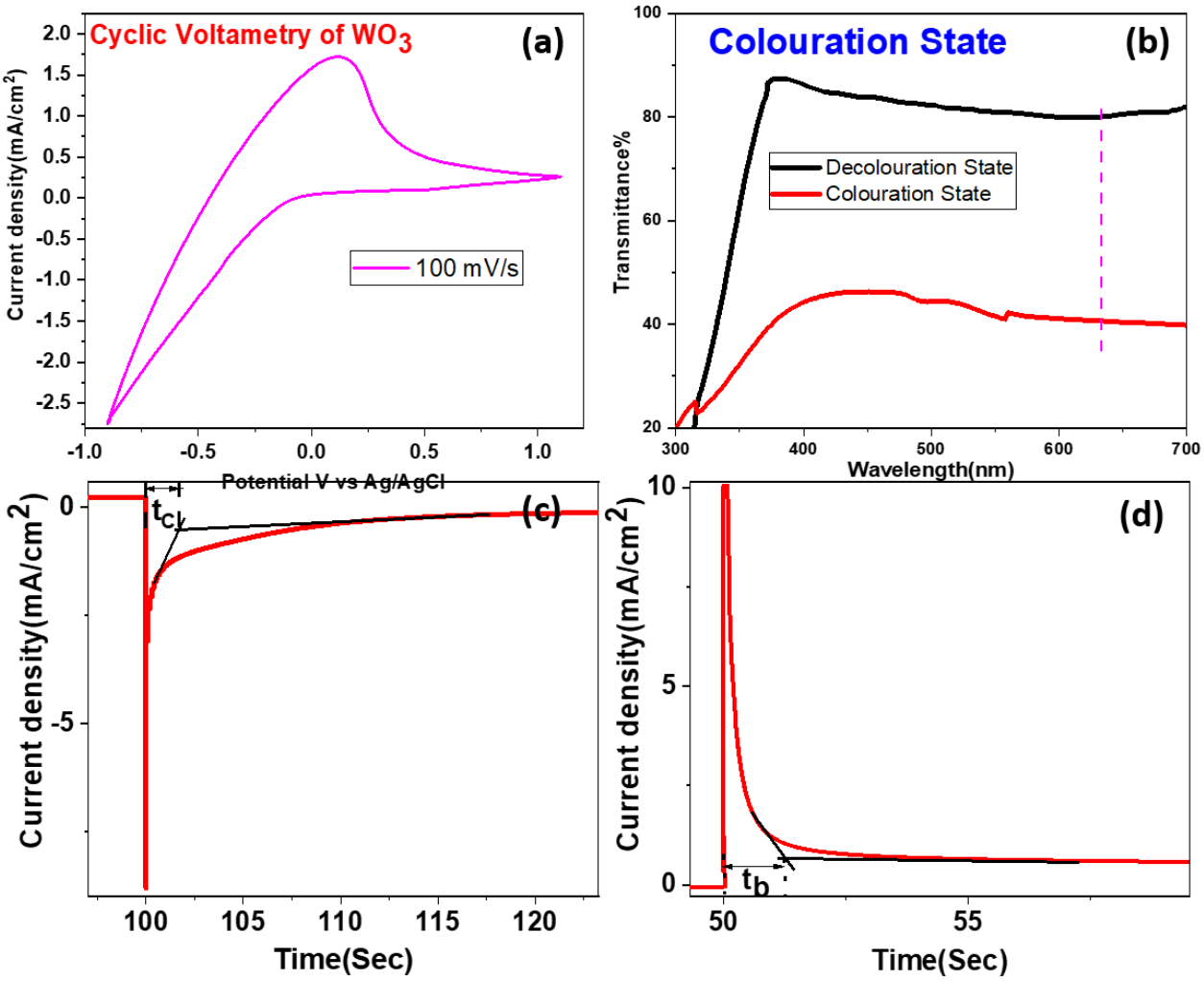

Fig. 4 (a) Cyclic Voltammetry (CV) curves (b) CE analysis coloration curve, (C) coloration state response time curve (d) Bleaching state response time curve of binder-free WO_3 films.

In figure 4(b), we observed the reversible nature of the blue to transparent color [9] and the CE was calculated using the following relations [9].

$$\text{Coloration Efficiency (CE)} = \frac{\Delta OD}{Q_i} \text{ ---------- (4)}$$

$$\text{Optical Density } (\Delta OD) = \log_{10}\left(\frac{T_b}{T_c}\right) \text{ ---------- (5)}$$

Where ΔOD is optical density, Q_i is the Coulombic charge accumulated during the coloration and de-coloration states, and T_b and T_c are the transmittances of the materials during the bleaching and coloration state. Here, the Q_i value observed during the coloration cycles is 0.0018 C, and ΔOD is 0.3444, also the coloration efficiency value for WO_3 deposited onto FTO is 193.20 cm^2C^{-1}, at 633 nm wavelength. The required response/switching time of WO_3 was measured using chronoamperometry (CA) analysis of -0.8 to 1.1V for 50 seconds (Fig. 4 (c&d)). The WO_3 electrodes exhibit the coloration states at the negative sweep potential owing to the Li^+ ions intercalated in bulk materials. Similarly, this material shows the de-coloration

state at anodic potentials due to Li^+ deintercalation. The observed response time of the WO_3 nanomaterials for coloration is 2.62 s and de-coloration is 3.0 s from the CA analysis.

IV. CONCLUSIONS

One-step WO_3 nanomaterials were successfully deposited on FTO by using electrodeposition. The analysis of XRD and FTIR confirmed that the WO_3 can be successfully deposited on various substrates. The SEM analysis shows that WO_3 is a crack morphology. The CV analysis revealed that the as-deposited WO_3 is highly reversible at a potential of -0.9V to 1.1V. The observed maximum coloration efficiency of the FTO is sss193.20 cm^2C^{-1} at 633 nm wavelength. The fastest electrochromic coloration and beaching response times of nanostructured WO_3 are 1.29 and 1.22 s. Thus, prepared one-step binder-free WO_3 nanostructured materials on FTO substrate are highly efficient for electrochromic (EC) applications.

V. REFERENCES

[1]. John R. Platt, Electrochromism, a Possible Change of Color Producible in Dyes by an Electric Field; J. Chem. Phys. 34, 862 (1961);

[2]. S.K. Deb, A novel electrophotographic system, Appl. Opt. Suppl. 3 (1969) 192–195.

[3]. D.T. Gillaspie, R.C. Tenent, A.C. Dillon, Metal oxide films for electrochromic applications: present technology and future directions, J. Mater. Chem.20(2010) 9585.

[4]. W.C. Dautremont-Smith, L.M. Schiavone, S. Hackwood, G. Ben and J.L. Shay, Electrochromic Cells with Iridium Oxide Display Electrodes, Solid State Ionics 2 (1981) 13-18.

[5]. C.G. Granqvist, Electrochromic tungsten oxide films: a review of progress, Sol. Energy Mater. Sol. Cells 60 (2000) 201–262.

[6]. R. Vijayalakshmi, M.Jayachandran, et al, Electrochromic Characterization of Electrodeposited WO3 Thin films, solid state ionics: trends in the new millennium, (2002) pp. 445-452

[7]. Rosana Balzer, Valderez Drago, Wido H. Schreiner, Luiz F. D. Probst, Synthesis and Structure-Activity Relationship of a WO3 Catalyst for the Total Oxidation of BTX, J. Braz. Chem. Soc., Vol. 25, No. 11, 2026-2031, 2014

[8]. M.M. Uplane, S.H. Mujawar, A.I. Inamdar, P.S. Shinde, A.C. Sonavane, P.S. Patil, Structural, optical and electrochromic properties of nickel oxide thin films grown from electrodeposited nickel sulphide, Applied Surface Science, 253, (2007), 9365–9371.

[9]. Bhalchandra K. Mandlekar, Amar L. Jadhav, Sharad L. Jadhav, Ayesha Khan, Anamika V. Kadam, Binder-free room-temperature synthesis of amorphous- WO3 thin film on FTO, ITO, and stainless steel by electrodeposition for electrochromic application, Optical Materials,136,2023, 113460

International e-Conference on Recent Trends in Nano-Materials and Its Applications
In Association with International Journal of Scientific Research in Science and Technology
Volume 10 | Issue 9 | Print ISSN: 2395-6011 | Online ISSN: 2395-602X (www.ijsrst.com)

Effect of Composition on Structural and Magnetic Properties of Nano-Crystalline $Mg_{0.6-x}ni_xzn_{0.4}Fe_2O_4$ Spinal Ferrite

Aparna T. Mane[1], D.P. Shinde[2], D.H. Bobade[3], T.R. Mane[4], Sohail Bagwan[5]

[1]Research Scholar, Department of Physics, JJT University, Junjunu, Rajasthan, India

[2]Department of Physics, K.B.P. College, Pandharpur, Maharashtra, India

[3]Department of Physics, C. T. Bora college, Shirur, Pune, Maharashtra, India

[4]Department of Physics, Sangola College, Sangola, Maharashtra, India

[5]Department of Physics, Abeda Inamdar Senior College, Pune, Maharashtra, India

ABSTRACT

In the present work nanoparticles of Magnesium Nickel Zink Ferrite ($Mg_{0.6-x}Ni_xZn_{0.4}Fe_2O_4$) for x = 0.3 synthesized by sol-gel auto combustion method. Prepared sample were sintered at different temperature such as 150^{0}C, 300^{0}C and 450^{0}C. Formation of single phase cubic spinel structure without addition of other peaks confirmed from XRD pattern. Infrared spectra were recorded at room temperature in which wave number ranging from 250 – 500 cm^{-1}. Surface morphology of sintered sample was studied by using SEM. The magnetic properties of prepared sample for different sintering temperature are carried out by using VSM. Chemical composition for prepared sample is confirmed by using EDAX.

I. INTRODUCTION

Now a day spinal ferrite nanocrystal has been widely investigated due to their remarkable electrical, magnetic properties and wide practical application in memory storage system, medical diagnosis, magneto-caloric refrigeration and ferrofluide technology [1]. To see the demand of high performance device, an important step is to synthesis ferrite crystals in nanoscale. At the nanoscale crystal exibit in a single domain state hence the domain wall resonance is avoided and material can work at higher frequencies [2]. Large number of techniques are used to the formation of nano-sized ferrites such as organic precursors [3], cathodic electrophoretic deposition (EDP) [4], mechanochemical synthesis [5], reverse micelle [6], electrochemical deposition [7] and utilizing egg-white [8]. More recently, cost effective sol-gel auto combustion method is used.

II. EXPERIMENTAL

Magnesium Nickel Zink nanoparticle ferrite was synthesized by sol-gel auto combustion method by using precursor such as zinc nitrate, ferric nitrate, magnesium nitrate and citric acid. All reagents are analytical

reagent (AR) grade. The stoichiometry formula used for the preparation of nanoparticles is $Mg_{0.6-x}Ni_xZn_{0.4}Fe_2O_4$ (where x = o.3). For the formation of sol all the analytical reagent grade precursors are dissolved in distilled water separately. Then transfer all the solution in 1000ml biker put it on magnetic stirrer. Start continuous stirring and simultaneously heating to the solution for 4 hour. Then sol gets converted into gel formation. After completion of half hour gel get converted into ash form. After that prepared powder was cursed by using agate mortar for the formation of nanoparticles. Lastly prepared powder was sintered at different temperature such as 150^{0}C, 300^{0}C and 450^{0}C for an hour.

III. RESULT AND DISCUSSION

Prepared sample was characterized by using X-ray diffraction (XRD), Scanning electron microscopy (SEM), Energy dispersive analyzing X-ray (EDAX), Fourier transformation infrared spectroscopy (FTIR) and Vibrating sample magnetometer (VSM) and results are discussed below.

3.1. XRD

The variation of diffraction intensity verses diffraction angle 2θ for the composition of $Mg_{0.6-x}Ni_xZn_{0.4}Fe_2O_4$ nanoparticles for x = 0.3 for different sintering temperature such as 150^{0}C, 300^{0}C and 450^{0}C is show in fig. at this temperature, the single phase spinel, $Mg_{0.6-x}Ni_xZn_{0.4}Fe_2O_4$ was formed. There is a formation of most instance pack (311) which shows Fe_2O_4 and all other miller indices (220), (400), (422), (333) and (440) matches well with the reflections of the magnesium-nickel-zinc ferrite which reported in the standard card. The 2θ position are in agreement with standard JCPDS. The value of these peak positions are used to find the value of interplaner spacing (d) among the Bragg planes. By using Scherer formula average crystalline size (D) of all powder samples was calculated and is gradually decreases as sintering temperature go on increasing. In addition of these lattices parameter (a) can be calculated by using Millar indices (hkl) and interplaner spacing (d). These values found to be increases as sintering temperature decreases.

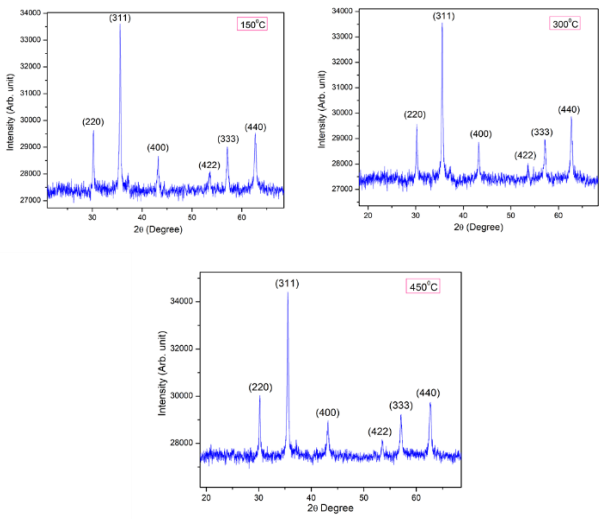

Fig. XRD of $Mg_{0.6-x}Ni_xZn_{0.4}Fe_2O_4$ for x = 0.3 at temperature 150^{0}C, 300^{0}C and 450^{0}C

Different parameters calculated from XRD:

Temperature	150⁰C	300⁰C	450⁰C
X-Ray density (gm/cc)	5.245	5.156	5.128
Lattice Constant (Å)	8.311	8.359	8.374
Ionic Bond Length (A-O) (Å)	1.799	1.803	1.81
Ionic Bond Length (A-O) (Å)	2.07	2.089	2.093
Ionic radii R_A (Å)	0.399	0.403	0.413
Ionic radii R_B (Å)	0.677	0.689	0.6936
Particle size (nm)	38	37	34

3.2. SEM

Scanning electron microscopy (SEM) of $Mg_{0.6-x}Ni_xZn_{0.4}Fe_2O_4$ nanoparticles for x = 0.3 for different sintering temperature such as 150⁰C, 300⁰C and 450⁰C is show in fig. Average grain size are calculated it is found to be 200nm – 300nm.

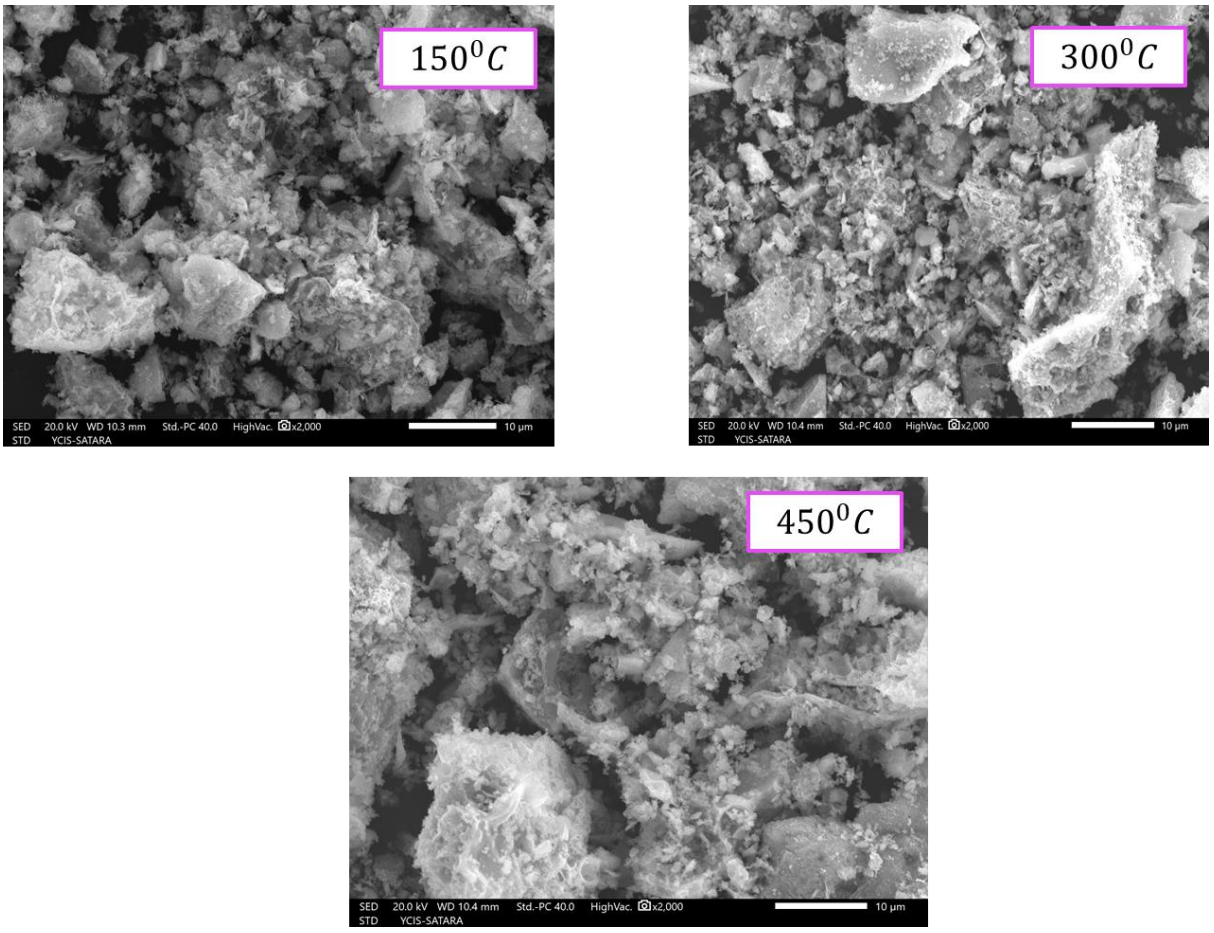

Fig. SEM of $Mg_{0.6-x}Ni_xZn_{0.4}Fe_2O_4$ for x = 0.3 at temperature 150⁰C, 300⁰C and 450⁰C

3.3. EDAX

Energy dispersive analyzing X-ray (EDAX) analysis of $Mg_{0.6-x}Ni_xZn_{0.4}Fe_2O_4$ nanoparticles for x = 0.3 for different sintering temperature such as 150⁰C, 300⁰C and 450⁰C is carried out for the conformation of element which are present in the prepared sample those which are used in precursor. The presence of elements Fe, Mg, O, Ni and Zn is clearly shown in all area of the sample.

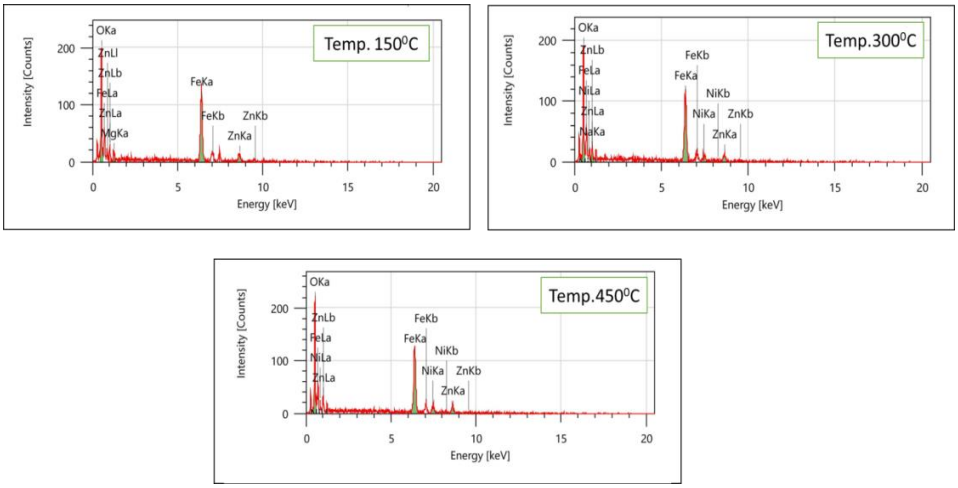

Fig. EDAX of $Mg_{0.6-x}Ni_xZn_{0.4}Fe_2O_4$ for x = 0.3 at temperature 150⁰C, 300⁰C and 450⁰C

3.4. FTIR

FTIR spectrum analysis can be used for identify information about molecular bond attachment as a residual functional group of the chemical which are used in the synthesis of the sample. The formation of $Mg_{0.6-x}Ni_xZn_{0.4}Fe_2O_4$ nanoparticles for x = 0.3 for different sintering temperature such as 150⁰C, 300⁰C and 450⁰C between 250–500 cm^{-1} is investigated by using Fourier transform infrared spectroscopy (FTIR) and results are presented in fig. from fig. high wave number ν_1 = 350 cm^{-1} and low wave number ν_2 = 300 cm^{-1} shows as the tetrahedron complex (M_{tetra}-O) and octahedral complex (M_{octa}-O). The vibrational mode for tetrahedral cluster are generally higher than the vibrational mode of octahedral cluster which is observed due to longer and shorter bond length of each cluster.

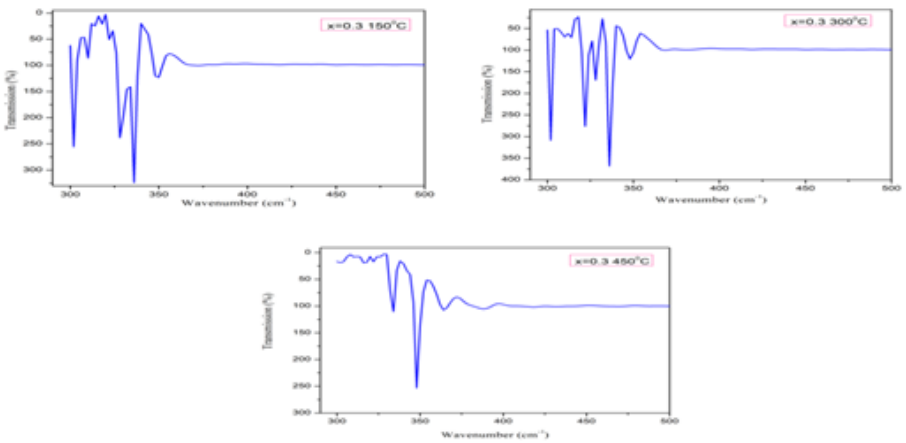

Fig. FTIR spectra of $Mg_{0.6-x}Ni_xZn_{0.4}Fe_2O_4$ for x = 0.3 at temperature 150⁰C, 300⁰C and 450⁰C

3.5. VSM:

The magnetic characteristic of $Mg_{0.6-x}Ni_xZn_{0.4}Fe_2O_4$ nanoparticles for x = 0.3 for different sintering temperature such as 150^{0}C, 300^{0}C and 450^{0}C were carried by using Vibrating Sample Magnetometer (VSM) at room temperature. VSM of the sample is shown in fig. The saturation magnetization is quite high of 32emu/gm. From graph there is a formation of loop which shows the prepared material is ferromagnetic in nature at room temperature.

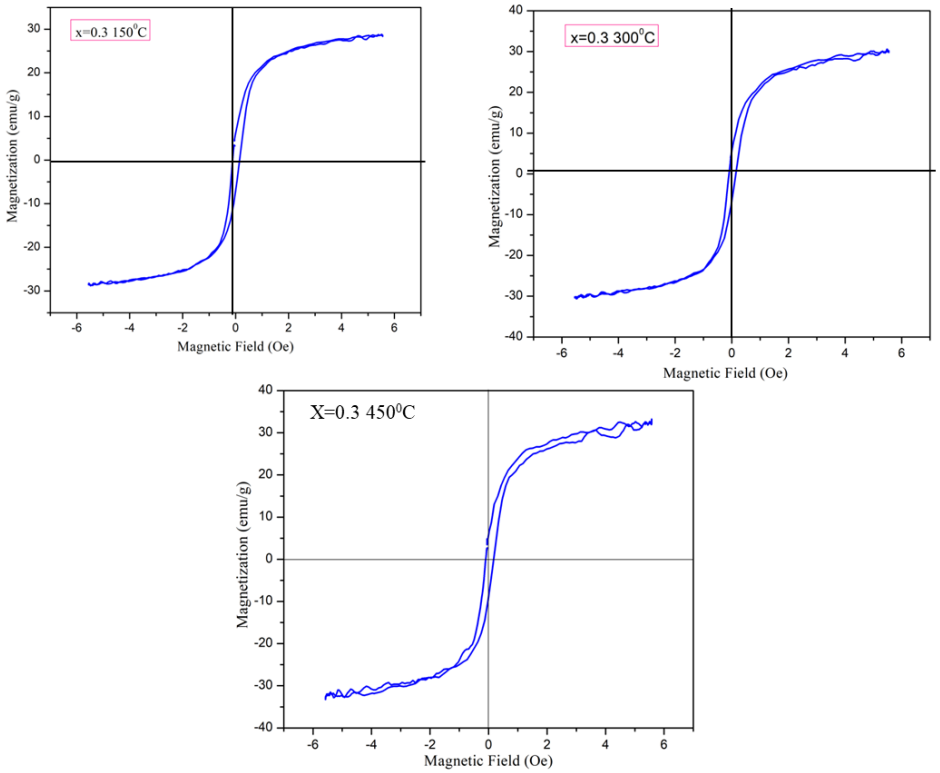

Fig. M-H Hysteresis loop of $Mg_{0.6-x}Ni_xZn_{0.4}Fe_2O_4$ for x = 0.3 at temperature 150^{0}C, 300^{0}C and 450^{0}C

IV. 4. CONCLUSION

$Mg_{0.6-x}Ni_xZn_{0.4}Fe_2O_4$ for x = 0.3 nanoparticle have been successfully synthesized by using metal nitrate and citrate sol-gel auto combustion route with enhanced magnetic properties. X-ray diffraction confirms the formation of single phase cubic spinal structure of sample. SEM analysis revealed average grain size of 200nm to 300nm. The magnetic properties of prepared sample for different sintering temperature are carried out by using VSM. FT-IR Spectra confirmed the formation of ferrite.

Acknowledgement:

Authors are grateful to thank Dr. D. H. Bobade (C.T. Bora College, Shirur, Pune) for providing X-Ray Diffraction (XRD) and Magnetic Hysteresis facility, Dr. S. H. Mujawar (Y. C. College satara) for providing SEM, EDAX Facility and Department of Chemistry, KBP College Pandharpur for providing FT-IR Facility.

V. REFERENCES

[1]. S. Kumar, V. Singh, S. Aggarwal, U. Mandal, R. Kotnala, Mater. Sci. Eng. B 166 (2010) 76
[2]. B.P. Rao, A.M. Kumar, K.H. Rao, Y.L.N. Murthy, O.F. Caltun, I. Dumitru, L. Spinu, J. Optoelectric. Adv. Mater. 8 (2006) 1703
[3]. U.R. Lima, M.C. Nasar, R.S. Nasar, M.C. Rezende, J.H. Arajo, J. Magn. Magn. Mater. 320 (2008) 1666.
[4]. C. Washburn, J. Jorne, S. Kurinec, Key Eng. Mater. 314 (2006) 127
[5]. M. Jalaly, M.H. Enayati, F. Karimazadeh, P. Kameli, Powder Technol. 193 (2009)
[6]. S. Thakar, S.C. Katyal, M. Singh, J. Magn. Magn. Mater. 321 (2009) 1
[7]. C. Washburn, J. Jorne, S. Kurinec, Key Eng. Mater. 314 (2006) 127
[8]. M.A.Gabal, W.A.Bayoumy polyhedron 29 (2010) 2569-257

International e-Conference on Recent Trends in Nano-Materials and Its Applications
In Association with International Journal of Scientific Research in Science and Technology
Volume 10 | Issue 9 | Print ISSN: 2395-6011 | Online ISSN: 2395-602X (www.ijsrst.com)

Analytical Method Development and Validation of RP-HPLC Method for The Estimation of Methocarbamol in Bulk and Formulation

Ankush Pawar*, Dr Varsha Tegeli, Vanita Choukhande, Dr.Meenakshi Menerikar, Dr.Yogesh Thorat
Department of Pharmaceutical Quality Assurance, D.S.T.S Mandal's College of Pharmacy, Solapur, Maharashtra, India

ABSTRACT

A Reverse Phase High Performance Liquid Chromatographic (RP-HPLC) method was developed and validated for the estimation of Methocarbamol which is a new antiviral drug. The RP-HPLC was succeeded on a Phenomenex Luna® LC C18 column (150×4.6mm, 5µm). The mobile phase was effective according to the polarity of studied drug. The mobile phase was consisting of Acetonitrile: Methanol: Water in the ratio of 30:50:20 v/v/v using at flow rate of 1ml/min. with injection volume of 20 µL was selected for this present work. Detection was made by using UV detector at 274nm. Retention time was found to be 1.9min. The developed method was validated according to the ICH guidelines. The calibration curve was linear for Methocarbamol in the concentration range of 10-50 µg/ml was good. The developed method was validated for Linearity, Precision, Accuracy and Robustness of Methocarbamol drug and was accurate, precise and reliable for the analysis of Methocarbamol in formulation. The Relative Standard Deviation for all the parameters were found to be less than 2 which shows the validated method and results obtained by this method is with fair agreement. Hence, this developed method can be easily effortlessly adopted for routine analysis for Methocarbamol in bulk and formulation.

Keywords: Methocarbamol, Method Development, Validation, RP-HPLC, ICH.

I. INTRODUCTION

High-Performance Liquid Chromatography (HPLC) is a technique in analytical chemistry commonly used to separate, identify, and quantify each component in a mixture. Analytical method development is the process of selecting an accurate assay procedure for the determination of composition of formulation. The analytical method must be developed using the protocol and acceptance criteria set out in International Council for Harmonization (ICH) guidelines Q2(R1). An analytical procedure is developed to test a defining characteristic of a drug substance or drug product against the predetermined acceptance criteria for that characteristic. Analytical method development and validation can be best understood as the process of showing that the analytical procedures are adequate for assessing the drugs, particularly the Active Pharmaceutical Product (API). Analytical test method validation provides a documented process,

demonstrating that the analytical procedure employed for a specific test is suitable for its intended purpose, provides evidence of method's performance and ensures quality and reliability of results[1].

The chemical name of methocarbamol is 3-(2-methoxyphenoxy) -1,2 propanediol 1-carbamate Its molecular formula $C_{11}H_{15}NO_5$and Its molecular weight is 241.41g/mol[2,3].

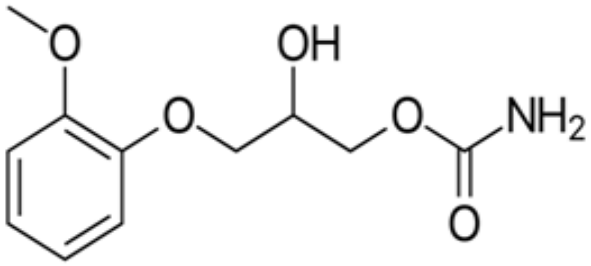

Fig.1: Structure of Methocarbamol

Methocarbamol is a muscle relaxant used to treat acute, painful musculoskeletal spasms in a variety of musculoskeletal conditions.There is, however, little published data on the drug's effectiveness and safety in treating musculoskeletal problems, particularly neck and back pain[4,5].

Methocarbamol may inhibit the effects of pyridostigmine bromide. Therefore, persons with myasthenia gravis who are using anticholinesterase drugs should utilize methocarbamol with caution[6].

Side effects: -

- Most commonly drowsiness, blurred vision, headache, nausea, and skin rash[7].
- Possible clumsiness (ataxia), upset stomach, flushing, mood changes, trouble urinating, itchiness, and fever [7, 8].
- Bothtachycardia(fast heart rate) andbradycardia(slow heart rate) have been reported[9]
- May cause respiratory depression when combined with benzodiazepines, barbiturates, codeine, or other muscle relaxants[10].

Although methocarbamol can cause jaundice, there is little evidence to support the claim that it also damages the liver.No laboratory evaluations of liver damage indicators, such as serum amino transferase (AST/ALT) levels, were performed during methocarbamol clinical trials to confirm hepatotoxicity.Although unlikely, it is impossible to rule out that methocarbamol may cause mild liver injury with use.

There is currently no known mechanism of action for methocarbamol. Instead of having a direct impact on skeletal muscles, its effect is assumed to be restricted to the central nervous system.

In the literature survey, it was found that few RP-HPLC[11]and UV-Vis Spectrophotometric methods were reported for the determination of Methocarbamol in the formulation.

The objective of this work is to establish the ideal chromatographic conditions for estimating methocarbamol in bulk and a formulation using the RP-HPLC method and to validate the results following ICH guidelines.

II. MATERIAL AND METHODS

Chemicals and reagents:

Methocarbamol was obtained as gift sample from Callidus Reserach Laboratories Pvt. Ltd Pune Maharashtra India.Acetonitrile Li Chrosolv® and Methanol Li Chrosolv® was purchased from Merck Life Science Private LTD, Mumbai.Robinax500mg tablet was purchased local market.

Instrumentation:

Younglin Acme 9000 with UV detector (UV730D), Software (Autochro-3000),Ultras onicator(Oscar Microclean 103), RC membrane 0.45µm, 25mmSyringe filters of Phenomenex and, Ultipor® N_{66}® Nylon 6,6 membrane 0.45µm, 47mm(Pall Life Sciences Pvt. Ltd, Mumbai) filters were used, electronic balance (Shimadzu AY220).

Chromatographic equipment and conditions

Chromatographic separation was achieved on a Phenomenex Luna® LC C18 Column (150 × 4.6mm, 5µm). The mobile phase used for the separation of Methocarbamol was Acetonitrile: Methanol: Water in the ratio of 30:50:20 v/v/v. Flow rate was set at a 1ml/min at ambient temperature 30°C, an injection volume of 20µL. Using UV-Visible detector (UV730D) at wavelength of 274nm. The mobile phase was ultrasonicated for degassing and filtered through 0.45µm membrane nylon filter using vacuum pump before pumping into HPLC system.

Preparation of Mobile Phase

HPLC grade Acetonitrile, Methanol and Water were used for the preparation of mobile phase in the ratio 30:50:20v/v/v. Each component of mobile phase was filtered twice using 0.45µm membrane filter and degassed for 15min by sonicating each component of mobile phase.

III. PREPARATION OF SOLUTION

Preparation of Standard stock solution

Standard stock solution of Methocarbamol was prepared by transferring 10mg in 10 ml volumetric flask by using methanol as a diluent and volume was made up to mark and sonicated for 5min. (Conc.= 1000µg/ml). 2ml standard stock solution was pipette out and transferred in to10ml of volumetric flask and volume was made up to the mark with same diluent and further added 20 ml of same diluent to get concentration 100µg/ml.

Preparation of sample solution

Twenty Robinax 500mg of uncoated tablets were weighed, crushed, finely powdered and mixed well. A portion of tablet powder equivalent to weight of 10 mg of Methocarbamol was transferred to a 10 ml of volumetric flask and volume was made up to the mark with same diluent (Methanol) and sonicated for 15 minutes to complete dissolution of drug. The solution was filtered through Whatman filter paper no.1 to remove insoluble residue. The above prepared solution was further diluted to get required concentrations then analyzed the by proposed procedures.

Analytical Method Development [19]

The proposed RP-HPLC method of analysis was validated following ICH Q2 (R1) guidelines by studying the parameters like system linearity, accuracy, assay, precision, suitability, specificity, LOD, LOQ and robustness.

IV. RESULTS AND DISCUSSION

Method Development The proposed RP-HPLC method was developed and optimized for a series of trials in a terms of mobile phase selection, composition, wavelength, choice of stationary phase of column, flow rate and column temperature. Methocarbamol showed the absorbance maxima at 274nm. Hence, the wavelength was selected as a working wavelength for the proposed RP-HPLC method.

Linearity and Range

The calibration curve was constructed between concentrations versus peak area by preparing in the concentration range of 10-50µg/ml. The regression equation was found to be Y=11.38x+48 and correlation coefficient of Methocarbamol was noted at 0.997 (Fig. 2). Overlay of chromatograms of concentration 10-50µg/ml of Methocarbamol is shown in Fig.3. The ranged from 10-50µg/ml.

Table 1: Results of linearity

Sr. No.	Concentration(µg/mL)	Peak Area
1	10	169
2	20	275
3	30	379
4	40	497
5	50	627

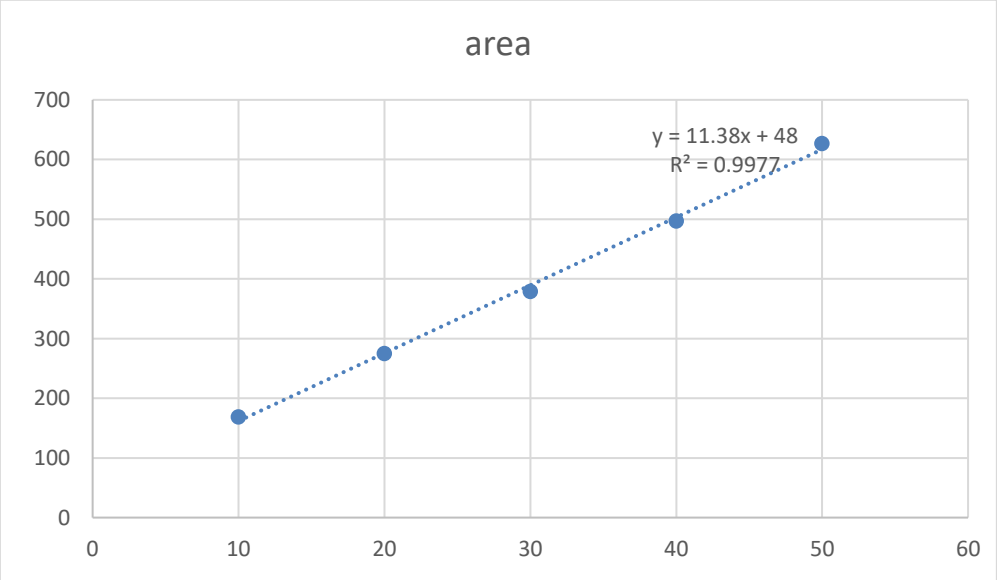

Fig. 2: Calibration curve of Methocarbamol

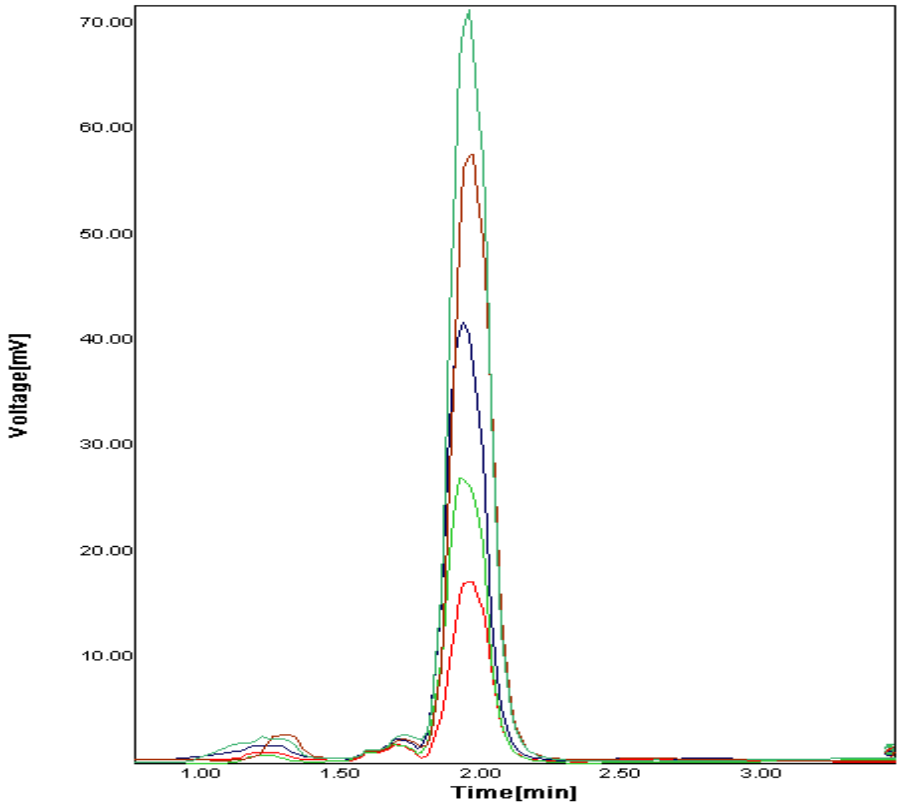

Fig. 3: Overlay of chromatograms of concentration 10-50µg/ml of Methocarbamol

Accuracy

The accuracy of the method was validated by analyzing three quality control samples of Methocarbamol representing three concentration levels covering the specified linearity range and then calculating the percentage recovery. It was obtained from 98.8-100% for the method which confirms the accuracy of developed method (Table 2).

Table 2: Accuracy result of Methocarbamol

Sr. no.	Recovery level in %	Concentration (µg/mL)	Amount recovered (µg/mL)	% Recovery
1	80	16	15.90	99.37
2	100	20	19.6	98
3	120	24	23.9	99.5

Assay

The proposed method was successfully adopted for the determination of Methocarbamol in Robinax 500mg uncoated tablet. Percentage recovery of Methocarbamol was found to be 101.4% (Table 3). The method can be employed for routine analysis of estimation of Methocarbamol in the formulation.

Table 3: Assay result of Methocarbamol formulation

Tablet form	Amount taken	Amount found	% Content
Robinax 500mg	20µg/mL	20.29µg/mL	101.4

Precision

The % RSD values for intra-day and inter-day precisions were found to be < 2% for the proposed method which confirms the good precision of the method (table 4).

Table 4: Intraday and Interday Precision results of Methocarbamol

Injection	Peak Area		
	Repeatability	Intermediate precision	
		Day-1	Day-2
1	395	395	412
2	402	384	408
3	410	389	425
4	408	395	412
5	412	402	415
6	395	386	408
SD	7.50	6.73	6.31
%RSD	1.85	1.71	1.52

System suitability and Specificity

All the system suitability parameters such as retention time, tailing factor and theoretical plates were studied from standard chromatogram and to evaluate system suitability are given in Table 5. The analytical parameter of specificity study is to determine whether the effect of excipients and other additives that are usually present in the pharmaceutical formulations of Methocarbamol are interfering with the peaks of the analytes or not in optimum chromatographic conditions. The specificity of the study was determined by comparing test results of standard solution and sample solution. Chromatograms were observed and compared for interference of excipients (Fig.4)

Table 5: System suitability results of Methocarbamol

Sr. No.	Parameters	Observed Value
1.	Retention Time	1.9
2.	Theoretical Plates	2127
3.	Tailing Factor	1.13
4.	Resolution	2.9

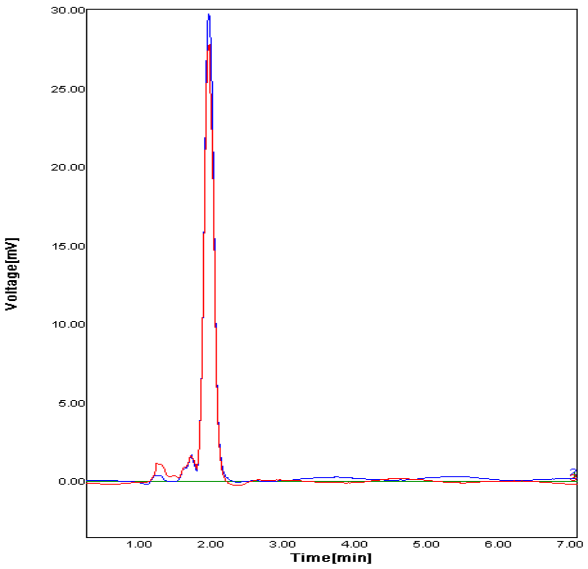

Fig. 4: Overlay of 20µg/ml standard solution chromatogram (Red), 30µg/ml of sample solution chromatogram (Blue) and blank (Green)

Limit of Detection & Limit of Quantification

The developed method was highly sensitive with LOD of 6.79µg/ml and LOQ of 20.39µg/ml.

Robustness

The robustness of the developed method was accessed by small changes in method parameters such as flow rate (±0.1ml/min), mobile phase composition (±1%) and detection wavelength (±1nm). The %RSD of robustness was found to be less than 2% of the proposed method (Table 6).

Table 6: Robustness result of Methocarbamol

Parameters	**Area**
Wavelength of UV detector	
273	395
274	390
275	394
Mean ± SD	393± 2.64
% RSD	0.673
Flow Rate	
0.9 mL/min	389
1 mL/min	394
1.1 mL/min	382
Mean ± SD	388.6± 5.5
% RSD	1.41

Table 7: Summary of Methocarbamol

Sr. No.	Parameters	Methocarbamol
1.	Linearity range (µg/ml)	10-50µg
2.	Regression equation	Y=11.38X+48
3.	Slope	11.38
4.	Intercept	48
5.	Regression Coefficient	0.997
6.	% Recovery (Accuracy)	98
7.	LOD (µg/ml)	6.78
8.	LOQ (µg/ml)	20.38

V. CONCLUSION

A novel RP-HPLC method was developed and successfully validated as per ICH guidelines for the estimation of Methocarbamol. All the results of various parameters were found to be within the acceptance limits. Hence the proposed RP-HPLC method for the analysis of Methocarbamol in bulk and its formulation was found to be specific, precise, accurate and fast.

VI. ACKNOWLEDGEMENT

The authors are thankful to the Callidus Research Laboratories pvt.ltd. Pune, Maharashtra, India for providing gift sample of Methocarbamol. The corresponding author gratefully acknowledge to Principal to D.S.T.S. Mandal's College of Pharmacy, Solapur, Department of Pharmaceutical Quality Assurance, Assistance Professor Dr. M.S. Kalshetti and guide Assistance Professor Dr. V.S Tegeli for their constant caring support and guidance.

VII. REFERENCES

[1]. Chauhan A, Mittu B, Chauhan P. Analytical method development and validation: a concise review. J. Anal. Bioanal. Tech. 2015;6(1):1-5.

[2]. Nagamani, M., Ramana, H., Bhadru, B., Vasanthi, R.; Method development and validation of methocarbamol in bulk and its formulation by UV spectroscopy; International Journal of Pharmaceutical, Chemical and Biological Sciences, (2015); 5(1): 258–261.

[3]. Prabha, T., Caroline Grace, A., Nivethitha, B., Jagadeeshwaran, M.,Sivakumar, T.; Method development, validation and degradation studies of methocarbamol from methocarbamol injection; International Journal of Pharmaceutical Sciences Review and Research, (2018); 50(1):169–174.

[4]. "Methocarbamol Monograph for Professionals". Drugs.com. American Society of Health System Pharmacists.

[5]. "Robaxin- methocarbamol injection". DailyMed. 10 December 2018.
[6]. Methocarbamol.Liver Tox: Clinical and Research Information on Drug-Induced Liver Injury. National Institute of Diabetes and Digestive and Kidney Diseases. 30 January 2017. PMID 31643609.
[7]. Methocarbamol Side Effects: Common, Severe, Long Term". Drugs.com. Retrieved 18 April 2020.
[8]. See, Sharon; Ginzburg, Regina (1 August 2008). Choosing a skeletal muscle relaxant.American Family Physician.78(3): 365–70.ISSN 0002-838X. PMID 18711953.
[9]. Teja LR. Ravi, Rao C.M. Pradada, Dhachinamoorthi D. Analytical Method Development and Validation of Methocarbamol and its Impurities in API, Dosage Form by using RPHPLC. Eur. J. Biomedical Pharm Sci. 2018;5(1):698-708.
[10]. Meher, C., Vani, M.; Simple UV spectrometric method for estimation of methocarbamol in bulk and its formulation; International Research Journal of Pharmacy, (2013); 4(8): 231–233.

International e-Conference on Recent Trends in Nano-Materials and Its Applications
In Association with International Journal of Scientific Research in Science and Technology
Volume 10 | Issue 9 | Print ISSN: 2395-6011 | Online ISSN: 2395-602X (www.ijsrst.com)

Smoking Status in Young Generation : A Review of Available Reports

Aniket Ganesh Sapkal[1], Utkarsha Shivsharan[2]
[1]B-pharm Final Year Student, D S.T.S. Mandal's College of Pharmacy, Solapur, Maharashtra, India
[2]Associate Professor, D.S.T.S. Mandal's College of Pharmacy, Solapur

ABSTRACT

India is the world's fastest growing large economy, is Home to over 11% of the world's cigarette smokers but also has significantly larger proportion of population including in smoking tobacco in its alternative forms (e.g. bidis, hookah, chilam, shisha, and water pipes). In Maharashtra around 35% of men, 17% of women and 26.6% of adults either smoke tobacco or use smokeless tobacco. This increasing number of smoking habits in adults is a sign of danger for the government, because even after performing numbers of awareness programs by the Maharashtra State Government the numbers are rising. This study aimed to develop a questionnaire to assess smoking habits, attitudes, knowledge, and needs among the young generation. A questionnaire was developed starting from literature review and existing questionnaires which includes a total of 30 questions. Around 300 participants participated in the survey, out of which 39 females smoke cigarettes and 141 male smokes regularly, occasionally or only under the stressful condition patterns. This questionnaire will be used in a survey among students from College and universities to assess addiction habits among students and to spread more awareness about hazardous effects of smoking on health as a regular smoker or passive smoker.
Keywords: Smoking, Tobacco, Student's, Cigarettes, Health care etc.

I. INTRODUCTION

to Health is the most important factor of life [1]. Smoking is the leading cause of death worldwide [2]. Tobacco use among youth is increasing day by day and it's estimated that most of the tobacco users start using tobacco products before the age of 18 years [3, 4]. Tobacco smoking is the biggest preventable cause of non-communicable disease affecting both users and bystanders [5, 6]. The WHO states that there are more than 1.1 billion smokers globally and predicts 1 billion premature smoking related deaths during the twenty first century [7]. Globally out of every 10 girls 1 girl and out of every 5 boy's 1 boy use tobacco as smoking or in any other form [8, 9]. Smoking during adolescence and early adulthood has profound public health implications [10, 11]. Smoking has been consistently linked to heart disease, cancers, and premature mortality [12]. Smoking is a leading cause of illness and death worldwide [12]. Both active and passive smoking has dangerous effects on health, and the youth smoking habit is the leading cause of concern nowadays [13]. Smoking not only affects the smoker, but it also has detrimental effects on other people's health, especially children and women. Youth smoking is a time-bomb and needs to be curbed urgently, given its multifaceted

harmful effects. India represents a complex public health challenge [14]. Each year in India more than 1 million adults die due to smoking and smokeless tobacco use accounting for 9.5% of overall deaths [15]. According to the Global Adult Tobacco Survey, the overall prevalence of smoking tobacco use is 10.38% and smokeless tobacco use is 21.38% in India [16]. Of all adults, 28.6% currently consume tobacco either in smoke or smokeless form, including 42.4% of men and 14.25 women [17-20]. There are 267 million tobacco users in India [21, 22], making it the country with the second largest number of tobacco users in the world (behind China) [23]. Approximately 100 million people ages 15 and older currently smoke tobacco [24, 25]. Tobacco use is higher in rural areas, among those with lower socioeconomic status and lower levels of education [26]. Various forms of tobacco use are responsible for an estimated 27% of all cancers in India [27]. Tobacco causes a substantial economic burden. Total costs attributed to all disease and deaths for those above 35 years was USD 27.5 billion [28]. In 2011, India banned food products containing nicotine, however a substantial number of people continue to use such products [29-33]. Tobacco harm reduction products such as e-cigarettes and heated tobacco products face a nationwide government ban. Electronic cigarettes is the recent invention that can deliver nicotine without combustion. This can be a viable option for those who are unable to quit smoking [34, 35].

Firstly, smoking poses health risks that are often ignored by the youth who consider it a fashion statement [36]. Smoking can cause various types of cancer, including lung, bladder, pancreatic, and oral cancer. It can also lead to heart diseases, chronic obstructive pulmonary diseases, and stroke. Youth who start smoking early find it challenging to quit later, leading to long-term health effects. The addiction to nicotine makes smoking cessation an uphill task, leading to premature death. Smoking has social and psychological effects that impact youth's mental health and self-esteem. Smoking seems like an act of independence and rebellion by the youth, but it has negative social effects on their lives.

Smokers are often shunned from social events, and being ostracized by peers can lead to depression and low self-esteem. Moreover, addiction to nicotine can lead to irritability, anxiety disorder, and mood swings, further increasing stress levels and hampering the mental well-being of youth. Smoking has financial repercussions, leading to reduced social mobility, and ultimately leaving the youth dependent on others. The habit is expensive, and a smoker who spends around 22 rupees daily can quickly accumulate into thousands of rupees every year [37], leading to a strain on his financial capability. Moreover, smoking can lead to decreased productivity and physical and mental sickness, forcing youth to take time off work or limit their work opportunities, leading to a less-empowered life. 3 Passive smoking has serious side effects, particularly for non-smoking children and women. Young people, who passively inhale smoke, risk developing fatal diseases like lung and heart diseases, cancer, and respiratory problems, impeding their physical and mental growth. Pregnant women who come in contact with secondhand smoke may pass on serious health risks to their unborn child, leading to premature death or disability [38].

II. METHODOLOGY

A cross-sectional descriptive survey was conducted among university students to investigate the perception, level of knowledge, smoking trends, and its association with various diseases. The objectives of this study were explained to the respondents before taking their consent. To acquire the trust of participants, information about their national identity card, residents, name, and the mobile number was avoided. A Google form was created under the guidance of a project guide containing 30 questions and circulated in whatsapp groups and individual contacts of students, and asked them to fill the form while helping them with their queries.

III. RESULTS

About 400 participants were approached, 301 questionnaires were found complete which complies with the criteria of further analysis. The targeted audience age was in the range of 15-35 years old. 200(66.4%) of the respondents were male and 101(33.6%) were female. About 283(94.33%) of the respondents were students of graduation, diploma or 12th boards etc. 69(22.9%) students were regular smokers while 70(23.3%) smoked occasionally and 42(14%) students preferred smoking only in stress-full conditions or when they were under any stress. 120(39.9%) of the targeted population claimed to be non-smokers(Fig.1). After smoking 115(38.2%) population use clove cigarettes or bidis as another addiction, 44 chews tobacco, 78(25.9% population uses Nicotine replacement products, 112(40.5%) uses E-cigarettes and 21 supari while 27 people use cigar and 21 people uses tobacco pipes. For 155 people it is very easy to get tobacco products but 77 got it somewhat easy and it is not easy at all for 69 persons (Fig.2)

The prevalence of smoking among different age groups was 7.3% in 14-17 years old, 30.9% in 18-21 years, and 15.3% in 22 years old or older and 37(12.3%) of the population never became a regular smoker. Further details are given in table-1. The 135(44.9%) population thinks that smoking is cool out of which 103 are males and 32 are females. But 126 (68 Male/58 Female) think that smoking cigarettes isn't a cool thing (Fig.3). 6 students have tried smoking before the age of 8-9 years old, while the maximum number of population 100 tried a single puff when they were 14-17 years old, out of which 29 are female candidates and 66 students tried it after the age of 18-22 years old or older. After the age of 14 years 28 (99.3%) of the population had tried whole cigarette, 44(14.6%) 16-17 years old, 61(20.3%) 18-21 years old and 21(7%) after the age of 22 or older (Table-1).

14.3% population craved cigarettes if they didn't smoke regularly, while 23.6% people claimed that smoking relaxes them, 15.99% smoking helps them in better concentration and focus while 18.3% population feels less stressed after smoking. 60 people gets buzz after smoking and 53 enjoyed the taste (further details in Table-1). 20.3% population smokes 2-5 cigarettes in one day in which 14 are females and 47 are male students. 6 females smokes 6-10 cigarettes per day and 15 females smoke 1 or less than 1 cigarette per day. While in male population 47 smokes 2-cigarettes per day, 34(6-10 per day), 20(11-20 per day) and 9(21 or more cigarettes

per day)(Fig.6). The most common period of time for which the experimental smoking phase lasts is at least 1 year with 76 votes and at least 6 months with 46 votes.

The money expenditure on cigarettes of 64(21.3%) population is three thousand rupees while 50 people spend more than 5 thousands and 60 people spend 1 or 2 thousands. 92 persons have smoked 1 or more cigarettes per day for 30 days straight and 164 haven't. (32.3%) of the population smoke their first cigarette after 60 minutes of waking up, 34(11.3%) after 31-60 minutes, 21(7%) 6-30 minutes, and 11(3.7%) within 5 minutes. The most preferred places for smoking are friend's home, social events, and in public places (e.g. parks, shopping centers, street corners) with 87, 86 and 84 respective votes followed with at home 47, school 30, and at work 45(Fig.5). When the audience were asked about will they smoke even if they are so ill that they are in bed most of the day, 26.2 %(68 males and 11 females) population said yes and 57.1% people said no.

Talking about the cigarette habits in the younger generation, 100(32.2%) of the population thinks that about half the people of their age smoked, 56(18.6%) people think that almost every one of their age smoke and 49 people said that it's not at all common to smoke. About 52(17.3%) people said yes when they were asked about whether they had discussed the reasons why people smoke in their school, and 140(46.5%) said no. When asked about while they were growing up, did their parents/guardians smoke inside their home, 34(11.3%) said yes and 209(69.4%) said no. Most of the population don't have any brothers or sisters who lived with them smoke 53.5% and 11.3% have addicted siblings. Near about 60 person's parents smoked in their house (Table-1)

In this survey it is found that the rate of smoking amongst is increasing because almost 50% target audience confirmed the smoking habit of their friends who have been allowed smoking in their workplace or in designated smoking area. 32.9% of the population smoke cigarettes during the past 30 days almost every day, and 18.9% smoked for some days while 56 people didn't smoke. Although 67.1% of the population believe that smoking cigarettes could be harmful to their health. Some of the targeted audience are suffering from heart disease, eating disorders, manic depression etc. Hence 42.5% of the population have agreed that health issues, self-initiation including disease prevention can be the reason to quit smoking, 41.9% people are interested in quitting smoking very strongly (89 males & 37 females), 58 strongly(Fig.4), and if they decided to quit smoking completely, 41.5% population is very strongly confident that they will succeed.

IV. CONCLUSION

The average age of being a regular smoker was discovered to be 18-21 years in this study. The possible reason could be the social influence because, at this age, students are influenced more by their companions than guardians. A comparable pattern was found in a study claiming that the average age of onset of smoking is 18 years for males and 24 years for females. Several factors were found associated with smoking and may have a critical impact on smoking initiation; however, anxiety, stress, and social influence were the fundamental reasons cited by the people. A possible explanation could be that at a certain age students tend to be friends with smokers and would prefer not to be left out of the group of companions merely on the reason for not smoking cigarettes. Several youths believe that "smoking makes you cool" and that smokers have more

friends. There exist many perceptions that relate smoking with the facts that it enhances one's image, relieves boredom, and helps in easing stress-related issues. This study suggests that smoking initiation among young adults is stimulated by smoker peers, the attitude of family members, their educational performance, gender, ethnic belonging, socioeconomic status, and psychological distress. About half of the respondents do not believe to be at risk of any disease associated with smoking while the other half believe to be at risk of respiratory problems or might have suffered from respiratory problems due to cigarette smoking. That most of the students is aware of the harms of both active and passive smoking on health but proper counseling and training were required for smoking cessation and that training should be the part of the education. The administrative staff of universities and accredited bodies should work in the same direction for the implementation of separate integrated programs about smoking awareness and cessation. Health education programs should be promoted considering the baseline data of the students' own beliefs relating to their behaviors about smoking attitudes. In conclusion, the youth smoking habit is a matter of grave concern, and its effects range from physical, mental, social, and financial implications. The government and other stakeholders must implement policies and programs that educate the youth on the harmful effects of smoking and provide assistance to help people quit smoking altogether. The youth must also take responsibility for their lives and say no to smoking, as their health, future, and that of those around them are at stake. Therefore, it is essential to create awareness among the youth about the risks of smoking and reduce the prevalence of smoking habits among them.

Table: 1 Smoking behavior and exposure

Questions	Anchors	Responses
Age(years)		15-35 years
Sex	Male	200 (66.4%)
	Female	101(33.6%)
	Transgender	0
Do you use any of the following tobacco or nicotine products? Chewing tobacco or snuff, cigars, tobacco pipes, clove cigarettes or bidis, nicotine replacement products such as gum, patch, or any other tobacco products besides cigarettes?	Chewing tobacco	44(14.6%)
	Cigar	27(7%)
	Tobacco pipes	21(7%)
	Clove cigarettes	115(38.2%)
	Nicotine replacement products	78(25.9%)

Questions	Anchors	Responses
	E-cigarettes	112(40.5%)
	Mawa supari	66(21.9%)
	None	125(41.5%)
How easy would it be for you to get tobacco products if you wanted some?	Very easy	155(51.5%)
	Somewhat easy	77(25.6%)
	Not easy at all	69(22.9%)
Do you smoke?	Yes	69(22.9%)
	No	120(39.9%)
	Occasionally	70(23.3%)
	When I am under stress	42(14%)
When did you become a regular smoker?	I have never being a regular smoker	37(12.3%)
	Before age of 10	3(1%)
	10-13 years old	6(2%)
	14-17 years old	22(7.3%)
	18-21 years old	93(30.9%)
	22 years old or older	46(15.3%)
	NA	94(31.2%)
Why did you become a regular smoker?	I have never been a regular smoker	39(13%)
	I craved cigarettes if I didn't smoke regularly	433(14.3%)
		44(14.6%)

Questions	Anchors	Responses
	I was around smokers a lot of the time	41(13.6%)
	I found smoking pleasurable	60(19.9%)
	I got a “buzz” when I smoked	53(17.6%)
	I enjoyed the taste	71(23.6%)
	Smoking relaxed me	48(15.9%)
	Smoking helped me focus and concentrate better	55(18.3%)
	Smoking made me feel less stressed	30(10%)
	I smoked to fit with other people	13(4.3%)
	I liked the image of the smoker	4(1.3%)
	Smoking helped me to control my weight	8(2.7%)
	Since others in my family smoked, it was easy to see myself as a smoker too	6(2%)
	Other	96(31%)
	NA	
Do you think that smoking is cool?	Yes	135(44.9%)
	No	126(41.9%)
	Don’t know/not sure	40(13.3)

Questions	Anchors	Responses
How old where you when you tried a cigarette, even a single puff?	I have never smoked cigarette	111(36.9%)
	7years old or younger	3(1%)
	8 or 9 years old	6(2%)
	10 or 11years old	21(7%)
	12 or 13 years old	20(6.6%)
	14 or 15 years old	24(8%)
	16 or 17 years old	50(16.6%)
	18 or 21 years old	50(16.6%)
	22 year old or older	16(5.3%)
How old were you when you smoked an entire cigarette?	I have never smoked cigarette	111(36.9%)
	7 years old or younger	0
	10 or 11 years old	10(3.3%)
	12 or 13 years old	25(8.3%)
	14 or 15 years old	28(9.3%)
	16 or 17 years old	44(14.6%)
	18-21 years old	61(20.3%)
	22 years old or older	21(7%)
How long did your experimental smoking phase last? If you are a current non-smoker, please indicate the length of time you experimented with smoking before you stopped completely. If you are a current smoker, please indicate the amount of time	Less than 1 month	10(3.3%)
	At least 1 month, but less than 6 months	13(4.3%)

Questions	Anchors	Responses
you experimented with smoking before becoming a regular (daily or almost daily) smoker.	At least 6 months, but less than 12 months (1 year)	46(15.3%)
	At least 1 year, but less than 2 years	76(25.2%)
	4 years or more	19(6.3%)
	Don't know/ not sure	30(10%)
	NA	107(35.5%)
How many cigarette did you smoke in a day?	Less than 1 Cigarette per day	19(6.3%)
	1 Cigarette per day	25(8.3%)
	2-5 cigarette per day	61(20.3%)
	6-10 Cigarette per day	40(13.3%)
	11-20 Cigarette per day	23(7.6%)
	21 or more cigarette per day	9(3%)
	NA	124(41.2%)
How much do you spend per month on smoking?	1 k	30(10%)
	2 k	30(10%)
	3 k	64(21.3%)
	More than 5 k	50(16.6%)
	NA	127(42.2%)
At any time in your life, have you smoked 1 or more cigarettes per day for 30 days straight?	Yes	92(30.6%)
	No	164(54.5%)

Questions	Anchors	Responses
	NA	45(15%)
How soon after waking up, do you smoke your first Cigarette?	After 60 minutes	97(32.2%)
	31-60 minutes	34(11.3%)
	6-30 minutes	21(7%)
	Within 5 minutes	11(3.7%)
	NA	138(45.8%)
Where did you smoke usually?	At home	47(15.6)
	At school	30(10%)
	At work	45(15%)
	At friend's home	87(28.9%)
	At social events	86(28.6%)
	In public places (e.g. parks, shopping centers, street corners)	84(27.9%)
		121(40.2%)
	NA	
Do you smoke even if you are so ill that you are in bed most of the day?	Yes	79(26.2%)
	No	172(57.1%)
	NA	50(16.6%)
Is it common for people of your age to smoke cigarettes?	Not at all common	49(16.3%)
	Less than half the people my age smoked	42(14%)
		100(32.2%)
	About half the people my age	

Questions	Anchors	Responses
	smoked	56(18.6%)
	Almost everyone my age smoked	54(17.9%)
	Don't know/Not sure	
When you were in school, did you discuss the reasons why people smoke in any of your classes?	Yes	52(17.3%)
	No	140(46.5%)
	I didn't attend	63(20.9%)
	Don't know/Not sure	46(15.33%)
While you were growing up, did your parents/guardians ever ask nearby smokers to stop smoking?	Yes	106(35.2%)
	No	151(50.2%)
	Don't know/Not sure	44(14.6%)
While you were growing up, did any of your parents/guardians smoke inside your home?	Yes	53(17.6%)
	No	209(69.4%)
	Don't know/Not sure	39(13%)
. While you were growing up, did any of your brothers or sisters who lived with you smoke?	Yes	34(11.3%)
	No	161(53.5%)
	Don’t know/not sure	69(22.9%)
	I don't have any brother or sister who lived with me while I was growing up	37(12.3%)
While you were growing up, what was your oldest age when at least one of your parent/guardians smoked?	None of my parents/guardians smoked when I was growing up	171(56.8%)
	10(3.3%)	
	6 years old or less	12(4%)

Questions	Anchors	Responses
	7-10 years old	30(10%)
	11-13 years old	30(10%)
	14-21 years old	48(15.9%)
	Don't know/not sure	
Did any of your closest friends smoke cigarettes?	None	76(25.2%)
	Yes	60(19.9%)
	Most of all	138(45.8%)
	Don't know/not sure	27(9%)
23. Is smoking allowed in any of the following areas in your workplace?	In my work area	58(19.3)
	In common area (lobbies, rest rooms, lunch rooms	79(26.2%)
	In designated smoking areas	93(30.99%)
	Don't know/not sure	63(20.9%)
	Smoking was not allowed anywhere in my work place	71(23.6%)
	I was not working during my experimental smoking phase	51(16.9%)
	I don’t smoke	69(22.9%)
During the past 30 days (1 month) on how many days did you smoke cigarettes?	Every day or almost every day	99(32.9)
	Some	57(18.9%)

Questions	Anchors	Responses
	No days	56(18.6%)
	NA	89(29.6%)
Do you believe that smoking cigarettes could be harmful to your health?	Yes	202(67.1%)
	No	62(20.6%)
	Don't know/not sure	37(12.3%)
Have you ever suffered from any of the following health problems?	Heart disease	11(3.7%)
	Cancer	5(1.7%)
	Stroke	7(2.3%)
	Chronic bronchitis/ Emphysema	6(2%)
	Chronic cough	7(2.3%)
	Asthma	9(3%)
	Stomach or Duodenal ulcers	9(3%)
	Epilepsy, Seizures or Fits	10(3.3%)
	Previous Head injury	9(3%)
	Brain tumor	3(1%)
	Eating disorders	15(5%)
	Liver disease	6(2%)
	Manic-depression disease	22(7.3%)
	Kidney disease or Dysfunction	9(3%)

Questions	Anchors	Responses
	None	280(93%)
What will be the main reason if you quit smoking?	Advice of physician	28(9.3%)
	Health reasons, self-initiated including disease prevention	128(42.5%)
	Pressure from others, excluding physician	65(21.6%)
		55(18.3%)
	NA	
	Other	
How interested are you in quitting smoking?	Strongly	58(19.3%)
	Very strongly	126(41.9%)
	A little	46(15.3%)
	Not at all	11(3.7%)
	I don't smoke	60(19.3%)
If you decide to quit smoking completely, how confident are you that you will succeed?	Strongly	56(18.6%)
	Very strongly	125(41.5%)
	Some	42(14%)
	A little	10(3.3%)
	Not at all	10(3.3%)
	NA	58(19.3%)

V. REFERENCES

[1]. Reitsma, M.B.; Fullman, N.; Ng, M.; Salama, J.S.; Abajobir, A.; Abate, K.H.; Abbafati, C.; Abera, S.F.; Abraham, B.; Abyu, G.Y.; et al. Smoking prevalence and attributable disease burden in 195 countries and territories, 1990–2015: A systematic analysis from the Global Burden of Disease Study 2015. Lancet 2017, 389, 1885–1906. [CrossRef].

[2]. Hanawi, S A , Saat, N Z M, Zulkafly, M, Hazlenah, H, Taibukahn, NH, Yoganathan, D et al. Impact of a Healthy Lifestyle on the Psychological Well-being of University Students. Int. J. Pharm. Res. Allied Sci 2020;9(2):1-7

[3]. Kiaee KG, Tabarsy B, Zare M. Effectiveness of problem solving skills and impulse control on the knowledge and attitude of students towards smoking. J. Adv. Pharm. Educ. Res| Apr-Jun. 2019;9(S2):134-138.

[4]. World Health Organization. Tobacco. 2018; Available from https://www.who.int/en/news-room/fact-sheets/detail/tobacco.

[5]. World Health Organization. Tobacco-Free Initiative (TFI). 2015 November 11; Available from https://www.who.int/tobacco/about/partners/bloomberg/pak/en/.

[6]. Nichter, M., et al., Project Quit Tobacco International: laying the groundwork for tobacco cessation in low-and middle-income countries. Asia Pacific Journal of Public Health, 2010. 22(3_suppl): p. 181S-188S.

[7]. Chen+, X., et al., To text or not to text? Acceptability of WeChat and text messaging intervention to promote tobacco control assistance among parents who smoke in rural China. Tobacco Induced Diseases,2019. 17(December).

[8]. The World Bank. India. https://data.worldbank.org/country/india. Accessed August 25, 2019.

[9]. CentralIntelligence Agency. The World Factbook. https://www.cia.gov/library/publications/the-world-factbook/geos/in.html. Updated January 20, 2018. Accessed August 25, 2019.

[10]. TheWorldBank. GDP (current US$): India.https://data.worldbank.org/indicator/NY.GDP.MKTP.CD. Accessed January 24, 2020.

[11]. TheWorldBank.GDPgrowth(annual%)–India. https://data.worldbank.org/indicator/NY.GDP.MKTP.KD.ZG?locations=IN&name_desc=false. Accessed January 24, 2020.

[12]. The World Bank. The World Bank in India. https://www.worldbank.org/en/country/india/overview. Updated October 25, 2019. Accessed January 24, 2020.

[13]. United Nations Development Programme. Human Development Report 2019. http://hdr.undp.org/sites/default/files/hdr2019.pdf. Published 2019. Accessed March 11, 2020.

[14]. Oxfam International. India Extreme Inequality in Numbers. https://www.oxfam.org/en/even-it/india-extreme-inequality-numbers. Accessed August 25, 2019.

[15]. The World Bank. GINI Index (World Bank Estimate) - India. https://data.worldbank.org/indicator/SI.POV.GINI?locations=IN. Accessed August 25, 2019.

[16]. Kanbur R, Zhuang J. Urbanization and inequality in Asia. Asian Dev Rev. 2013;30(1):131-147.https://www.mitpressjournals.org/doi/pdf/10.1162/ADEV_a_00006. Accessed August 25, 2019.

[17]. Asaria M, Mazumdar S, Chowdhury S, Mazumdar P, Mukhopadhyay A, Gupta I. Socioeconomic inequality in life Expectancy in India. BMJ Glob Health. 2019;4(3):e001445. https://gh.bmj.com/content/4/3/e001445. Accessed August 25, 2019.

[18]. Indian states by GDP per capita. Statistics Times website. http://statisticstimes.com/economy/gdp-capita-of-indian-states.php. Updated September 28, 2019. Accessed October 4, 2019.

[19]. Chakravarty M. The Class Divide in Indian Education System. https://www.livemint.com/Opinion/DuRPMPSqaaqCDLoNMgRAbL/The-class-divide-in Indian education-system.html. Published January 23, 2018. Accessed August 25, 2019.

[20]. Mazumdar I. Approach Paper: Vulnerabilities of Women Home-based Workers. New Delhi, India: Centre for Women's Development Studies; 2005. https://www.academia.edu/1187411/Approach_paper_Vulnerabilities_of_women_home_based_workers. Accessed August 25, 2019.

[21]. Geetika, Singh T, Gupta A. Women working in informal sector in India: a saga of lopsided utilization of human Capital. International Proceedings of Economics Development and Research. 2011; 4:534-538.

[22]. McKinsey Global Institute. The Power of Parity: How Advancing Women's Equality Can Add Growth.https://www.mckinsey.com/~/media/McKinsey/Featured%20Insights/Employment%20and%20Growth/How%20advancing%20womens%20equality%20can%20add%2012%20trillion%20to%20global%20growth/MGI%20Power%20of%20parity_Full%20report_September%202015.ashx. Published September 2015. Accessed August 25, 2019.

[23]. TheEconomist.WhyIndianeedswomentowork.https://www.economist.com. Leaders/2018/07/05/why-India- Needs-women-to-work. July 5, 2018. Accessed January 24, 2020.

[24]. The World Bank. Rural Population: India. https://data.worldbank.org/indicator/SP.RUR.TOTL?locations=IN.https://data.worldbank.org/indicator/SP.RUR.TOTL?locations=IN. Revised 2018. Accessed August 25, 2019.

[25]. The World Bank. Urban Population: India. https://data.worldbank.org/indicator/SP.URB.TOTL?locations=IN. Revised 2018. Accessed August 25, 2019.

[26]. Sivaramakrishnan KC, Singh BN. Paper on urbanization. http://planningcommission.nic.in/reports/sereport/ser/vision2025/urban.pdf. Accessed October 4,

[27]. GATS Global Adult Tobacco Survey FACT SHEET MAHARASHTRA 2016-17

[28]. Jha P, Chaloupka FJ, eds . Curbing the Epidemic: Governments and the Economics of Tobacco Control. Washington DC: The World Bank; 1999. [Google Scholar] Warren CW, Riley L, Asma S, Eriksen MP, Green L, Blanton C, Loo C, Batchelor S, Yach D. 29.Tobacco use in youth: a surveillance report from the Global Youth Tobacco Survey Project. Vol. 78. Bulletin of World Health Organization; 2000. pp. 868–876. [PMC free article] [PubMed] [Google Scholar]

[29]. Krishnamurthy S, Ramaswamy R, Trivedi U, Zachariah V. Tobacco use in rural Indian children. Indian Pediatrics. 1997;34:923–927. [PubMed] [Google Scholar]
[30]. Venkatraman S, Mukhopadhyay A, Muliyil J. Trends of smoking in medical students. Indian Journal of Medical Research. 1996;104:316–320. [PubMed] [Google Scholar]
[31]. Vaidya SG, Naik UD, Vaidya JS. Effect of sports sponsorship by tobacco companies on children's experimentation with tobacco. British Medical Journal. 1996;313(7054):375. [PMC free article] [PubMed] [Google Scholar]
[32]. George A, Varghese C, Sankaranarayanan R, Nair MK. Use of tobacco and alcoholic beverages by children and teenagers in a low income coastal community in south India. Journal of Cancer Research. 1994;9:111–113. [PubMed] [Google Scholar]
[33]. Jayant K, Notani PN, Gulati SS, Gadre VV. Tobacco use in school children in Bombay, India. A study of knowledge, attitude and practice. Indian Journal of Cancer. 1991;28:139–147. [PubMed] [Google Scholar]
[34]. Gavarasana S, Doddi VP, Prasad GV, Allam A, Murthy BS. A smoking survey of college students in India: Implications for designing an antismoking policy. Japanese Journal of Cancer Research. 1991;82:142–145. [PMC free article] [PubMed] [Google Scholar]
[35]. Gavarasana S, Gorty PV, Allam A. Illiteracy, ignorance and willingness to quit smoking among villagers in India. Japanese Journal of Cancer Research. 1992;83:340–343. [PMC free article] [PubMed] [Google Scholar]
[36]. Singh SK, Narang RK, Chandra S, Chaturvedi PK, Dubey AL. Smoking habits of the medical students. Indian Journal of Chest Diseases and Allied Sciences. 1989; 31:73–75. [PubMed] [Google Scholar]
[37]. Singhi S, Broca JS, Mathur GM. Smoking behavior of rural schoolboys. Indian Pediatrics. 1987;24:655–659. [PubMed] [Google Scholar].

Graphical Representation:

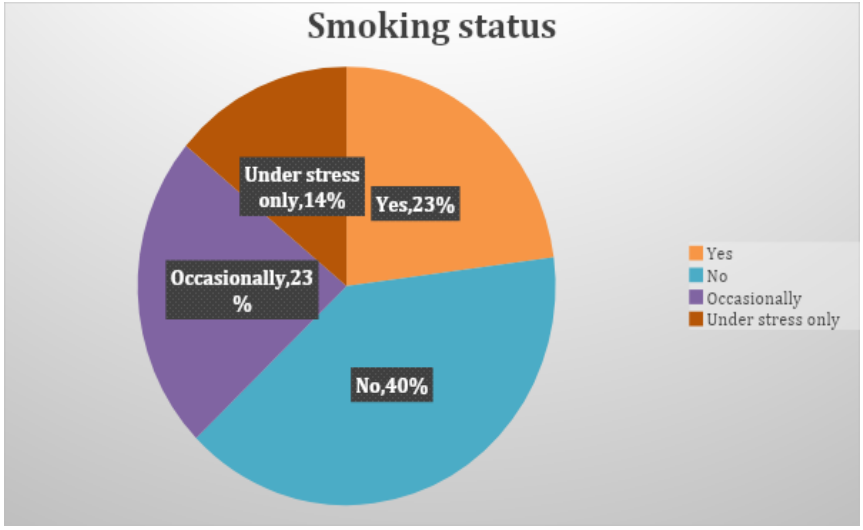

Figure 1 : Smoking Status

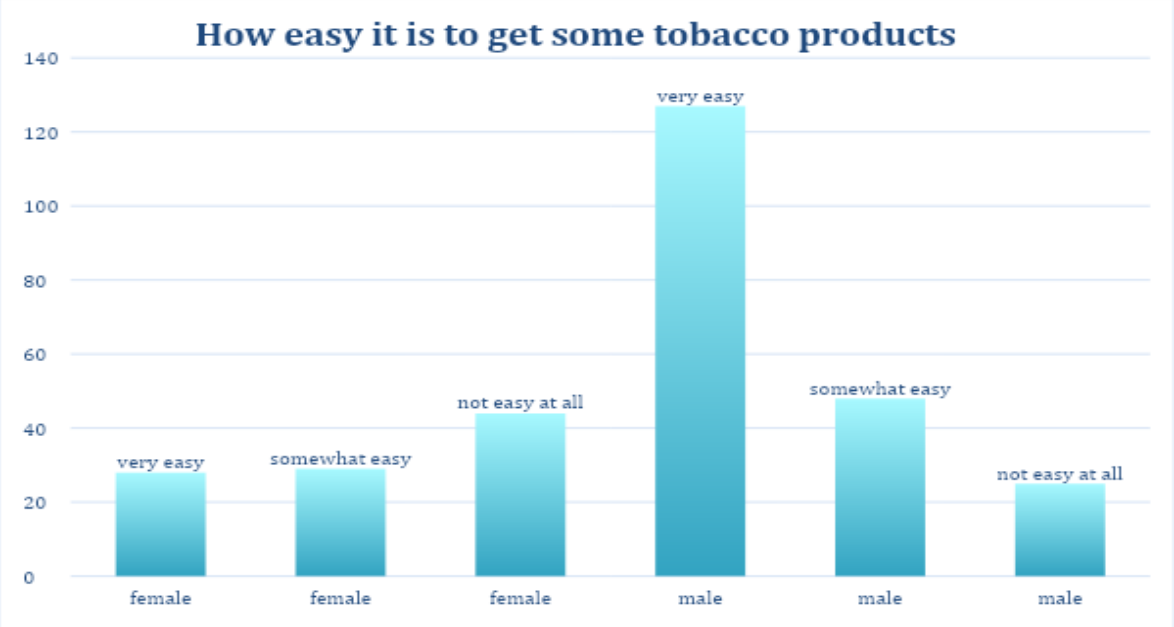

Figure 2: How easy it is to get some tobacco products

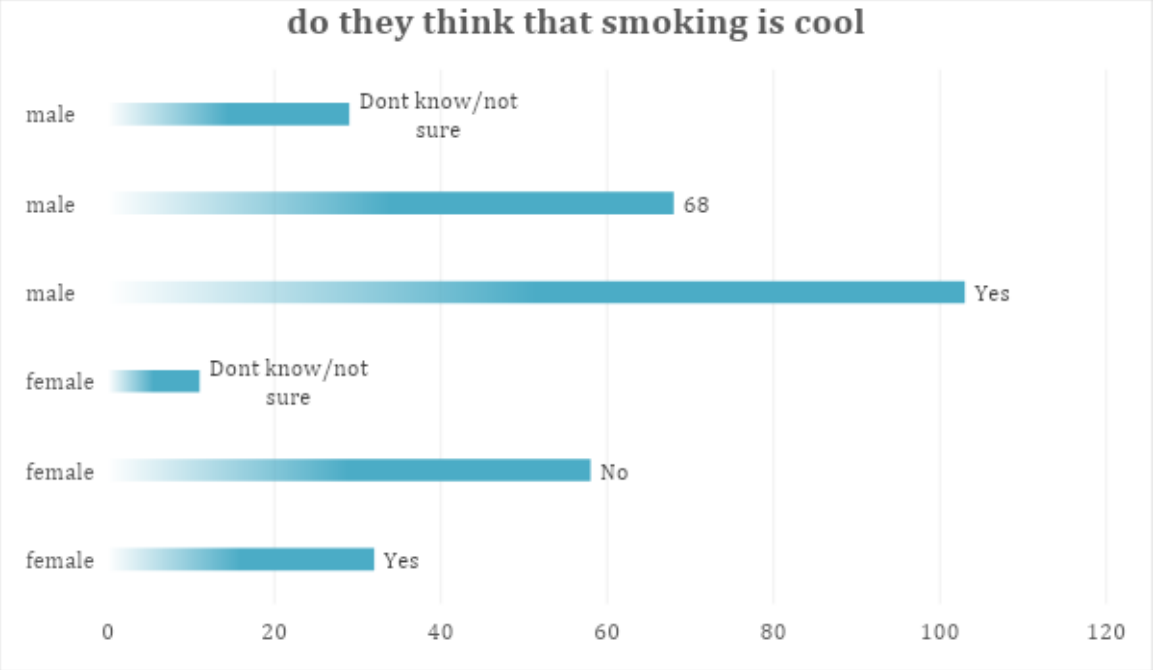

Figure 3 : Do they think that smoking is cool

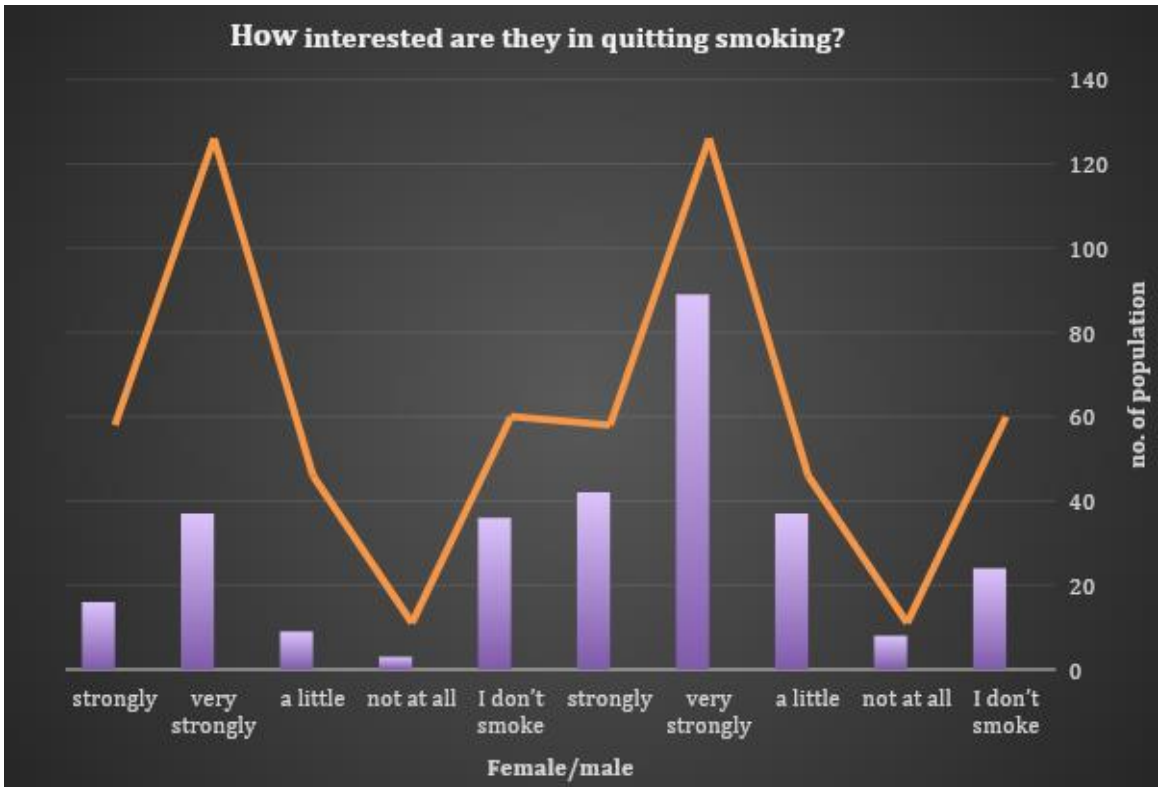

Figure 4 : How interested are they in quitting smoking

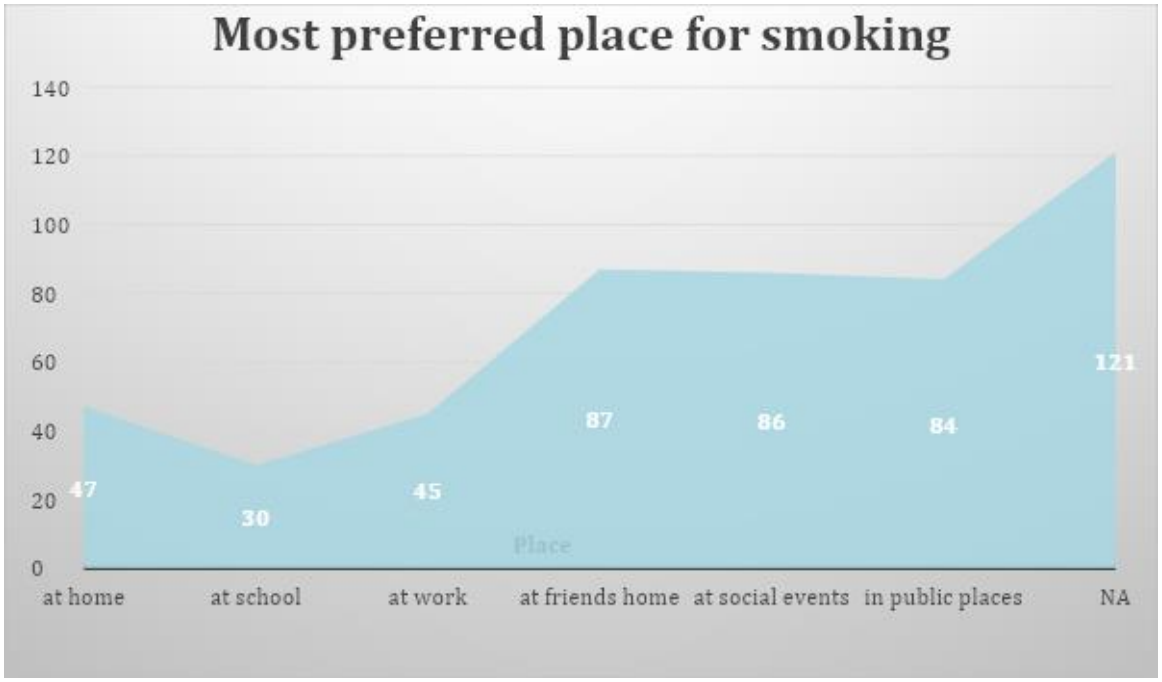

Figure 5 : Most preferred place foe smoking

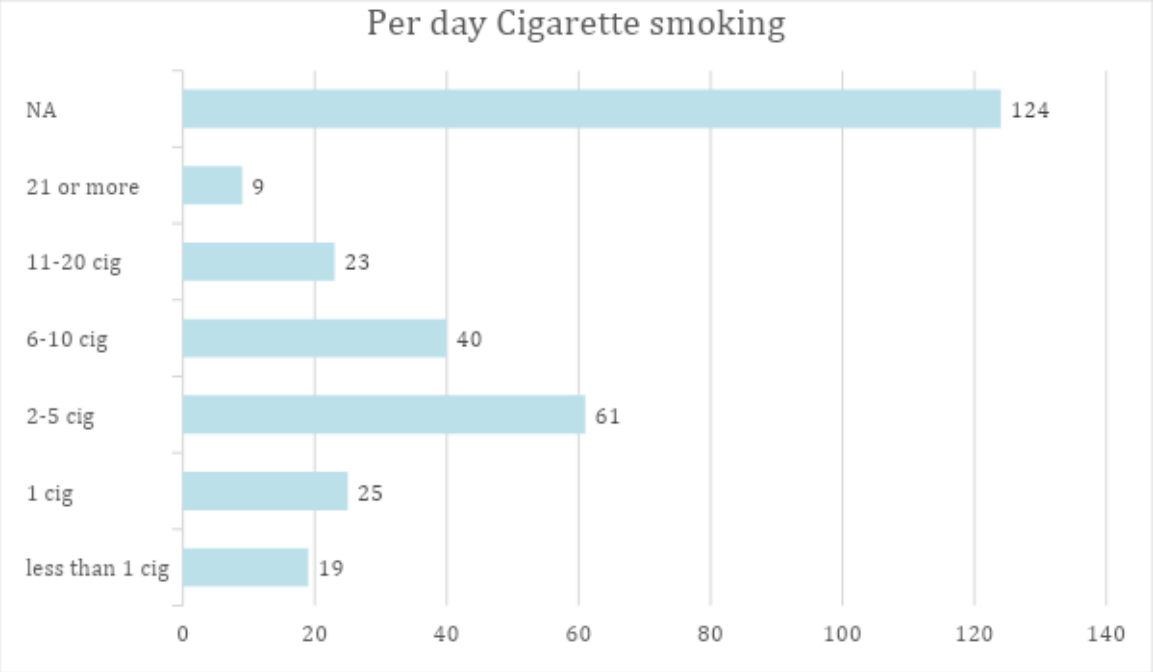

Figure 6 : Per day cigarette smoking

International e-Conference on Recent Trends in Nano-Materials and Its Applications
In Association with International Journal of Scientific Research in Science and Technology
Volume 10 | Issue 9 | Print ISSN: 2395-6011 | Online ISSN: 2395-602X (www.ijsrst.com)

Green Approach to the Design of Synthesis of Benzopyran Derivatives by Using as Greener Gel Entrapped Catalysts

Shital Shinde, Rajashri Salunkhe*

Vidnyan Mahavidyalaya Sangola, Department of Chemistry, PSAH Solapur University, Solapur, 413001, Maharashtra, India

ABSTRACT

A protocol has been developed for the efficient synthesis of structurally diverse terahydrobenzo[b]pyran via three-component reactions of dimedone, malanonitrile with various aldehydes and in the presence of gel entrapped NaOH as a catalyst.

Keywords: Gel Entrapped Base Catalyst, terahydrobenzo[b]pyran, recyclability

I. INTRODUCTION

Multicomponent reactions (MCRs) have attracted considerable attention owing to high synthetic efficiency, and, in many cases, the facile construction of novel molecular libraries. These methodologies are of particularly great utility when they lead to the formation of privileged medicinal scaffolds. Tetrahydrobenzo[*b*]pyransare an important class of heterocyclic scaffolds in the field of drugs and pharmaceuticals. These compounds are widely used anti-coagulant, anti-cancer and anti-ancaphylactiaspasmolytic agents.[1-4] In addition, they have been shown to act as cognitive enhancers, for the treatment of neurodegenerative disease, including Huntington's disease, amyotrophic lateral Sclerosis, Alzheimer's disease, AIDS associated dementia and Down's syndrome as well as for the treatment of Schizophrenia and myoclonus.[5, 6] The polyfunctionalized benzopyrans are used as cosmetics, pigments and biodegradable agrochemicals.[7] Other than their biological importance, some tetrahydrobenzo[*b*]pyrans have been widely used as photoactive materials.[8] Looking at their importance from pharmacological and industrial point of view, several methods for the multi-component synthesis of tetrahydrobenzo[*b*]pyrans have been reported. These include both homogeneous as well as heterogeneous conditions, catalyzed by Na_2SeO_4, hexadecyldimethylbenzyl ammonium bromide,[9] NaBr,[10] tetra-methyl ammonium hydroxide $(CH_3)_4N^+OH^-$,[11] TEBA,[12] KF-montmorillonite,[13] KF-alumina,[14] organocatalysts,[15] acetic acid,[16] diammonium hydrogen phosphate[17] and hexadecyltrimethylammonium bromide.[18] Microwaves[19] and ultrasonic irradiation[20] have also been used to promote the reaction. Although the literature on synthesis of tetrahydrobenzo[*b*]pyrans enjoys a rich array of versatile methodologies, new efficient approaches can be valuable additions to the contemporary arsenal of synthetic strategies.

The concept of gel entrapped base catalysts (GEBCs) combines the advantages of alkali and organic bases with those of heterogeneous supports.[21] These catalysts are prepared by immobilization of alkali or organic bases by entrapping them in an aqueous gel matrix of agar-agar which is a polymer composed of repeating agarobiose units alternating between 3-linked β-D-galactopyranosyl (G) and 4-linked 3, 6-anhydro-α-L-galactopyranosyl (LA) units. The use of GEBCs in organic transformations abates the amount of bases used and affords easy and efficient separation of products from the catalyst simply by filtration. Often, bases like alkalis absorb moisture when exposed to air and get spoiled. On the contrary, the GEBCs do not absorb moisture on exposure to air and remain intact. They also provide excellent opportunity of recyclability and reusability which is rarely possible using bases alone as catalyst. Further advantages of GEBCs include their ease of handling and being less corrosive. However, despite of their well recognized advantages, there have been only limited and sporadic reports dealing with the use of GEBCs in organic synthesis.[22]

In continuation to our research work devoted to the development of green methodologies for MCRs.[23] we report herein an efficient synthesis of tetrahydrobenzo[*b*]pyransfrom dimedone, malanonitrileand aryl aldehydes in the presence of Gel entrapped NaOH as a catalyst.

II. RESULTS AND DISCUSSION

We focused our initial studies on synthesis of Gel entrapped NaOH (acronymed as GENaOH). A series of experiments were under taken in which different concentrations of NaOH (5-25 %) were dissolved in a varying amount of agar-agar in water. After a considerable experimentation, we found that 20 % *w/w* of agar-agar aqua gel containing 10 % NaOH resulted in the formation of soft gel that served as GEBC in the present work. The GENaOH was light yellow jelly like substance that could be cut into pieces .The changes in physical nature of GENaOH were studied in different solvents. The GENaOH swelled in water and become soft. The nature of gel remained intact in organic solvents like ethanol, acetone, dichloromethane, toluene and isopropanol.

The TGA analysis of agar-agar and GENaOH are displayed in fig. The TGA profiles shows three different weight losses at different temperatures. The forth weight loss which occure below 150 ^{0}C for GENaOH as well as agar could be due to removal of physisorbed or occluded water. The second step of decomposition which is initial above 240 ^{0}C in both agar-agar as well as GENaOH differed in their amount of respective weight losses (GENaOH ~ 8%, agar- agar 63.5% could be assigned to thermal decomposition of agar polymer was agar-agar. The decomposition of remaining polymer matrix is accompanied with ~21 % weight loss. Third step in the temperature range of 440-480 ^{0}C. On the other hand the additional exothermic weight loss centered at 710 ^{0}C is observed and could be assigned the decomposition of carbonates frame if any. The entrappment of NaOH in gel matrix is evidenced by the comparatively large residual weight observed in the TGA profile of GENaOH than that of agar-agar.

In order to assess the catalytic activity of GENaOH in the synthesis of tetrahydrobenzo[*b*]pyrans **(Scheme 1),** an equimolar mixture of dimedone, malanonitrile and benzaldehyde (5 mmol each) was stirred in the presence of 1 gm of GENaOH in ethanol at ambient temperature till the completion of reaction as monitored by thin layer chromatography. The reaction proceeded efficiently yielding the corresponding

tetrahydrobenzo[*b*]pyran in 91% yield in just 5-15 minutes. In order to check the generality of this methodology, a series of tetrahydrobenzo[*b*]pyrans were prepared by reaction of dimedone, malanonitrile with various aryl aldehydes. We were gratified to find that with both electron-poor and electron-rich benzaldehydes, the corresponding products were obtained in excellent yields. The reaction of the sterically hindered *o*-nitrobenzaldehyde even gave higher yields high lightening the general applicability of the protocol. The striking feature of all the reactions was the isolation of products. During the course of the reaction the product precipitates out and can be isolated simply by filtration.The product obtained after sufficient washing with water was found to be practically pure. The identity of all the compounds was ascertained on the basis of IR, ^{1}H NMR, ^{13}C NMR and mass spectroscopy data. The physical and spectroscopic data are in consistent with the proposed structures.

It has been well established that in case of the GEBCs, the reagent trapped in the gel may leach into the solvent. To study the leaching of NaOH in solvent, 1 gm GENaOH was stirred in 5 mL of ethanol at room temperature. The GENaOH was filtered and water (3 mL) was added to the filtrate. The NaOH leached out was determined by titration with 0.1 N succinic acid solution using phenolphthalein as an indicator. The study revealed that only 3.91 % NaOH leached out from gel into ethanol. Using the amount of NaOH same as that leached out, the reaction between dimedone, malanonitrile and benzaldehyde did not gave quantitative yield of the corresponding product. This clearly demonstrated that catalysis was solely due to intact GENaOH rather than leached NaOH.

A proposed mechanism for the formation of tetrahydrobenzo[*b*]pyrans using GENaOH. The mechanism suggests that in step-1 Knoevenagel condensation takes place to form the α-cynocinnamonitrile derivative. In step-2 the active methylene of dimedone react with the electrophilic C=C double of α-cynocinnamonitrile giving the intermediate 6, which tautomerizes into 7. The latter is then cyclized by nucleophilic attack of the OH group on the cyano (CN) moiety, giving intermediate 8. Finally, the expected product 4 is afforded by tautomerizeation (8-4).

The use of catalyst is especially interesting when it can be used several times. To investigate the possibility of catalyst recycling, the reaction of dimedone, malanonitrile with benzaldehyde using GENaOH in ethanol was carried out. After completion of the reaction, the GENaOH was recovered by simple filtration, washed with ethanol and reused in another reaction with identical substrates. The catalyst could be reused for five runs without noticeable drop in the yield of product.

III. EXPERIMENTAL

Infrared spectra were recorded on a Perkin-Elmer FTIR spectrometer. The samples were examined as KBr discs ~5% w/w. ^{1}H NMR and ^{13}C NMR spectra were recorded on a Bruker Avon 300 MHz spectrometer using DMSO/$CDCl_3$ as solvent and TMS as internal reference. Mass spectra were recorded on a Shimadzu QP2010 GCMS with an ion source temperature of 280 ^{0}C. The thermal gravimetric analysis (TGA) curves were obtained by using the instrument STA 1500 in the presence of static air at a linear heating rate of 10 °C/min

from 25 ° to 1000 °C. Melting points were determined in an open capillary and are uncorrected. All chemicals were obtained from local suppliers and used without further purification.

Preparation of gel entrapped NaOH

To a boiling mixture of agar-agar (20 Mg) in water (60 mL) was added a solution of NaOH (10 gm) in water (100 mL). The resultant solution was boiled with stirring for five minutes and cooled in ice bath to yield the desired GENaOH.

General procedure for the multi-component synthesis of tetrahydrobenzo[b]pyrans

A mixture of dimedone (5 mmol), malanonirile (5 mmol) and aryl aldehyde (5 mmol) was stirred in the presence of GENaOH (1 gm) in 5 mL of ethanol at ambient temperature till the completion of the reaction as monitored by TLC. The resulting crude product was filtered off, washed with water and recrystallized from ethanol to afford the desired product.

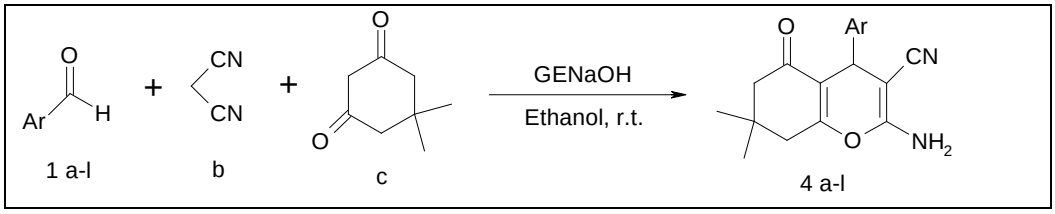

Scheme 1: GENaOH catalyzed multicomponent synthesis of tetrahydrobenzo[b]pyrans

Spectral data of representative compounds

2-Amino-3-cyano-5,6,7,8-tetrahydro-7,7-dimethyl-5-oxo-4-phenyl-4H-benzopyra: IR (KBr): υ 3396, 3323, 3213, 2961, 2199, 1976, 1660, 1371 cm^{-1}; ^{1}H NMR (300 MHz, DMSO-d_6): δ 1.05 (s, 3H), 1.12 (s, 3H), 2.21 (d, 1H), 2.22 (d, 1H), 2.44 (s, 2H), 4.39 (s, 1H), 4.50 (s, 2H), 7.17-7.31 (m, 5H); ^{13}C NMR (75 MHz, DMSO-d_6): 27.39, 28.92, 32.13, 35.88, 50.52, 59.03, 113.36, 120.03, 126.92, 127.50, 128.57, 144.78, 158.91, 162.73, 196.05; MS (EI): m/z = 294 (M^+).

IV. CONCLUSION

We have described a general and highly efficient procedure for the preparation of multi-component synthesis of tetrahydrobenzo[b]pyrans from dimedone, malanonitrile and aryl aldehydes in the presence of gel entrapped NaOH. The method offers several significant advantages, such as high conversions, easy handling, clean reaction profile, no energy consumption, high conversions, cost effective short reaction time and green methodology which make it a useful and an attractive addition to the existing methodologies.

Acknowledgements

We gratefully acknowledge the financial support from the Department of Science Technology and University Grants Commission for FIST and SAP respectively.

V. REFERENCES

[1]. Zhang Y L, Chen B Z, Zheng K Q, Xu M L, Zhang L Z and Lei X H, Yao Xue Xue Bao.,1982, 17(1), 17-22.

[2]. Zhang Y L, Chen B Z, Zheng K Q,Xu M L and Lei X H, ChemAbstr., 1982, 96, 135383e.

[3]. Andreani L L and Lapi E, Bull Chim Fr., 1960, 99, 583.

[4]. Witte E C, Neubert P and Roesch A, ChemAbstr., 1986, 104, 224915f.

[5]. Konkoy C S, Fick D B, Cai S X, Lan N C and Keana J F W, PCT IntAppl WO, 00, 75 2000, 123.

[6]. Konkoy S, Fick D B, Cai S X, Lan N C and Keana J F W, PCT IntAppl WO 0075123 ChemAbstr., 2000, 134, 29313a.

[7]. Hafez E AA, Elnagdi M H, Elagamey A G A and EL-Taweel F M AA, Heterocycles, 1987, 26, 903; (b) Abdel Galil F M, Riad B Y, Sherif, S M and Elnagdi M H, ChemLett., 1982, 1123.

[8]. Arnesto D, Horspool WM, Martin N, Ramos A, Seaone C (1989) J Org Chem 54:3069

[9]. (a) Jin T S, Wang A Q, Shi F, Han L S, Liu, L B and Li T S, ARKIVOC, 2006, (xiv), 78-86; (b) Wang X S, Shi D Q, Tu S J and Yao C S, Synth Commun., 2003, 33, 119.

[10]. Devi I and Bhuyan P J, Tetrahedron Lett., 2004, 45, 8625-8627.

[11]. Balalaie S, Sheikh-Ahmadi M and Bararjanian M, CatalCommun., 2007, 8, 1724- 1728.

[12]. Rong L, Li X, Wang H, Shi D, Tu S and Zhuang Q, Synth Commun., 2006, 36, 2363.

[13]. Zhuang Q Y, Wu N, Shi D Q, Tu S J and Wang X S, Chin J Org Chem., 2006, 26, 1217.

[14]. Wang X S, Shi D Q, Tu S J and Yao C S, Synth Commun., 2003, 33, 119-126.

[15]. Lian X Z, Huang Y, Li Y Q and Zheng W J, Monatshefte fur Chemie, 2008, 139, 129.

[16]. Kamaljit S, Jasbir S and Harjit S, Tetrahedron, 1996, 52, 14273.

[17]. a) Balalaie S, Bararjanian M, Sheikh-Ahmadi M, Hekmat S and Salehi P, Synth Commun., 2007, 37, 1097; (b) Balalaie S,Bararjanian M, Amani A M and Movassagh B, Synlett., 2006, 263-266.

[18]. (a) Jin T S, Wang A Q, Wang X, Zhang J S and Li T S, Synlett., 2004, 871; (b) Wang L M, Shao J H, Tian H, Wang Y H and Liu B, J Fluorine Chem., 2006, 127, 97; (c) Seifi M and Sheibani H, CatalLett., 2008, 126, 275; (d) Gao S, Tsai C H, Tseng C and Yao C F, Tetrahedron, 2008, 64, 9143.

[19]. Devi I, Bhuyan PJ. Tetrahedron Lett.2004, 45, 8625.

[20]. Tu SJ, Jiang H, Zhuang QY, Miu CB, Shi DQ, Wang XS, Gao Y. Chin. J. Org. Chem. 2003, 23(5), 488.

[21]. R. S. Natekar, S. D. Samant, Ind. J. Chem. 35B (1996) 1347

[22]. S. S. Chaphekar, S. D. Samant, J. Chem. Technol. Biotechnol. 2004, 79, 769; B. P. Bandgar, L. S. Uppalla, Synth. Commun. 2000, 30, 2071.

[23]. G. Rashinkar, R. Salunkhe, J. Mol. Catal. A: Chem. 2010, 316, 146;

[24]. S. Gurumurthi, V. Sundari and R. Valliappan, E-Journal of Chemistry ,2009, 6(S1),S466- S472

[25]. Naglaa M. Abd El-Rahman, Ahmed A. El-Kateb, Mohamed F. Mady, Synth. Commun., 37;22, 3961-3970

[26]. Li-Min Wang,Jue-Hua Shao, He Tian, Yong-Hong Wang, Bo Liu, Journal of Fluorine Chemistry 127 (2006) 97-100

International e-Conference on Recent Trends in Nano-Materials and Its Applications
In Association with International Journal of Scientific Research in Science and Technology
Volume 10 | Issue 9 | Print ISSN: 2395-6011 | Online ISSN: 2395-602X (www.ijsrst.com)

Synthesis and Characterization of CuO –Co_3O_4@NiO core shell Nanoplates

Savita Vasantrao Thakare*[1], Komal Dadaji Khairnar[1], Akanksha Milind Sajgure[1]
[1]M.V.P. Samaj's K.S.K.W. Arts, Science and Commerce College, CIDCO, Nasik, Maharashtra, India

ABSTRACT

The research work presents synthesis and characterization CuO –Co3O4 composite supported on NiO nanoplates. Synthesis of NiO nanoplates by co precipitation method. The coreshell paticles were developed by the impregnation method using aqueous solutions of copper and cobalt nitrates. The structural and morphological properties of synthesized core shell CuO –Co_3O_4@NiO have been determine by characterisation techniques such as UV-DRS, X-ray diffraction analysis (XRD) and scanning electron microscopy (SEM).

Keywords: -NiO nanoplates, CuO–Co3O4 Coprecipitation method, XRD, SEM

I. INTRODUCTION

Recently, In the Nanotechnology field the development of advanced core-shell materials is proposed. Due to enormous application this class of nanostructure has received considerable attention It has uses in physics [1-3], chemistry [4-6], and biological area [7-9] because of the collective properties and function of the core and shell.Core shell nanoparticles consist of various types of inorganic nanoparticles like metal oxides.

Metal oxide nanoparticles have drawn large attention as they possess distinctive chemical, electronic, mechanical, magnetic and optical properties which are significantly unlike from those of analogous bulk ones. Transition metal oxides shows a expansive structural variety due to changeable oxidation states so being measured as potential materials for many applications. Nanoscale transition metal oxides are acquiring unbroken significance than its bulk equivalents. Nanoparticles expose unique properties because of their small size and high surface area. Owing to chemical stability, novel optical , electronic, magnetic , thermal and mechanical properties, nickel oxide (NiO) is remarkable transition metal oxide nanoparticles. In view of all the mentioned properties NiO material has potential application in catalyst , battery electrodes , gas sensors, electro chromic material etc. Various methods have been employed to synthesize metal oxides like solvothermal, hydrothermal, chemical bath deposition, chemical precipitation, microwave assisted, electrophoretic deposition and sonochemical with different morphologies. From all said methods Co-precipitation is a easy and cost effective method for synthesizing nanoparticles that can be made in a variety of sizes [13]. The core shell formation with NiO leading to modification of their properties and made desirable for many applications [10]. Co_3O_4 and CuO are the promising materials in formation of core shell nanostructure [11-12].

In the present work, we report a promising strategy to improve the performance of Nickel Oxide,we have describe a simple method to synthesize CuO–Co_3O_4@NiO core shell Nanoplates .Structure determination of synthesizing material were characterized by UV-DRS, X-ray diffraction (XRD) and scanning electron microscopy (SEM) .

II. EXPERIMENTAL

Material

The chemicals used are nickel nitrate (Ni(NO3)2.6H2O(SigmaAldrich 99.99%), Cobalt nitrate (Co(NO3)2.6H2O) (SigmaAldrich 99.99%),($Cu(NO_3)_2.3H_2O$) copper nitrate(SigmaAldrich 99.99%), sodium hydroxide (NaOH, Merck 99%) Triton X100 (Sigma-Aldrich). Double distilled water (DDW) was used as a solvent in all the experiments.

Preparation of NiO Nanoplates

The NiO nanoparticles were synthesized by the coprecipitation method using Nickel nitrate Ni (NO3)2.6H2O (1M) used as precursor and Triton X100 as surfactant was dissolved in 100 ml double distilled water. The sodium hydroxide (0.1M) was slowly added drop wise under continuous stirring. The green colored precipitates of Nickel hydroxide were obtained. The mixtures were stirred for 3 h at 80.0^{0}C The precipitate obtained was filtered and washed with double distilled water .The washed precipitate was dried at 80 °C for 12 h. The dried precipitate was calcined at 450°C for 5h.

Preparation of CuO–Co_3O_4@NiO core shell Nanoplates

CuO–Co_3O_4@NiO core shell Nanoplates was obtained an impregnation method. The method involve loading aqueous solution of stochiometric amount of ($Cu(NO_3)_2.3H_2O$) copper nitrate and Cobalt nitrate ($Co(NO_3)_2$ of of.$6H_2O$) on prepared NiO Nanoplates. The mixture obtained was refluxed at 110^{0}C for 12 h then filtered and washed with double distilled water. The product obtained was dried at 100^{0}C in the oven and calcined at 750 ^{0}C for 4 h in air. The synthesized CFA@CuO catalyst was characterized by UV DRS, XRD and SEM techniques.

III. RESULT AND DISCUSSION

UV– DRS absorption spectra of the synthesized CuO–Co_3O_4@NiO core shell Nanoplates recorded in the range 200– 1000 nm are shown in Fig. 1. Spectra reveals peaks at 245 , 320, 380 and 690 nm confirm the formation of product.

In XRD analysis Fig.2., the diffraction peaks of CuO–Co_3O_4@NiO core shell Nanoplates at 37.26,62.93.73.34,79.20 originate from crystal planes (111), (220), (311) and (222) of NiO (JCPDS No.47-1049). The formation of CuO and Co_3O_4 on the surface NiO of was confirmed by the XRD pattern show peaks at 38.78, 48.84, 53.42, 67.98 of CuO (JCPDS card No. 05-661). The peaks at 36.93, 44.93, 59.39 and 65.33 of Co_3O_4 (JCPDS card No: 74-2120). No extra peak is observed which confirms the purity of product.

To characterize and analyze the morphology, the synthesized material are analyzed by SEM as shown in Fig.3. The scanning electron microscopy is used to determine the shape or morphology of the synthesized material. The particles have plate-like morphology and they are aggregated together. In the aggregates, the size of the particles is not uniform .

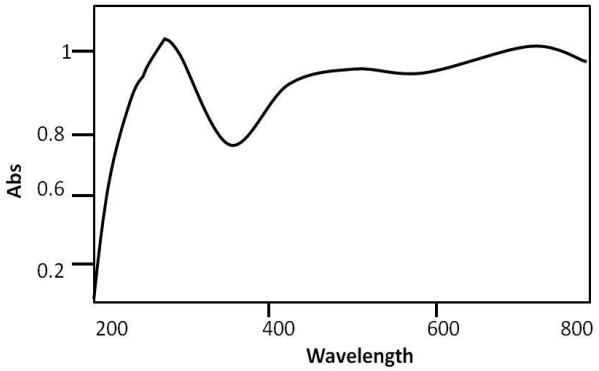

Fig 1 UV-DRS of CuO–Co_3O_4@NiO

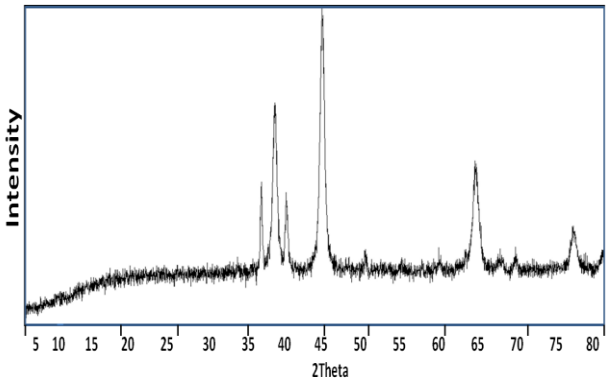

Fig 2 XRD pattern of CuO–Co_3O_4@NiO .

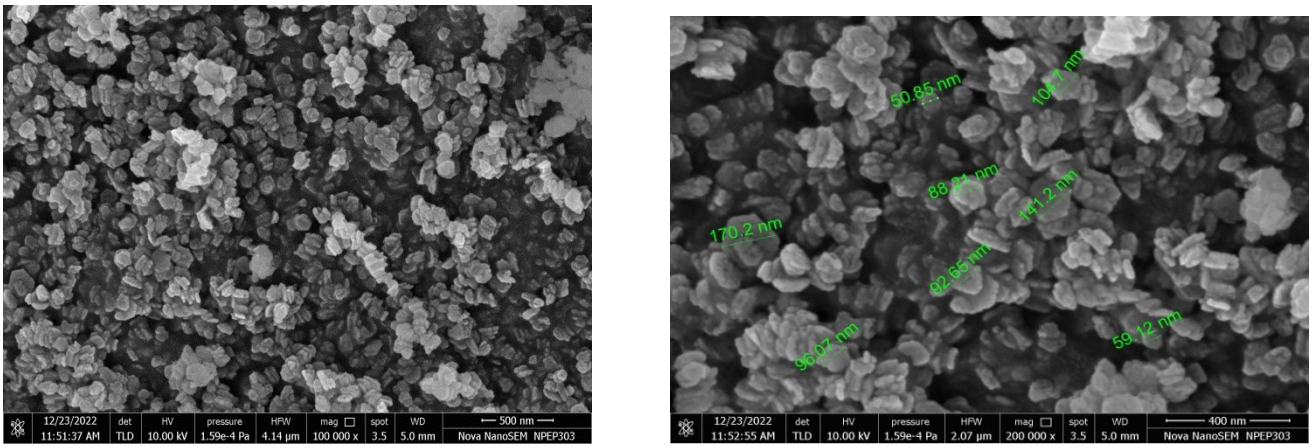

Fig 3 SEM pattern of CuO–Co_3O_4@NiO

IV. CONCLUSION

CuO–Co_3O_4@NiO core shell Nanoplates have been effectively synthesized using an impregnation method. By this method get an opportunity to synthesize nanoparticles with controlled morphology. Characterization of the precursors and the oxides by various analytical techniques UV DRS and XRD indicate the formation of core-shell nanoparticles. The SEM images of CuO–Co_3O_4@NiO show core-shell morphology.

V. REFERENCES

[1]. L Theil Kuhn, A Bojesen, L Timmermann, M Meedom Nielsen, S Mørup Structural and magnetic properties of core–shell iron–iron oxide nanoparticles Journal of Physics: Condensed Matter 2002 ,14, 13551.

[2]. C. L. Dennis, A. J. Jackson, J. A. Borchers, R. Ivkov, A. R. Foreman, J. W. Lau, E. Goernitz, C. Gruettner The influence of collective behavior on the magnetic and heating properties of iron oxide nanoparticles Journal of Applied Physics 2008,103, 07A319.

[3]. X. Xia, J.Tu, Y.i Zhang, X.i Wang, C. Gu, X.Zhao, H. Jin Fan, High-Quality Metal Oxide Core/Shell Nanowire Arrays on Conductive Substrates for Electrochemical Energy Storage ACS Nano 2012, 6, 6, 5531.

[4]. M. Lukosi, H. Zhu, S. Dai Recent advances in gold-metal oxide core-shell nanoparticles: Synthesis, characterization, and their application for heterogeneous catalysis Frontiers of Chemical Science and Engineering volume 2016, 10,39.

[5]. Z. Ai, Z. Gao, L. Zhang, W. He, J. Jie Yin Core–Shell Structure Dependent Reactivity of Fe@Fe2O3 Nanowires on Aerobic Degradation of 4-Chlorophenol Environmental Science & Technology 2013, 47, 10, 5344.

[6]. M. Mazloum-Ardakani, F. Sabaghian, M. Yavari, A. Ebady, N. Sahraie Enhance the performance of iron oxide nanoparticles in supercapacitor applications through internal contact of α-Fe2O3@CeO2 core-shell Journal of Alloys and Compounds 2020, 819, 5,152949.

[7]. H.Y. Park, M. J. Schadt, Wang, I-Im Stephanie Lim, P. N. Njoki, S. Hong Kim, M.Y. Jang, J. Luo, C.J. Zhong Fabrication of Magnetic Core@Shell Fe Oxide@Au Nanoparticles for Interfacial Bioactivity and Bio-separation Langmuir 2007, 23, 17, 9050.

[8]. A. Noormohamadi , M. Homayoonfal , M. R. Mehrnia , F. Davar Synergistic effect of concurrent presence of zirconium oxide and iron oxide in the form of core-shell nanoparticles on the performance of Fe3O4@ZrO2 /PAN nanocomposite membrane Ceramics International 2017, 43, 18, 15 ,17174.

[9]. T. Seto, H. Akinaga, F. Takano, K. Koga, T. Orii, M. Hirasawa Magnetic Properties of Mono dispersed Ni/NiO Core–Shell Nanoparticles Journal of Physical Chemistry B 2005, 109, 28, 13403.

[10]. N. Bayal, P. Jeevanandam Synthesis of CuO@NiO core-shell nanoparticles by homogeneous precipitation method Journal of Alloys and Compounds 2012, 537, 232.

[11]. H.Ming, Y. Zhang, F. L. Zhongchang, W. Ning, H. Z. Wen, Q. Liu, Merging of Kirkendall growth and Ostwald ripening: CuO@ MnO2 core-shell architectures for asymmetric supercapacitors Scientific reports 2014 1,4, 4, 1.

[12]. F. Yang , K. Xu , J. Hu Hierarchical multicomponent electrode with NiMoO4 nanosheets coated on Co3O4 nanowire arrays for enhanced electrochemical properties Journal of Alloys and Compounds, 2019,781, 1127.

[13]. J. M. Ramzan, S. Ashraf. Synthesis of Co3O4 Nano Aggregates by Co-precipitation Method and its Catalytic and Fuel Additive Applications Open Chemistry, 2019, 17, 1, 865.

International e-Conference on Recent Trends in Nano-Materials and Its Applications
In Association with International Journal of Scientific Research in Science and Technology
Volume 10 | Issue 9 | Print ISSN: 2395-6011 | Online ISSN: 2395-602X (www.ijsrst.com)

Development And Evaluation of Dental Gel Containing Clove Oil and Neem Oil for The Treatment of Periodontal Diseases

Baburao N. Chandakavathe[1], Shubham P. Bet[2]*, Omkar J. Shiddanagoudar[3], Akash D. Rajmane[4]

Department of pharmaceutics, D.S.T.S. Mandal's College of pharmacy, Solapur, Maharashtra, India

ABSTRACT

Aim: The goal of the study was to formulate and evaluate a dental gel for the treatment of periodontal diseases that contained clove oil and neem oil as its primary ingredients.

Methods: It is chosen moreover the treatment of periodontitis because it has a broad spectrum of antibacterial activity against a variety of periodontal infections. Clove oil and neem oil gel is developed using Carbopol 940 as the gelling agent, polyethylene glycol as the cosolvent, methyl and propyl parabens as the preservatives, and the necessary amount of distilled water as the vehicle.

Results: Clove oil and neem oil both performed satisfactorily in tests for physical characteristics such as acid value, saponification value, solubility, density, refractive index, and specific gravity. The produced gel was tested for a number of characteristics, including drug content, pH, spreadability, extrudability, and antibacterial activity. The formulation F4 is an acceptable dosage form for the treatment of periodontitis, according to *in-vitro* tests. Neem oil and clove oil indicated a zone inhibition that was around 26.04±0.6 mm.

Conclusion: The gel formulations of clove oil F4 exhibited good physicochemical properties as well as good drug content in comparison to other formulations, according to the outcomes of the current investigation.

Key words: Periodontitis, Tooth gel, antimicrobial activity, Carbopol-940, Herbal.

I. INTRODUCTION

The popularity of therapeutic herbs is booming in both developed and developing countries. One of the most active study fields worldwide is herbal medicine. The usefulness of herbal treatments in both treating and preventing oral disorders has recently been the subject of substantial research. Herbs have traditionally been used to cure a variety of oral disorders as well as to clean teeth and gums. One of the most significant issues with oral health is oral diseases such periodontal disease, dental caries, and oral cancer. The interactions between oral illnesses and the microbial species that make up the microbiota of the mouth are well-established. An increase in the prevalence of diseases has resulted in a significant need for alternative medicines, products, and solutions for secure, affordable, and efficient contraceptive methods. Historically, A rise in the prevalence of diseases, especially in developing countries, an increase in the resistance to pathogenic bacteria in the current use of chemotherapeutics and antibiotic opportunistic infections in

vulnerable people, and commercially viable options for secure, affordable, and beneficial oral contraceptives are all contributing factors. In a developing nation like India, allopathic medication is also exceedingly costly and unsuccessful at both preventing and treating mouth and oral disease. So, the practice of herbal treatments in traditional medicine and other products is still regarded as one of the best alternatives to synthetic over natural medications. [1,2]

All groups, ethnicities, races, genders, and socioeconomic levels are affected by periodontal disease, which is acknowledged as a major public health issue worldwide. The gums, supporting alveolar bone, periodontal ligament, dental cementum, and buildup of bacterial pathogens are all characterized by inflammation and deterioration. It is a localized inflammatory response brought on by a periodontal pocket's bacterial infection along with subgingival plaque. Periodontal disease is mostly brought on by bacteria, but periodontitis may not always lead from the presence of microbial pathogenic agents. [3,4] Gingivitis and periodontitis are two inflammatory conditions caused by plaque that are frequently referred as periodontal disease. The early stage of the disease, known as gingivitis, is characterized by swelling, minor bleeding, and redness of the marginal gingiva. It is caused by an accumulation of supragingival plaque. The microbiota changes during gingivitis, moving from a Gram-positive anaerobic flora to a more Gram-negative one. The degradation of the alveolar bone and the separation of the periodontal ligament supporting the tooth are signs of periodontitis, a more advanced stage of periodontal disease. [5] According to Morris, 40–45% of adults in the United Kingdom have moderately damaging periodontal disease, and 5–10% have a severe form of the condition. They also noted that the main cause to periodontal disease, visible plaque, is observed in 72% of individuals. In the US, half of all individuals have gingivitis that affects at least three to four teeth; two thirds have subgingival calculus; and approximately one third have periodontitis. [6,7]

Moreover, it has been linked to the bacteria *Porphyromonas gingivalis* [8], the *Tannerella forsythia* [9], the *Actinobacillus actinomycetemcomitans,* the *Treponema denticola,* the *Dialister pneumosintes,* the Bacteroides *forsythus,* the *Capnocytophaga* species, and *Eikenella corrodens.* [10] The traditional methods for treating periodontal disease, including oral, topical, and systemic dosage forms, have significant drawbacks, including superinfection, low or non-compliance, low levels of antibiotics in gingival crevicular fluid, systemic side effects, short duration, and high relative costs. [11] Poor oral hygiene, alcohol, stress, cigarettes, nutrition, immune system problems, and systemic diseases are the main causes of periodontitis. On the tooth's supporting tissue, gram-negative and gram-positive bacteria combine to produce a bacterial plaque, which grows over time. Collagenase's enzymes, antigens, bacterial lipopolysaccharides, endotoxins, ammonia, and hydrogen sulphide are all released by these bacteria. In response, the flow of gingival crevicular fluid, which carries a significant amount of β-glucuronidase, elastase, prostaglandin, neutrophil, and proteoglycans conducive to gingival inflammation, increases in the gingival crevice. [12] The goals of periodontal therapy are to treat inflammatory tissue, lessen the number of pathogenic germs, and heal diseased pockets.

New advances in dentistry have encouraged the use of herbal and natural remedies to treat a variety of oral illnesses. Neem oil and clove oil are two products with many advantages that have grown in significance in herbal remedies. [13] Clove oil is extremely helpful in dentistry since it has minimal intrinsic toxicity and a wide range of biological effects, including analgesics, bactericidal, antispasmodic, anti-neuralgic, carminative,

anti-infectious, antiseptic, insecticide, stimulant, and stomachic properties. [14] The neem tree has been deeply rooted in Indian culture. The neem leaves are cheap and easily available as well as widely accepted socially in the Indian society. It has been tested for its antibacterial activity, including its therapeutic use for gingivitis and periodontitis. [15,16,17] The present study was aimed to formulate dental gel containing clove oil and neem oil for the treatment of periodontal disease and then evaluated for their physicochemical properties including drug content, spreadability, extrude ability, *in-vitro* antibacterial activity.

METHODS AND MATERIAL

MATERIALS AND METHODS

Materials:

Clove oil and neem oil is purchased from local market in Solapur. Carbopol 940 (research lab.Ltd),methyl paraben and propyl paraben (ozone international Mumbai),Glycerin (Vikash pharma),propylene glycol (Memba. chem. Corporation Mumbai).

Method:

Carbopol 940 gels were prepared by soaking Carbopol 940 in water and by neutralizing with triethanolamine to pH 6.4. Weighed amount of methyl and propyl paraben were added to the water prior to the addition of Carbopol 940 [18]. In another beaker, the needed quantity of propylene glycol was placed in another test tube to which accurately measured the amount of clove oil and neem oil corresponding to its MIC was incorporated and finally this mixture was added to the beaker containing Carbopol with stirring [19]. The sweetening agent was also added to the polymer dispersion and stirred continuously till it forms a homogenous product [20]. The volume was made up with distilled water and stirring was done vigorously. All the formulation were then subjected to evaluation tests in order to select the best formulation. Table 1 contains a list of several gel formulations ingredients.

Physicochemical characteristics of clove oil:

The physicochemical properties of the clove oil and neem oil, such as their acid value, saponification value, solubility, density, refractive index, and specific gravity, were examined. The results are listed in Table 2.

Evaluation of gel formulation

Physical appearance:

- Color

On a white background, the formulation's color was checked.

- Consistency

The consistency was tested by applying on skin.

- Greasiness

The greasiness was tested by the application on to the skin.

- Odor

The odor of the gels was tested by mixing the gel in water and taking the smell.

Determination of pH:

The pH of gel was determined using digital pH meter by immersing the glass electrode completely into the gel system. [21]

Determination of viscosity:

Brooke field viscometer was used to measure the viscosities of the formed gels; spindle number 7 and spindle speed of 60 rpm at 25 °C were used for gels; the corresponding dial reading on the viscometer was recorded [22] in table 3.

Determination of spreadability:

Using a modified wooden block and glass slide apparatus, spreadability was evaluated. The apparatus was made up of a pulley and a wooden block with a fixed glass slide. with the use of a string, a pan was tied to another glass slide that could be moved. For the purpose of determining spreadability, a fixed glass slide containing a measured amount of gel was placed. A moveable glass slide with a pan attached was then put on the fixed glass slide, causing the gel to be sandwiched between the two slides for five minutes. Time taken for the slides to separate was noted[23]. Spreadability was determined using following formula:

$$S = M.L/T$$

Where S is the spread ability in grams.cm/sec, M is the mass in grams, T is the time in seconds.

Determination of extrudability:

Standard collapsible aluminum tubes with caps were filled with the gel compositions, and the ends were crimped to the end. The tubes weights were recorded. The tubes were clamped after being placed between two glass slides. 500 gm was placed over the slides and then the cap was removed. The extruded gel's volume was collected and weighed. Calculated extrudability percentages are as follows: (>90% extrudability: excellent, >80%extrudability: good, >70% extrudability: fair). [24]

Determination of homogeneity:

All the developed gels were tested for homogeneity by visual inspection after the gels have been set in the container. [25] They were tested for their appearance and presence of any aggregates.

Determination of drug content:

For the determination of drug content of gel formulation, by thoroughly dissolving 1 g of the gel in 100 ml of solvent (a mixture of Methanol and phosphate buffer pH 6.8 for the formulation of clove oil and neem oil). The solutions were kept for shaking for 4 hr. and then kept for 6 hr. for complete dissolution of the formulations. The dissolved solutions were filtered through 0.45 mm membrane filters and proper dilutions were made and solutions were accustomed to the spectrophotometric analysis.[26] The linear regression equation constructed from the calibration data was used to calculate the drug content.

Determination of antimicrobial activity:

Clove oil and neem oil gel were tested for antibacterial properties using the agar cup plate method. The clove oil and neem oil formulation of about 2% were aseptically placed in cups of previously inoculated agar cultured media plate. The plates were kept at room temperature for 30 mins just before to incubation at 37◦C for 24 hrs. The antibiotic i.e., Penicillin and Antifungal i.e., Amphotericin B was used as standards for obtaining comparative results. Plates were examined after 24-48 hrs. incubation for the appearance of the

zone of inhibition. Antimicrobial and antifungal activity was determined by measuring the diameter of zones of inhibition (millimeters) of microbial growth.[25]

RESULTS AND DISCUSSION:

The following metrics were used to characterize the purchased clove oil and neem oil: acid value, saponification value, solubility, density, refractive index, and specific gravity (table 2).

The formulations were developed by using clove oil and neem oil of same concentration and Carbopol 940 at different concentrations. Formulation composition is given in (Table-1). Physical properties of each of the five batches of formulations were evaluated. All of the gel formulations were a light orange color and smelled strongly of neem and clove oils. The pH of all formulations ranged from 6.7 to 7.2, which corresponds to the buccal cavity's usual pH range of 6.2 to 7.6, supporting the claim that the formulated gels were irritant free to the skin.

Table no.1: Composition of Gel formulation

Ingredients	F1	F2	F3	F4	F5
Clove oil (ml)	0.5	0.5	0.5	0.5	0.5
Neem oil(ml)	0.5	0.5	0.5	0.5	0.5
Carbopol 940 (g)	0.3	0.4	0.5	0.6	0.1
Poly ethylene glycol (ml)	15	15	15	15	15
Glycerin (ml)	5	5	5	5	5
Methyl paraben (g)	0.18	0.18	0.18	0.18	0.18
Propyl paraben (g)	0.02	0.02	0.02	0.02	0.02
Aspartame (g)	0.4	0.4	0.4	0.4	0.4
Distilled water (ml)	q. s	q. s	q. s	q. s	q. s

Table no.2: Physicochemical characteristics of clove oil and neem oil.

Sr.no.	Parameter	Clove oil procured	Neem oil procured
1	Color	Pale yellow	Greenish yellow
2	Odor	Aromatic	Strong pungent
3	Acid value (mgKOH/g)	3.66	4.48
4	Saponification value (mgKOH/g)	42.07	195
5	Solubility	soluble in methanol	soluble in methanol
6	Density(g/ml)	1.02	0.918
7	Refractive index(n)	1.492	1.462
8	Specific gravity at 15^0C	1.042	0.932

Table no.3 : Characteristics of gel formulations

Formulations	Appearance	pH	Spreadability(g-cm/sec)	Extrudability (%)	Homogeneity	Viscosity(cps)	Drug content (%)
F1	Pale orange	6.7	18.24	92.20	Good	41330	95.03
F2	Pale orange	6.8	18.12	93.23	Good	41650	95.40
F3	Pale orange	6.7	16.52	90.16	Very good	42370	95.60
F4	Pale orange	6.9	17.86	94.28	Very good	42430	96.10
F5	Pale orange	6.8	15.64	89.30	Good	45420	90.80

Table sno.4: Antimicrobial activity of formulation (F4), clove and neem oil and tetracycline and Amphotericin B (standard)

Microorganisms	Zone of inhibition in mm(F4)	Clove and neem oil(mm)	Penicillin (mm) Standard	Amphotericin B(mm) Standard
Staphylococcus aureus	26.04±0.6	31.33±0.4	22.08±0.5	-
Candida albicans	25.33±0.4	26.02±0.4.	-	35.33±0.6
n=3, Mean ±S. D				

Table no.5 : Antimicrobial activity of clove and neem oil gel formulation

Formulation	Zone of inhibition(mm) (*Staphylococcus aureus)*	Zone of inhibition (mm) (*Candida albicans*)
F1	17.5±0.4	22.5±0.5
F2	16.2±0.1	21.02±0.4
F3	17.05±0.2	23.2±0.2
F4	19.5±0.5	25.33±0.6
F5	16.8±0.3	17.5±0.8
n=3, Mean ±S. D		

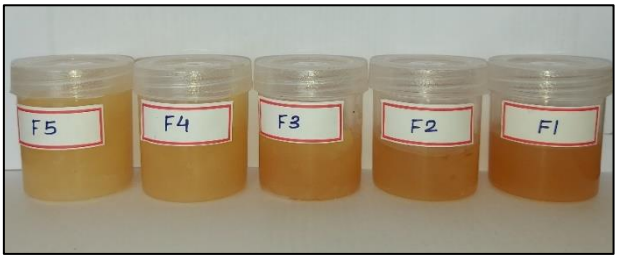

Fig 1: Formulation of clove oil and neem oil gel

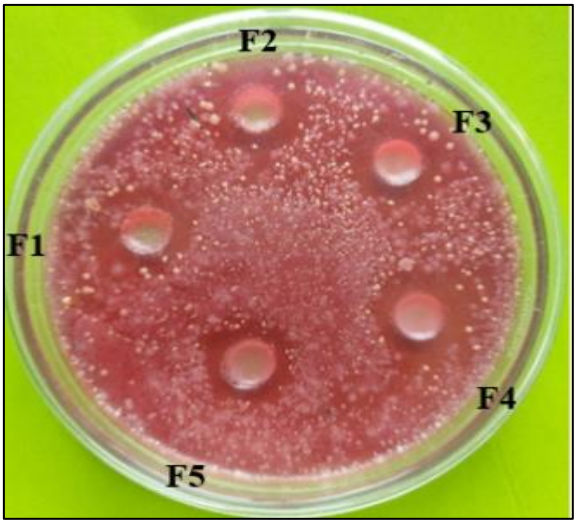

Fig 2: Antimicrobial activity of gel formulation on *S. Aureus*

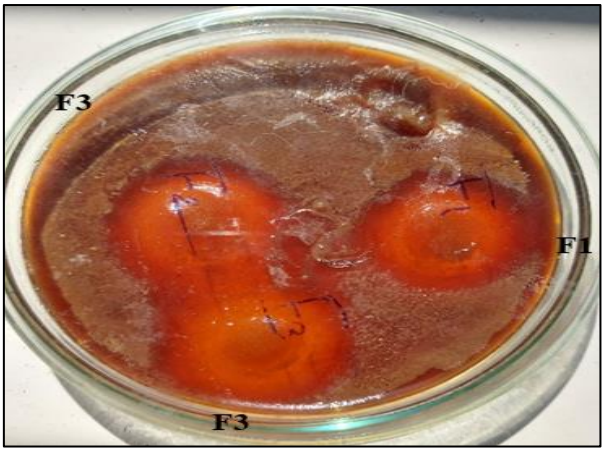

Fig 3: Antimicrobial activity of gel formulation on *C. Albicans*

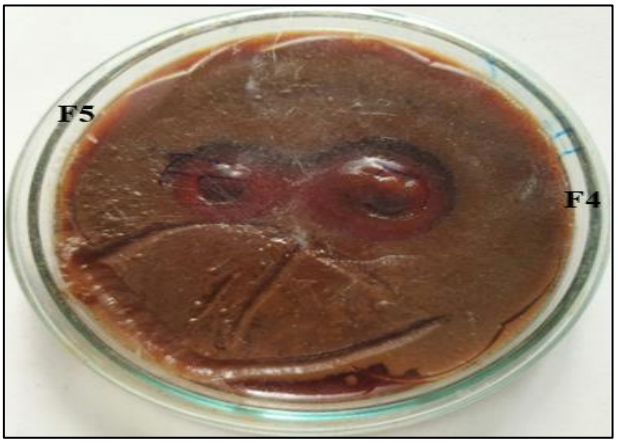

Fig 4: Antimicrobial activity of gel formulation on *C. Albicans*

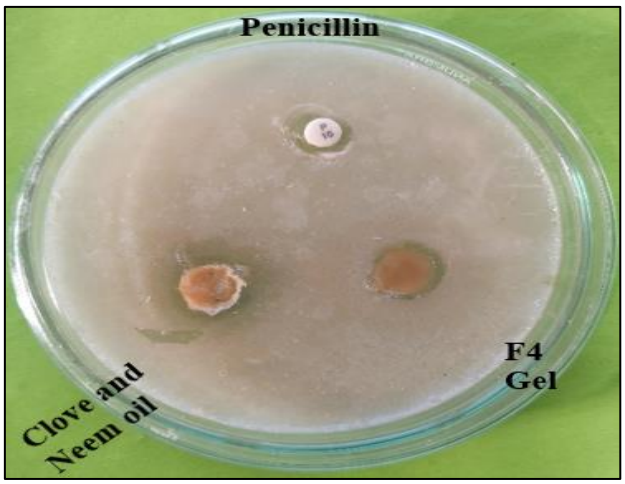

Fig 5: Antimicrobial activity on *S. Aureus*

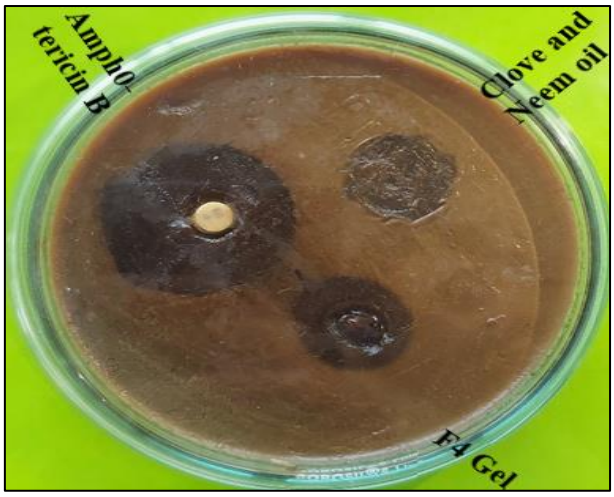

Fig 5: Antimicrobial activity on *C. Albicans*

The gel formulation's spreadability was determined to be between 15.64 to 18.24 gm/cm/sec, indicating that gels can spread consistently and smoothly. The compositions had a glossy, transparent appearance. In all formulations, the homogeneity and tube extrudability were excellent.

The formulations drug content ranged from 90.80% to 96.10%. (Table 3). It was found that there was no drug degradation during processing from the values obtained from the drug content. It was observed that the formulation F4 contained the greatest amount of drug. In comparison to previous formulations, the gel forms of clove oil and neem oil F4 demonstrated good physicochemical characteristics and good drug content (Table 3). According to the results of antimicrobial investigations, *candida albicans* and *staphylococcus aureus* were maximum zone of inhibition by the gel formulation of clove oil and neem oil i.e., F4.

CONCLUSION:

Staphylococcus aureus and *Candida albicans* were found to be resistant to the antibacterial effects of clove oil and neem oil. After performing human clinical trials, the formulations made from clove and neem were found to have considerable benefits and can be utilized commercially to design dental gels. However, more

investigation is still required to ascertain whether they can effectively replace synthetic antibiotics or be combined with them.

ACKNOWLEDEMENTS

We are thankful to the principal and management of D.S.T.S. Mandal's college of pharmacy Solapur for providing all the required facilities to complete this work successfully.

II. REFERENCES

1. Tribhuvan H, Mhaske S, Wayal V, Pawar P. Formulation and Evaluation of Pharmaceutical Aqueous Gel for Mouth Ulcer Treatment. International Journal of Scientific Research in Science and Technology,2022;9(4): 34-40.doi.org/10.32628/IJSRST2293165
2. Bhushan K, Chauhan G, Nagpal D, Prakash S. treatment of periodontal disease-A Herbal approach. Int.J.Pharm.Sci.Rev.Res.,2015;33(2):126-136.
3. Chaieb K, Hajlaoui H, Zmantar, Khla-Nakbi AB, Rouabhia M, Mahdouani K et al. The Chemical Composition and biological activity of clove essential oil, Eugenia caryophyllata (Syzigium aromaticum L. Myrtaceae): A short review. Phytother Res. 2007;21(6):501-506. doi: 10.1002/ptr.2124. PMID: 17380552.
4. Haffajee AD, Socransky SS. Attachment level changes in destructive periodontal diseases. J Clin Periodontol, 1986;13:461-75. doi: 10.1111/j.1600-051x.1986.tb01491.x. PMID: 3522651.
5. Gupta AK, Tandon N, Sharma M. Quality Standards of Indian Medicinal plants, Indian Council of Medical Research, 2011; New Delhi.
6. Oliver RC, Brown LJ, Löe H. Periodontal diseases in the United States population. J Periodontol, 1998; 69(2): 269-78. doi: 10.1902/jop.1998.69.2.269. PMID: 9526927.
7. Morris AJ, Steele J, White DA. The oral cleanliness and periodontal health of UK adults in 1998. Br Dent J, 2001;25;191(4):186-92. doi: 10.1038/sj.bdj.4801135. PMID: 11551090.
8. Yadav R, Kanwar IL, Haider T.In situ gel drug delivery system for periodontitis: an insight review. Futur J Pharm Sci,2020;33(6). doi: https://doi.org/10.1186/s43094-020-00053-x.
9. Hajishengallis G. Immunomicrobial pathogenesis of periodontitis: keystones, pathobionts, and host response. Trends Immunol, 2014;35(1): 3-11. DOI: 10.1016/j.it.2013.09.001
10. Oh TJ, Eber R, Wang HL. Periodontal diseases in the child and adolescent. J Clin Periodontol, 2002; 29(5): 400-10.doi: 10.1034/j.1600-051x.2002.290504.x. PMID: 12060422.
11. Pawar VA, Bhagat TB, Toshniwal MR, Mokashi ND, Khandelwal KR. Formulation and evaluation of dental gel containing essential oil of coriander against oral pathogens. Int Res J Pharm. 2013;4(10):48- 54.doi: 10.7897/2230-8407.041012
12. Juvekar S, Kathpalia H. Solvent removal precipitation based in situ forming implant for controlled drug delivery in periodontitis. J Control Release, 2017;10;251:75-81.doi: 10.1016/j.jconrel.2017.02.022. Epub 2017 Feb 24. PMID: 28242417.
13. Sharma A, Dwivedi S, Mishra GP, Joshi H. Formulation and Evaluation of Herbal Gel containing Extracts of Albezia Lebbeck linn. Am J Pharm Tech Res, 2012;2(4):663-668.
14. Gupta N, Patel AR, Ravindra RP. Design of Akkalkara (Spilanthes acmella) formulations for antimicrobial and topical anti-inflammatory activities. Int J Pharm Bio Sci 2012;3(4):161-170.
15. Mirpour M, Gholizadeh Siahmazgi Z, Sharifi Kiasaraie M. Antibacterial activity of clove, gall nut methanolic and ethanolic extracts on Streptococcus mutans PTCC 1683 and Streptococcus salivarius PTCC 1448. J Oral Biol Craniofac Res. 2015 Jan-Apr;5(1):7-10. doi: 10.1016/j.jobcr.2015.02.002.
16. Sharma A, Sankhla B, Parkar SM, Hongal S, K T, Cg A. Effect of traditionally used neem and babool chewing stick (datun) on streptococcus mutans: an in-vitro study. J Clin Diagn Res., 2014;8(7): ZC15-7. doi: 10.7860/JCDR/2014/9817.4549.
17. Chatterjee A, Saluja M, Singh N, Kandwal A. To evaluate the antigingivitis and antipalque effect of an Azadirachta indica (neem) mouthrinse on plaque induced gingivitis: A double-blind, randomized, controlled trial. J Indian Soc Periodontol. 2011;15(4):398-401. doi: 10.4103/0972-124X.92578.
18. Patil SC, Gadade DD, Rathis PB. Design, Development and Evaluation of Herbal Gel for Treatment of Psoriasis. JIPBS. 2015; l2(1):72-87.
19. Misal G, Dixit G, Gulkarni V. Formulation and Evaluation of herbal gel. Indian J nat prod resour. 2012;3(4):501-505.
20. Dheepika B, Uma Maheswari TN. Aloe Vera in Oral Diseases - A Review. Int J Pharm Pharm Sci. 2014;6(2):64-66. Doi:10.4103/0250-474X.22967.
21. Mastiholimath VS, Dandagi PM, Gadad AP, Patil MB, Manvi FV, Chandur VK. Formulation and evaluation of ornidazole dental implants for periodontitis. Ind J Pharm Sci. 2006;68(1):68-71.**doi:** 10.4103/0250-474X.22967.
22. Mitra J, Mohammad RR, Hedayte S. Mucoadhesive and drug release properties of benzocaine gel. Iranian J. Pharm Sci, 2006, (2):185-94.
23. Negi A, Sharma N, Singh M F. Formulation and evaluation an herbal anti-inflammatory gel containing Eupatorium leaves extract. J Pharmacognosy Phytochem, 2012;1(4): 112-116.
24. Mehta NJ, Patadiya ND, Patel J. Development and evaluation of antiarthritic herbal ointment. Research Journal of Pharmaceutical, Biological and Chemical Sciences,2013;(4) 221-228.
25. Vats A. Sharma P. Formulation and evaluation of topical anti acne formulation of coriander oil. International Journal of Pharmacy and Pharmaceutical Science Research 2012, 2(3) 61-66.
26. Voleti VK, Shaik SB, Konduru C, Peyam S, Yaramsetti CK, Pasala S, Pitchaimuthu SP. Formulation and development of dental gel containing clove oil for the treatment of human periodontal diseases. J Compr Phar 2016;3(1):1-7

International e-Conference on Recent Trends in Nano-Materials and Its Applications
In Association with International Journal of Scientific Research in Science and Technology
Volume 10 | Issue 9 | Print ISSN: 2395-6011 | Online ISSN: 2395-602X (www.ijsrst.com)

One Pot Environmental Benign Synthesis of Quinoline-3-Carbonitrile Derivatives

Kadam S. N*.[a], Adlinge N. P.[a]
[a]Vidnyan Mahavidyalaya Sangola, Solapur (MS) India 413307
Corresponding authors Email*siddhukadam214@gmail.com

ABSTRACT

Bleaching earth clay catalyzed multicomponent reaction of Heterocyclic aldehyde , 2-cyanoacetohydrazide and substituted Anilines, In PEG-400 is carried out. This method has been applied for the synthesis of quinoline-3-carbonitrile with good to excellet yield. In this study a comparison is made on triethylamine, piperidine, morpholine with Bleaching earth clay and with no catalyst. The studies revealed that bleaching earth clay and PEG-400 are more effective than other catalyst and solvents. It increasing the yield of product with less time consumption. All the synthesized compounds were characterized for their spectral analysis.
Keywords : Bleaching earth clay (BEC), PEG-400, Heterocyclic aldehyde, recyclability.

I. INTRODUCTION

The predominant occurrence of thequinoline-3-carbonitrile derivative in various natural products and established medicinal compounds[1-3] had proven to be a versatile scaffold in organic and medicinal chemistry. quinoline-3-carbonitrile have recognized to acquire varied biological activities such as antibacterial[4], antiviral[5], anticancer[6], antifungal[7], antimalarial[8], anti H.I.V[9], anti-inflammatory[10]. Quinoline-3-carbonitrile derivativeare acknowledged medicinal compounds known to be present in the bioactive natural products[11].Heterocyclic aldehydes are proven to contain varied biological activities[12]. By interpretating these points we combine the heterocyclic aldehydes with anilines and 2-cyanoacetohydrazide assuming that the present combination may lead to formation of improved biological hybrid.

There is always been quest for advancementof the synthetic rout for the conversion of readily available reagent in to widely used organic compounds. For accomplishing this multicomponent reaction (MCR) are recognized as an important tool from economic as well as environmental point of view[13]. Along with the MCR method, use of green solvent is also considered to be an environmental benign access. Amongst the green solvents used for MCR strategy PEG-400 is considered to be well known green solvent[14].

In the previous literature there are abundant synthetic strategies for the synthesis of quinoline-3-carbonitrile derivatives[15]. Development of an heterogenous catalyst for the synthesis of numerous important organic motifs was always been a center of interest for organic chemistry students[16-17].Ease of handling, reusability, easy extraction are some peculiar advantages of heterogenous catalysts. Amongst those

heterogeneous catalysts Bleaching earth clay (BEC) is considered as a remarkable heterogenous catalyst for various organic transformations[18].Taking in account these facts we represent an MCR protocol for synthesis of by Consolidation of heterocyclic aldehydes with anilines and 2-cyanoacetohydrazide Manipulating Bleaching earth clay as catalyst and PEG-400 as green solvent.

Result and discussion

A facile one pot three componentprotocol for the synthesis of new quinoline-3-carbonitrile derivative**4a-j**is reported by utilizing equimolar heterocyclic aldehydes**2a-j**, anilines**3a-c** and 2-cyanoacetohydrazide**1 Scheme 1**. The synthetic protocol commences with sequential addition of 2-cyanoacetohydrazide and heterocyclic aldehydes in round bottom flask previously filled with catalytic amount of BEC and PEG-400 as green solvent, after completion of reaction as indicated by TLC the anilineswas added in the same pot and the reaction mixture was further stirred at 80°C for the formation of product. the first attempt was made using the Triethylamine as a catalyst which results in formation of the product with 50% yield and time required for completion of reaction was 65 minutes Entry1 Table1. Observing these results, we moved for other catalysts piperidine and morpholine Entry 2and 3 Table 1 respectively which the outcomes of 40 and 30% yield with the time of 70 and 60 minutes. When we moved for using BEC as a catalyst 1 Wt%resulting in production of improved 60% yield Entry 4 table1. Enthused with these results we further investigate different wt% compositions of BEC (pH 12.5). We came to investigation that satisfactory yield was obtained when we utilized 15wt% of BEC. The yield was found to hampered when 10 wt% and 20wt% BEC were used Entry 5 and 7 Table 1. However, there was no formation of product when reaction was carried out in absence of catalyst when stirred at RT Entry 8. Even though when reaction mixture was stirred at 80°C without catalyst the formation of product was not observed Entry 9 Table 1. The optimized reaction conditions were found when 15wt% of BEC was used.

Table1: Optimized reaction conditions

Entry	Catalyst (Mol/wt%)	Temp (°C)	Time (Min)	Yield of 4a (%)
1	Triethylamine (Mol%)	70	65	50
2	Piperidine (Mol%)	80	70	40
3	Morpholine (Mol%)	80	60	30
4	Bleaching earth Clay 1 wt%	80	50	60
5	Bleaching earth Clay 10 wt%	80	40	70
6	Bleaching earth Clay 15 wt%	80	35	90
7	Bleaching earth Clay 20 wt%	80	20	70
8	No catalyst	**RT**	70	0
9	No catalyst	80	80	0

[a]Reaction progress was monitored by thin layer chromatography (TLC)

[b]Yield refers to isolated yield

With these optimized conditions we initiated to find the substrate scope the reaction condition was found to operate for varied substrate scope Table 2.

Scheme 1

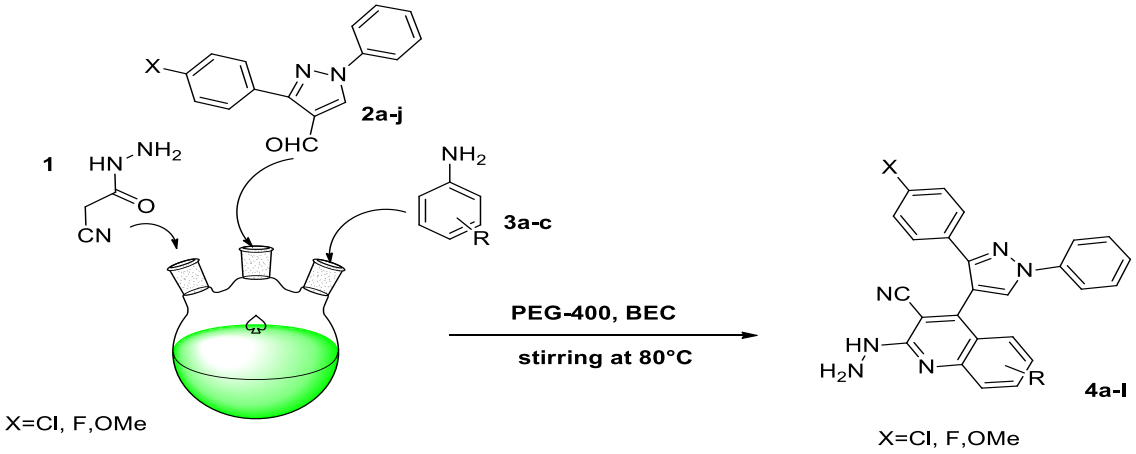

The finding of the substrate scope indicates that the MCR strategy allows variety of substrate to undergo smoothly with formation of product with satisfactory yield. Interpretation of the yield of the substrate scope indicate that the reactant with electron donating group either on aldehyde 2a-j or on the anilines 3a-c renders the productyield. The substrates with electron withdrawing groups on the aldehydes or on the anilines are providing the products with good yield.

Table 2 Substrate Scope

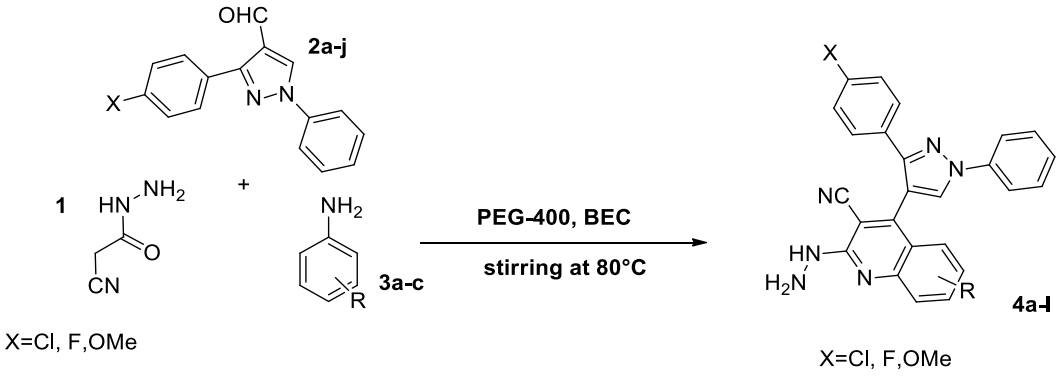

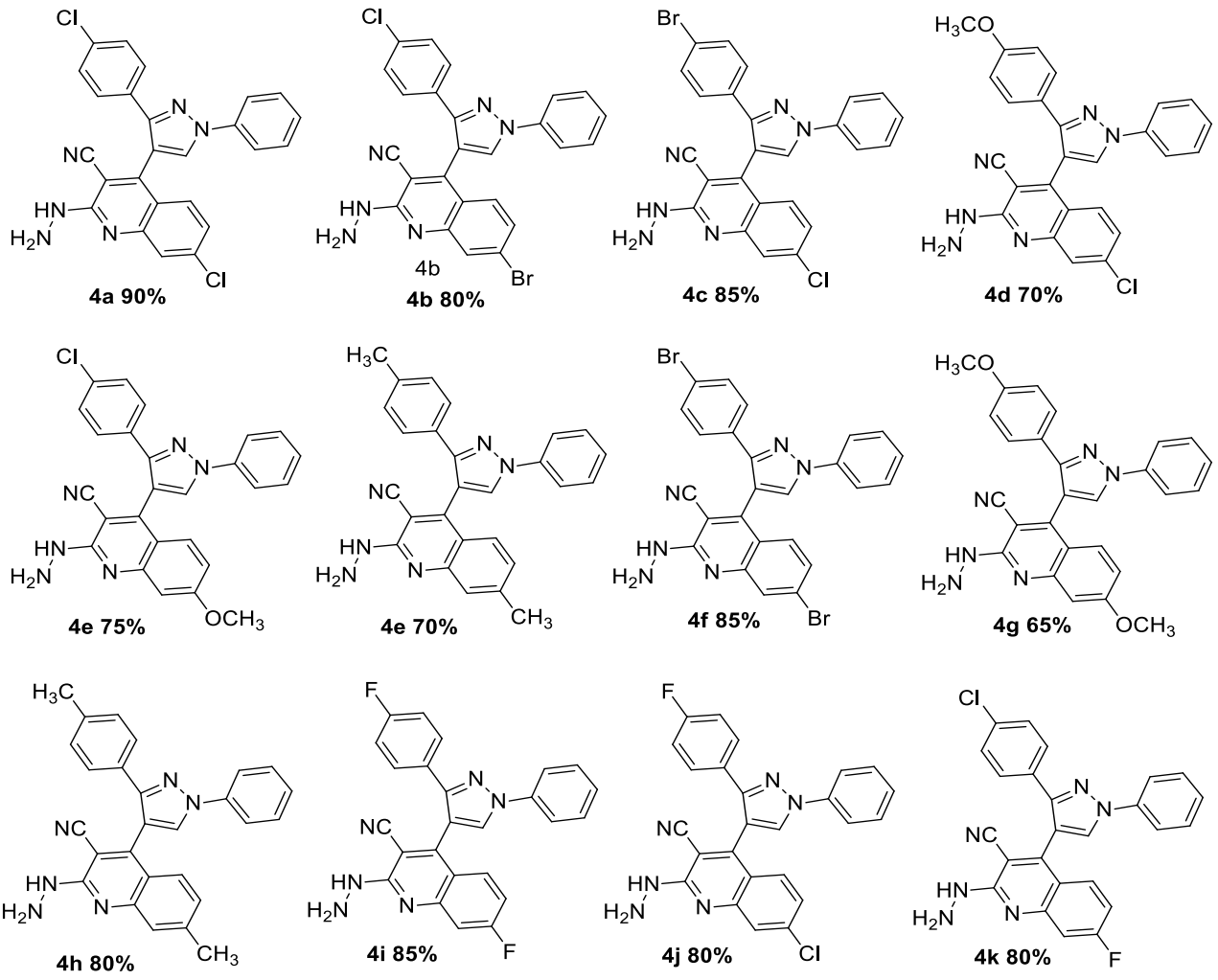

[a]Yield refers to the isolated product after column chromatography

The plausible mechanistic path was proposed in Scheme 2. The mechanism indicate reaction was proceed through abstraction of proton from 2-cyanoacetohydrazide by BEC then the anion attack on the carbonyl of heterocyclic aldehyde. Furthermore addition of substituted anilines leads to formation of final product.

Scheme 2 Plausible mechanism

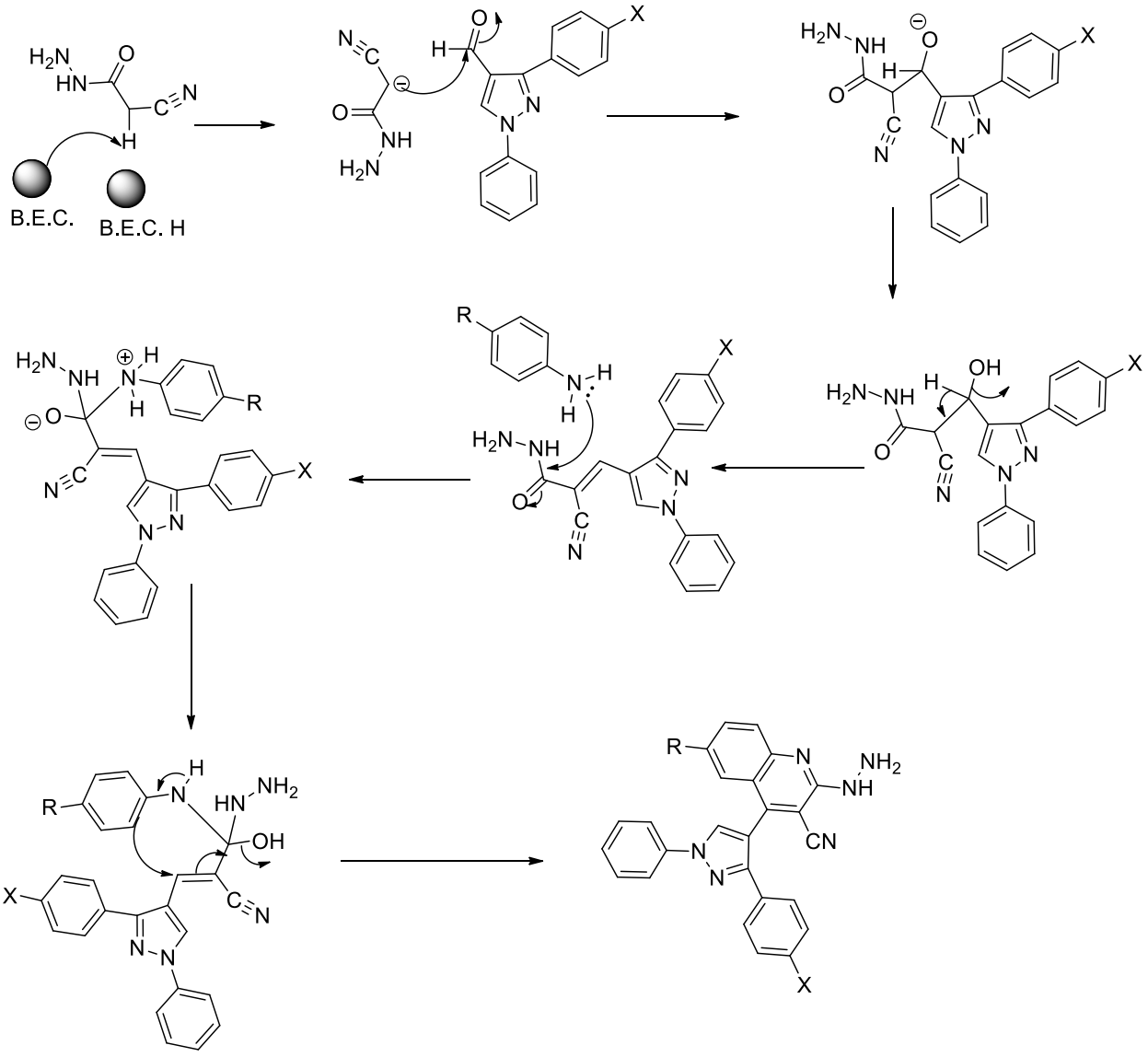

Conclusion:

The proposed protocol provides an easy access for the synthesis of quinoline-3-carbonitrile derivatives. the MCR strategy for the synthesis is woven with the environmental benign approach through the use of BEC as a catalyst and PEG-400 as a solvent. The protocol delivers an efficient access for the formation of new hybrid product with coupling of easily available reactants which may lead to improved biological activities.

References:

1. Nainwal, L. M., Tasneem, S., Akhtar, W., Verma, G., Khan, M. F., Parvez, S., Shaquiquzzaman, M., Akhter, M., Alam M. *Eur. J. Med. Chem.*2019, 164, 121-170.

2. Mukherjee, S., Pal, M. *Drug Discov. Today*, 2013, 18, 389-398.
3. Chung, P. Y., Bian, Z. X., Pun, H. Y., Chan, D., Chan, A.S.C., Chui, C. H., Tang, J.C.O., Lam, K. H. *Future Med. Chem.* 2015, 7, 947-967.
4. Khan, S. A., Asiri, A. M., Basisi, H. M., Asad, M., Zayed, M. E., Sharma, K., Wani, M. Y., *Bioorg. Chem.* 2019, 88, 102968.
5. Ibrahim, M. A., Badran, A. S. *Syn. Commun.* 2020, 50, 1871-1882.
6. Liu, B., You, Q. D., Li, Z. Y. *Chin. Chem. Lett.* 2010, 21, 554-557.
7. Gholap, A. R., Toti, K. S., Shirazi, F., Kumari, R., Bhat, M. K., Deshpande, M. V., Srinivasan, K. V. *Biorg. Med. Chem.* 2007, 15, 6705-6715.
8. Shah, N. M., Patel, M. P., Patel, R. G. *Eur. J. Med. Chem.* 2012, 54, 239-247.
9. Jentsch, N. G., Hart, A. P., Hume, J. D., Sun, J., McNeely, K. A., Lama, C., Julia, A., Pigza, M. G., Donahue G., Kessl, J. J., *ACS Med. Chem. Lett.* 2018, 9, 1007-1012.
10. Tu. S. J., Jiang, B., Jia, R. H., Zhang, J. Y., Zhang, Y., Yao, C. S., Shi, F.*Org. Biomol. Chem.* 2006, 4, 3664-3668.
11. Kawanishi, N., Sugimoto, T., Shibata, J., Nakamura, K., Masutani, K., Ikuta, M., Hirai, H. *Biorg. Med. Chem.* 2006, 16, 5122-5126.
12. Vo, C. V. T., Luescherf, M. U., Bode, J. W., *Nature Chemistry*, 2014, 6, 310-314.
13. Eydokimov, N. M., Kireev, A. S., Yakovenko, A. A., Antipin, M. Y., Magedov, I. V., Kornienko, A., *J. Org. Chem.*2007, 72, 3443-3453.
14. Shitole, N. V., Shelke. K. F., Sadaphal, S. A., Shingate, B. B., Shingare, M. S., *Green chem. Lett. Rev.* 2010, 3, 83-87.
15. Aly, R. M., Serya, R. A., El-Motwally, A. M., Esmat, A., Abbas, S., Abou El Ella, D. A., *Bioorg. Chem.* 2017, 75, 368-392.
16. Argyle, M. D., Bartholomew, C. H., *Catalysts*, 2015, 5, 145-269.
17. Boey, P. L., Maniam, G. P., Abd Hamid, S., *Chem. Eng. J.*, 2011, 168, 15-22.
18. Gaikwad, M. V., Kamble, R. D., Hese, S. V., Acharya, A. P., Mogle, P. P., Kadam, S. N., Dawane B. S., *Res. Chem, Intermed.* 2015, 41, 4673-4678.

International e-Conference on Recent Trends in Nano-Materials and Its Applications
In Association with International Journal of Scientific Research in Science and Technology
Volume 10 | Issue 9 | Print ISSN: 2395-6011 | Online ISSN: 2395-602X (www.ijsrst.com)

UV Spectrophotometric Method Development and Validation for Estimation of Cariprazine In Bulk and Tablet Dosage Form

Obaidullah Hundekari *, Ganesh B Gajeli
Correspondance Author: - Obaidullah Hundekari
Address: - D.S.T.S Mandal's College of Pharmacy, Solapur 413004 Maharashtra, India.
E-mail: o3aidis1@gmail.com

ABSTRACT

Objective: A new, simple, sensitive, precise and reproducible UV spectroscopic method was developed for the estimation of Cariprazine in bulk and tablet dosage from.

Method: The UV spectrum of Cariprazine in 50% Acetonitrile and 50% Water showed λ max at 216 nm. Beer's law is valid in the concentration range of 3.6-8.4 µg/ml. This method was validated for linearity, accuracy, precision, ruggedness and robustness.

Results: The method has demonstrated excellent linearity over the range of 3.6-8.4 µg/ml with regression equation y = 0.079x-0.002 and regression correlation coefficient r^2 = 0.999. Moreover, the method was found to be highly sensitive with LOD (0.15µg/ml) and LOQ (0.44µg/ml).

Conclusion : Depending on the results, the given method can be successfully applied of Cariprazine in Tablet formulation.

Keywords : Cariprazine, UV spectroscopy, method development and validation, tablet formulation.

I. INTRODUCTION

The purpose of analytical method development is to establish the identity, purity, physical characteristics and potency of drugs. The method development is to develop analytical method for drug product containing active pharmaceutical ingredients (API) to allow accurate and precise quantitation of drug. Validation of analytical method is intended to demonstrate that it is suitable for its intended use. The validation practice demonstrates that analytical method measures the correct substance in the correct amount and in appropriate range for the intended samples. Analytical method validation is an essential requirement to perform chemical evaluation and thinking about the utmost relevant overall performance indicators inclusive of accuracy, precision, linearity, range, selectivity, limit of detection (LOD) and limit of quantification (LOQ) are severely discussed in an effort that to prevent their misguided utilization and to ensure the scientific correctness and consistency among publication [1]

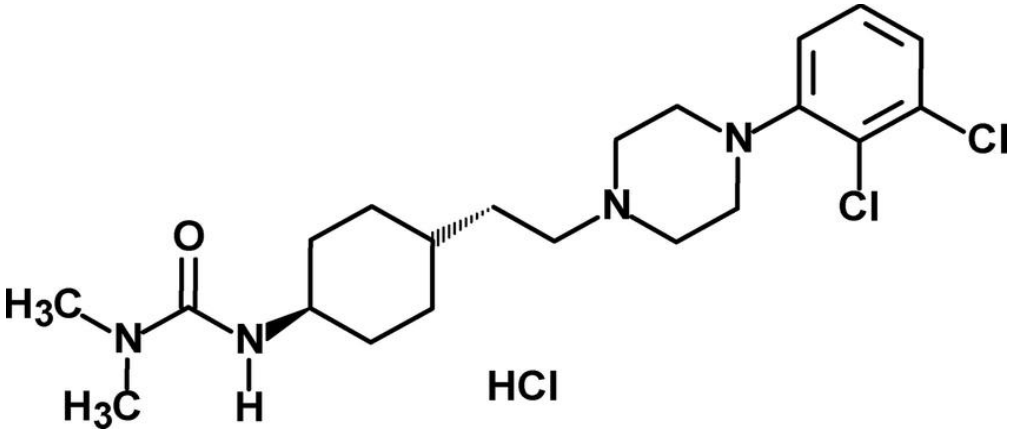

Cariprazine

The chemical name of Cariprazine is N'-[trans-4-[2-[4-(2,3-Dichlorophenyl)-1-piperazinyl]ethyl]cyclohexyl]-N,Ndimethylurea .

The molecular formula is $C_{21}H_{32}Cl_2N_4O$ and It has a molecular weight 427.411 g/mol [2] .

Cariprazine is an Atypical antipsychotic which is indicated in the treatment of schizophrenia and bipolar disorder. It acts as D2 and D3 receptor partial agonist, with high selectivity towards the D3 receptor. It is also preferably useful as an add-on therapy in major depressive disorder.

Cariprazine is used to treat schizophrenia and manic, depressive, or mixed episodes associated with bipolar I disorder. In the United States it is approved for schizophrenia in adults, acute treatment of manic or mixed episodes associated with bipolar I disorder in adults and treatment of depressive episodes associated with bipolar I disorder (bipolar depression). Cariprazine consistently improved depressive symptoms across a spectrum of patients with bipolar I depression. In Australia, UK and Europe it is currently approved only for schizophrenia.

MATERIALS AND METHOD:

Materials:

Cariprazine was obtained as a gift sample from Aadhar Life Science Pvt, Solapur Maharashtra, India. Tablets of Barkeit were purchased from local market; each tablet was labeled to contain 200 mg. All chemicals and reagents were of analytical grade.

Instruments :

A Double beam UV Visible Spectrophotometer (Systronic-2201 Spectrophotometer) was used for the detection of absorbance, Sonicator (Microclean-1103) and Weighing Balance (SHIMADZU AY220) was used for experimental purpose.

Chemical and Reagent:

Acetonitrile, water, Whatman filter papers were used.

METHOD DEVELOPMENT:

Selection of solvent:

Solubility of Cariprazine was performed in solvent Acetonitrile: Water and UV spectra of drug in this solution were recorded.

Determination of Wavelength:

The sample was scanned from 200-400 nm with PDA detector. The Wavelength selected for analysis chosen was 216 nm on basis of appropriate intensity of Cariprazine.

Preparation of standard stock solution:

Cariprazine Standard Stock Solution-I (SSS-I)

Prepare a Cariprazine Standard Stock Solution (SSS-I) by adding 6 mg of Cariprazine in 100 ml volumetric flask & add 50-70 ml diluent, mix for 2 minutes and make the volume to 100 ml with diluent. (Conc. of Cariprazine = 60 µg/ml) and add 1.0 ml of SSS-I in 10 ml volumetric flask and add 5 ml diluent and vortex and make up the volume with diluent. (Conc. of Cariprazine = 6 µg/ml)

Preparation of sample stock solution:

Sample Stock Solution:

Weigh 10 capsules content and calculate average weight of 1 capsule content. Weigh powder equivalent to 0.6 mg of Cariprazine and transfer to 100 ml volumetric flask & add 50-70 ml diluent, mix for 5 minutes and make the volume to 100 ml with diluent. (Conc. of Cariprazine = 6 µg/ml).

Method Validation:

The developed method was validated as per ICH guidelines. The ICH parameters assessed were specificity, linearity, range, accuracy, precision (repeatability), LOD and LOQ

1. **Linearity:**
   Five different concentration of Cariprazine solutions were prepared and analyzed at wavelength 216nm. The regression coefficient was found to be 0.999.
2. **Range:**
   The range of analytical method was decided for Cariprazine (2-10µg/ml).
3. **Accuracy :**
   The accuracy was determined by calculating % recovery of Cariprazine. It was carried out by adding known amounts of analyte corresponding to the concentration levels 80, 100, and 120% and results were expressed as % recovery.
4. **Precision:**
   The precision of analytical method was studied by performing repeatability studies by estimating responses of working standard solution (Conc. of Cariprazine: 40µg/ml) for 6 times. The results were reported in terms of percentage relative standard deviation (%RSD)
5. **Limit of Detector (LOD):**
   LOD is the lowest amount of analyte in sample that can be easily but not necessarily quantified. LOD was calculated by following formula.

LOD = 3.3 × STDV/ S

Where STDV and S are the standard deviation of the response and the slope of the calibration curve respectively.

6. **Limit of Quantification (LOQ) :**

LOQ is the lowest amount of analyte in sample that can be easily detected and quantified with suitable precision and accuracy. LOD was calculated by following formula.

LOD = 10 × STDV/ S

Where STDV and S are the standard deviation of the response and the slope of the calibration curve respectively.

RESULT AND DISSCUSSION:

The absorption spectrum shows λ max of Cariprazine at 216nm.

The proposed method was validated according to ICH Q28 R1 guidelines for validation of analytical procedure.[4-8]

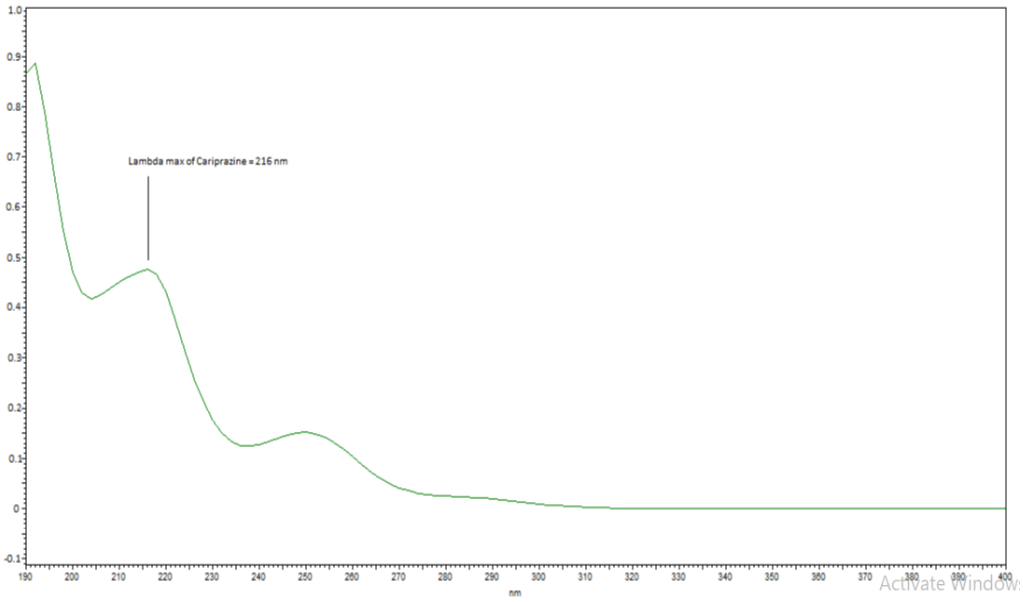

Fig: 2 UV –Visible spectra of Cariprazine.

Validation of method as per ICH guidelines:

1. **Linearity:**

Five different concentration of Cariprazine were prepared and analysed at wavelength 216 nm. The regression coefficient was found to be 0.999. The absorbance was found in limit i.e. 0-2. Hence the analysed parameter was found to be validated

Sr. No	Conc (µg/ml)	Absorbance
1	3.6	0.283
2	4.8	0.381
3	6.0	0.476
4	7.2	0.574
5	8.4	0.665

Table 1: Results of Linearity

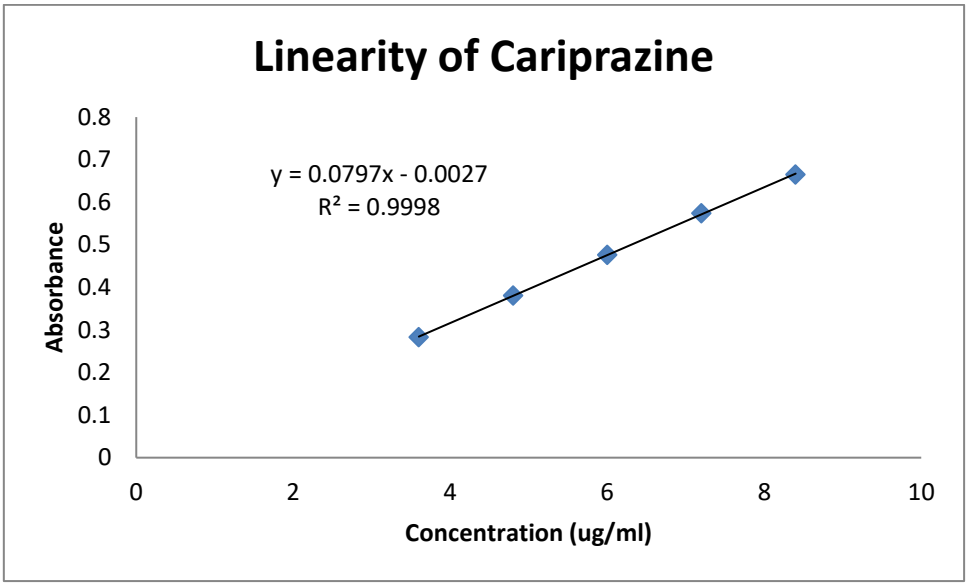

Figure 3: Calibration curve for Cariprazine (Conc.vs.Abs.)

Table: 2 Optimization parameter of Cariprazine

Parameter	**Method values**
Wavelength	216
Beers law	2-10ug/ml
Correlation Coefficient	0.999
Regression coefficient	Y=0.079x-0.002
Slope	0.079
Intercept	0.002

2. Accuracy:

The concentration 40, 50, 60µg/ml was taken as 80,100,120% and % recovery was found to be in range 99%-101%. Hence the parameter was found to be validated.

Table 3: Result of accuracy

Sample ID	Sample ID	Sample ID	Sample ID	Sample ID	Sample ID	Sample ID	Sample ID	Sample ID
80%	Rep 1	4.8	0.381	4.81	100.16	100.25	0.401558	0.40
	Rep 2		0.383	4.83	100.68			
	Rep 3		0.380	4.79	99.89			
100%	Rep 1	6	0.476	6.01	100.11	99.96	0.437785	0.44
	Rep 2		0.477	6.02	100.32			
	Rep 3		0.473	5.97	99.47			
120%	Rep 1	7.2	0.574	7.24	100.60	100.42	0.175254	0.17
	Rep 2		0.573	7.23	100.42			
	Rep 3		0.572	7.22	100.25			

3. Range:

Range is an interval between highest and lowest concentration limit of the analyte i.e. 2-10µg/ml.

4. Precision:

The prepared working standard was analysed in morning and at evening and % RSD was calculated to identify the stability of solution for intraday precision.

The same solution was analysed on second day and compared with morning results of intraday precision and % RSD was calculated.

Table 4: Result of intra-day precision

Sample ID	Absorbance	Conc (ug/ml)
Standard	0.476	6.00
Morning	0.473	5.96
Evening	0.472	5.95
% RSD	0.15	0.15

Table 5: Result of Inter- day precision

Sample ID	Area	Conc (ug/ml)
Day 1	0.473	5.96
Day 2	0.469	5.91
% RSD	0.60	0.60

5. Limit of Detection (LOD):

The limit of detection was found to be 0.15µg/ml.

6. Limit of Quantification:

The limit of quantification was found to be 0.44µg/ml.

7. Assay:

Sample solution of concentration 40 µg/ml was analysed at wavelength 216nm and the % purity was calculated.

Table 6: Result of Assay

Formulation	Concentration (µg/ml)	Amount obtained(µg/ml)	% Purity
Barkeit 200mg Tablets	40	39.70	99.25%

8. Robustness :

The Robustness was performed by changing the Diluent concentration by ± 2% and Wavelength by ± 2 nm.

Table 7: Robustness studies

Diluent Composition			
Condition	Sample ID	Absorbance	Assay
Increase	WS	0.477	-
	DP	0.475	99.58
Normal	WS	0.476	-
	DP	0.473	99.37
Decrease	WS	0.476	-
	DP	0.475	99.79
Wavelength Temperature			
Condition	Sample ID	Absorbance	Assay
Increase	WS	0.471	-
	DP	0.469	99.58
Normal	WS	0.476	-
	DP	0.473	99.37

Decrease	WS	0.468	-
	DP	0.463	98.93

Table 8: Result of Robustness

Condition	Increase	Normal	Decrease
Diluent Composition	A52-W48	A50-W50	A48-W52
Wavelength	218	216	214

Conclusion:

An analytical UV spectrophotometric method was developed & validated thoroughly for quantitative determination of Cariprazinein bulk and tablet formulation. The presented method was found to be simple, precise, accurate, rugged, and reproducible which gives an acceptable recovery of the analyte, which can be directly easily applied to the analysis of pharmaceutical semisolid formulation of Cariprazinein.

Acknowledgements:

The authors are thankful to the Aadhar Life Science pvt.ltd. Solapur, Maharashtra, India for providing gift sample of Cariprazine. We also grateful to Principal and management of D.S.T.S. Mandal's College of Pharmacy, Solapur for providing all facilities to complete this research work successfully.

References:

1. Chauhan A, Mittu B, Chauhan P. Analytical method development and validation: a concise review. J. Anal. Bioanal. Tech. 2015;6(1):1-5.
2. https://en.wikipedia.org/wiki/Cariprazine
3. Nagamani, M., Ramana, H., Bhadru, B., Vasanthi, R.; Method development and validation of cariprazine in bulk and its formulation by UV spectroscopy; International Journal of Pharmaceutical, Chemical and Biological Sciences, (2015); 5(1): 258–261.
4. Dr. Parag Gadkari; Challenges in Analytical Method Development for Drug Products, Pharma times, January 2012, 44(1): 22-26.
5. http://hplc.chem.shu.edu/HPLC/Theory/th_selrs.html
6. Agency, E. M. European Medicines Agency, June 1995, 2006, 2: 1–15.
7. Ravisankar, P.; Swathi, V.; Babu, P. S.; Sulthana, S.; Gousepeer, S. K. Current Trends in Performance of Forced Degradation Studies and Stability Indicating Studies of Drugs., 2017; 12(6): 17–36.
8. Vemuri Pavan Kumar; N. Vishal Gupta* ; A review on Quality by Design (QBD) approach for pharmaceuticals. Ijddr.
9. Ganorkar, A. V.; Gupta, K. R. Analytical Quality by Design: A mini review. BJSTR, 2017; 1(6).
10. ICH Pharmaceutical Quality System Q10. WHO Drug Inf, 2008; 22(3): 177–181.

International e-Conference on Recent Trends in Nano-Materials and Its Applications
In Association with International Journal of Scientific Research in Science and Technology
Volume 10 | Issue 9 | Print ISSN: 2395-6011 | Online ISSN: 2395-602X (www.ijsrst.com)

Analytical Method Development and Validation of RP-HPLC Method for the Estimation of Vancomycin Hydrochloride in Bulk and Formulation

Payal Ladda*,Ganesh Gajeli , Anup Dhange
Correspondance Author
Pharmaceutical Quality Assurance Department, D.S.T.S Mandal's College of Pharmacy, Solapur, Maharashtra, India
"*Corresponding author": payalladda742@gmail.com

ABSTRACT

A Reverse Phase High-Performance Liquid Chromatographic (RP-HPLC) method was developed and validated for the estimation of Vancomycin Hydrochloride which is an antibiotic drug. The RP-HPLC succeededAgilent Zorbax SB-Aq(250×4.6mm,5u). The mobile phase was effective according to the polarity of the studied drug. The mobile phase was consisting of 0.1%formic acid:Methanol (50:50% v/v) used at a flow rate of 0.5ml/min. with an injection volume of10 µL was selected for this present work. Detection was made by using a UV detector at 225nm. The retention time was found to be3.92min. The developed method was validated according to the ICH guidelines. The calibration curve was linear for vancomycin hydrochloride in the concentration range of 80-120µg/ml was good. The developed method was validated for Linearity, Precision, Accuracy, and Robustness of Vancomycin HCL drug and was accurate, precise, and reliable for the analysis of vancomycin HCLin formulation. The Relative Standard Deviation for all the parameters was found to be less than 2 which shows the validated method and results obtained by this method is in fair agreement. Hence, this developed method can be easily and effortlessly adopted for routine analysis for Vancomycin hydrochloride in bulk and formulation.

Keywords:Vancomycin Hydrochloride , Method Development, Validation, RP-HPLC, ICH.

I. INTRODUCTION

High Performance Liquid Chromatography (HPLC) is a technique in analytical chemistry commonly used to separate, identify, and quantify each component in a mixture. Analytical method development is the process of selecting an accurate assay procedure for determination of composition of formulation. Analytical method must be developed using the protocol and acceptance criteria set out in ICH (International Council for Harmonization) guidelines Q2(R1).[1]

Analytical method plays an important role in the discovery, development and manufacturing of pharmaceuticals. The aim of method development is to develop analytical method for drug product containing active ingredients to allow accurate and precise quantitation of drug.[2]High Performance Liquid

Chromatography (HPLC) is an essential analytical tool in assessing drug product. HPLC methods should be able to separate, detect, and quantify the various drugs and drug related degradants that can form on storage or manufacturing, detect and quantify the various drugs and drug related impurities that may be introduced during synthesis. Validation is the process of establishing the performance characteristics and limitations of a method and identification of the influences which may change these characteristics.[3]

In literature review, various methods are available for determination of vancomycin in human plasma by HPLC, stability indicating HPLC method for determination of vancomycin in pharmaceutical dosage form. In the present work, it is therefore focused on new ecological method development for the estimation of vancomycin in bulk and formulation. The objective of this work is to develop and validate a new analytical method faster, low cost, ecological and miniaturized for quantification of vancomycin in API and dosage form using HPLC. The use of non-toxic or less toxic solvent, it is possible to make this method greener.

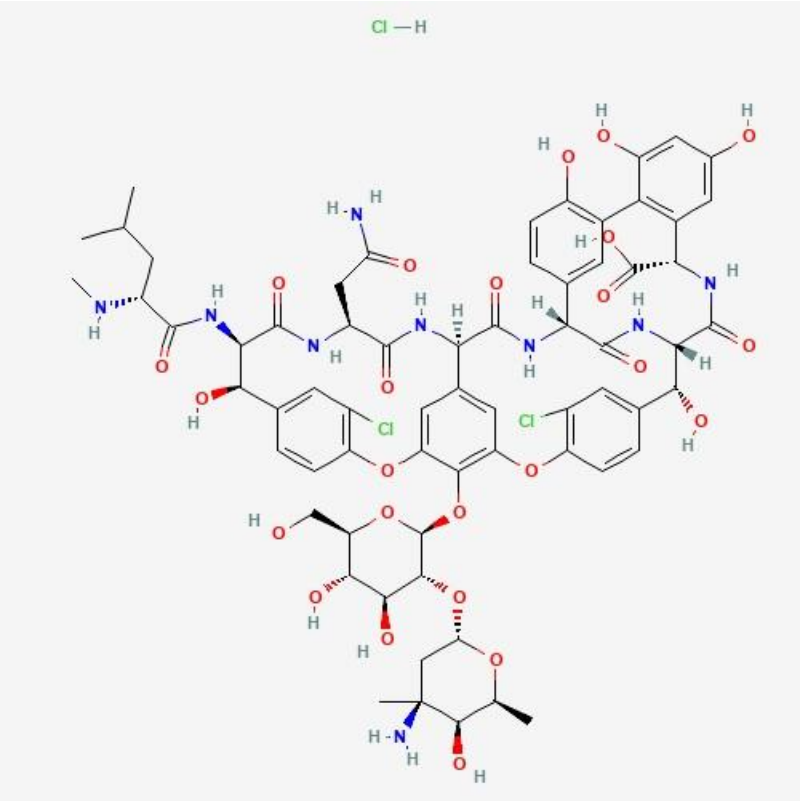

Fig no 1 . Vancomycin Hydrochloride

IUPAC NAME:

(1S,2R,18R,19R,22S,25R,28R,40S)-48-[(2S,3R,4S,5S)-3-[(2S,4S,5S,6S)-4-amino-5-hydroxy- 4,6-dimethyloxan-2-yl]oxy-4,5-dihydroxy-6-(hydroxymethyl)oxan-2-yl]oxy-22-(2-amino-2-oxoethyl)-5,15-dichloro-2,18,32,35,37-pentahydroxy-19-[[(2R)-4-methyl-2- (methylamino)pentanoyl]amino]-20,23,26,42,44-pentaoxo-7,13-dioxa-21,24,27,41,43-pentazaoctacyclo[26.14.2.23,6.214,17.18,12.129,33.010,25.034,39]pentaconta-3,5,8(48),9,11,14,16,29(45),30,32,34(39),35,37,46,49-pentadecaene-40-carboxylic acid;hydrochloride[4]

Its molecular formula is $C_{66}H_{76}Cl_3N_9O_{24}$ and its molecular weight is 1485.7[4]

Vancomycin is an amphoteric glycopeptide antibiotic, first isolated in 1956, that is active against a broad range of Gram-positive bacteria as well as some Gram-negative cocci. Vancomycin (VCM) is widely used to treat Methicillin-resistance Staphylococcus aureus (MRSA) infection[5]. It has a strong bactericidal activity, inhibiting the polymerization of peptidoglycans in the bacterial cell wall[6]. Because of toxicity, Vancomycin was used primarily for alternative therapy before the recent emergence of methicillin-resistant and penicillin-resistant organisms. For patients allergic to both penicillin and cephalosporins, vancomycin is often the only effective treatment Vancomycin is an antibacterial medication in the glycopeptide class like penicillin[7]. Vancomycin is FDA-approved for administration by either intravenous injection or oral route. Glycopeptide antibiotics such as vancomycin, ramoplanin and teicoplanin are lifesaving drugs in certain clinical situations where first-line antibiotics (e.g., penicillin's, cephalosporins) result in treatment failure[8,9]

MATERIAL AND METHODS:

Chemicals and reagents:

Vancomycin Hydrochloride was obtained as a gift sample from Hetero Labs Limited Telangana. 0.1 % FA , methanol.

Instrumentation:

Agilent Technologies Infinity II 1260, 1260 DAD Detector ,Electronic balance (Aczet CY224C),Syringe filter (Qualsil Nylon Membrane 0.45um, 15 mm.), Solvent filter (Pall Nylon 6.6 Membrane 0.45 um,47 mm filter),Glass filter Assembly Borosil All glass filter holder -47 mm, Ultra sonicator (Labman Scientific Pvt.Ltd)

Chromatographic equipment and conditions

Chromatographic separation was achieved onAgilent Zorbax SB-Aq(250×4.6mm,5u).The mobile phase used for the separation of Vancomycin hydrochloride was 0.1%formic acid :Methanolin the ratio of (50:50% v/v). The flow rate was set at 0.5ml/minat ambient temperature of 30°C, with an injection volume of10µL. Using DAD Detector at the wavelength of225 nm.

Preparation of Solution

Preparation of Standard stock solution

a. Vancomycin HCL Standard Stock Solution-I (VSSS-I):
   Initially Prepare a Standard Stock Solution (SSS-I) by adding 10 mg of Vancomycin HCL in a 10 ml volumetric flask & add 5 ml diluent, mix for 2 minutes and make the volume to 10 ml with diluent. (Conc. of Vancomycin in VSSS-I= 1000 µg/ml).
b. Then add 1 ml of VSSS-I in a 10 ml volumetric flask and add 5 ml diluent and vortex and make up the volume with diluent. (Conc. of Vancomycin =100 µg/ml)

Preparation of sample solution

1. **Drug Product Sample Preparation for Assay:**
   i. 10 tablets were weighed and the average weight was calculated. And tablets were crushed & mixed in mortar and pestle.
   ii. Powder weight equivalent to 10 mg Vancomycin was weighed into 10 ml volumetric flask & add 5 ml diluent, Sonicate for 5 minutes and make the volume to 10 ml with diluent. (Conc. of Vancomycin = 1000 µg/ml).
   iii. Further, pipette out 1.0 ml of the above solution in 10 ml volumetric flask and add 5 ml diluent and vortex and make up the volume with diluent. (Conc. of Vancomycin = 100 µg/ml).

Selection of Wavelength:

The sample was scanned from 190-400 nm with a DAD detector. The Wavelength selected for analysis chosen was 225 nm for appropriate identification of Vancomycin.

Analytical Method Development

The proposed RP-HPLC method of analysis was validated following ICH Q2 (R1) guidelines by studying the parameters like system linearity, accuracy, assay, precision, suitability, specificity, LOD, LOQ and robustness.

RESULTS AND DISCUSSION

Method Development The proposed RP-HPLC method was developed and optimized for a series of trials in a terms of mobile phase selection, composition, wavelength, choice of stationary phase of column, flow rate and column temperature . Vancomycin Hydrochloride showed the absorbance maxima at 225nm. Hence, the wavelength was selected as a working wavelength for the proposed RP-HPLC method.

Specificity & Assay:

- individual sample of Vancomycin working standard & drug product of 100 µg/ml was prepared and peaks were for identified from Retention Time.
- Blank was injected to ensure there is no blank peak interfering with the main analyte peak.

Table no 1. Result of specificity

VancomycinHCL			
Sample	RT	Area	Assay%
WS	3.91	14119427	-
DP	3.91	13985416	99.05

Repeatability & System Suitability:

i. A single sample was prepared as described and 6 injections were made from the same sample and checked for system suitability.

ii. System suitability parameters are as below:

1. Retention Time,
2. Theoretical plates,
3. Asymmetry (Tailing factor),
4. Peak purity.

Table no 2 . Result of Repeatability

Vancomycin HCL	
Sample ID	Area
Rep 1	14119427
Rep 2	14118712
Rep 3	14118715
Rep 4	14119554
Rep 5	14120021
Rep 6	14117877
Average	14119051
STDEV	766.99126
RSD	0.01

Table no 3. Result of System Suitability

Sample ID	RT(Min)	TP	Asymmetry	Peak Purity
Rep 1	3.91	5032	1.14	1.00
Rep 2	3.91	6001	1.12	1.00
Rep 3	3.91	5147	1.10	1.00
Rep 4	3.91	5671	1.11	1.00
Rep 5	3.91	5556	1.09	1.00
Rep 6	3.91	5232	1.08	1.00
Average	3.91			
STDEV	0			
RSD	0.00			

Linearity & Range:

- 5 samples of varying concentrations ranging from 80-120% were made.
- The concentrations are given below

% Level	Vancomycin Conc. (µg/ml)
80	80
90	90
100	100
110	110
120	120

- The sample preparations are given below;
- X ml of Vancomycin was added to 10 ml diluent to make up the concentrations given above

X ml of VSSS-I	Diluted to
0.8	10 ml
0.9	10 ml
1.0	10 ml
1.1	10 ml
1.2	10 ml

Table no 4. Linearity and Range

Vancomycin HCL		
% Level	Conc (ug/ml)	**Area**
80	80	**11290955**
90	90	**12708129**
100	100	**14119427**
110	110	**15485807**
120	120	**16890791**

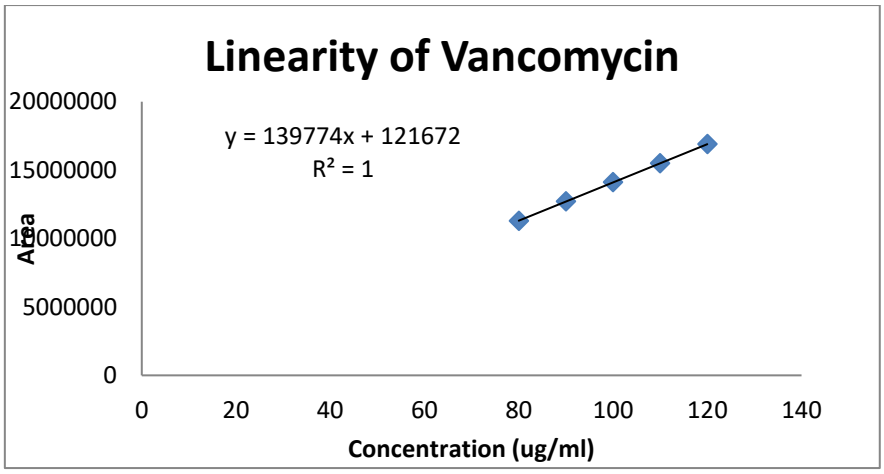

Fig. 2: Calibration curve of Vancomycin HCL

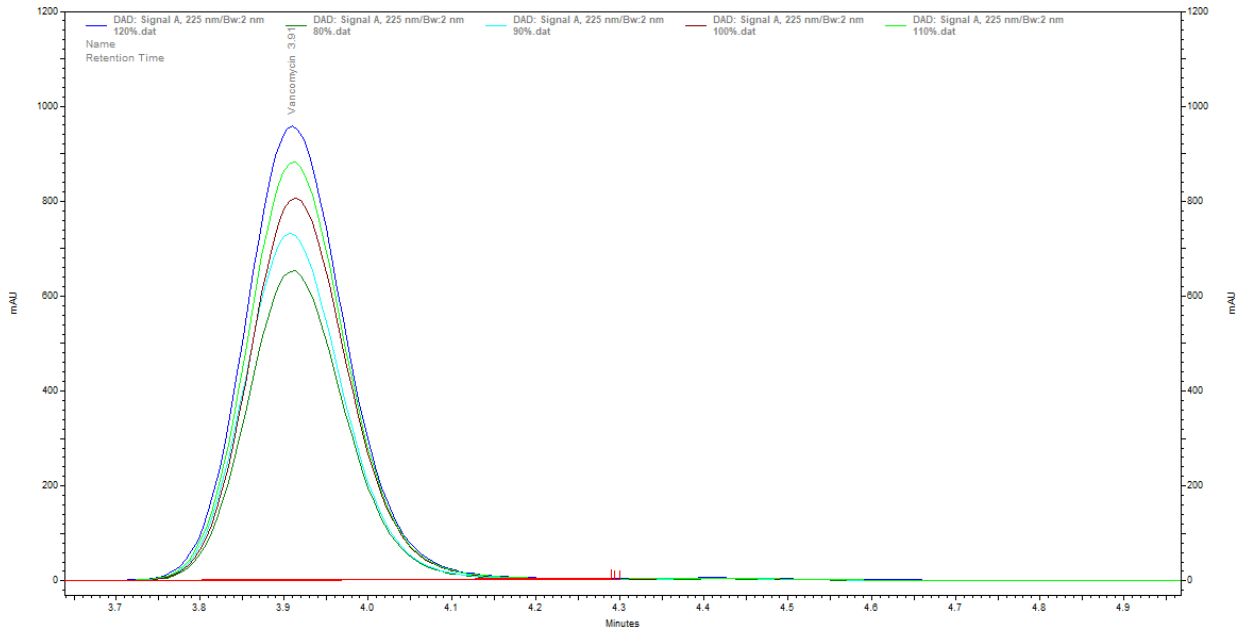

Fig. 3: Overlay of chromatograms of concentration 80-120 µg/ml of Vancomycin HCL.

Accuracy

i. Samples were prepared of 80%, 100% and 120% concentration by spiking the same amount of concentration given above in table for both Vancomycin.

ii. Samples were injected in triplicate to calculate % RSD

Table no 5 result of accuracy

Sample ID	Reps	Spiked Conc. (ug/ml)	Area	Amt Recovered (ug/ml)	% Recovery	Average	STDEV	RSD
80%	Rep 1	79.92	11290955	79.89	99.96	100.02	0.140382	0.14
	Rep 2	79.92	11315945	80.07	100.18			
	Rep 3	79.92	11286541	79.86	99.92			
100%	Rep 1	99.9	14119427	99.90	100.00	100.00	0.002918	0.00
	Rep 2	99.9	14118712	99.90	100.00			
	Rep	99.9	14118715	99.90	100.00			

	3							
120%	Rep 1	119.88	16890791	119.51	99.69	99.93	0.126077	0.13
	Rep 2	119.88	16915462	119.69	99.84			
	Rep 3	119.88	16945671	119.90	100.02			

LOD/ LOQ:

LOD and LOQwas calculated by using the ANOVA technique.The LOD found 1.20 ug/ml and a LOQ of 3.63ug/ml.

Robustness:

The Robustness was performed by changing the column temperature by ± 2˚C.

Each Sample was injected % Assay was calculated at each condition was calculated.

Condition	Increased	Normal	Decreased
Column Oven Temperature	32˚C	30˚C	28˚C

Table 6: Robustness result of Vancomycin Hydrochloride

Column Oven Temp Change				
Condition	Sample	Vancomycin		
		RT	Area	Assay
28°C	WS	3.91	14109845	-
	DP	3.91	14101456	99.94
30°C	WS	3.91	14119427	-
	DP	3.91	13985416	99.05
32°C	WS	3.91	14115541	-
	DP	3.91	13995418	99.15

Intra & Inter-day Precision:

- Single mixture working standard and drug product samples were prepared and injected twice in a day at different time intervals to evaluate intra-day precision.
- Same mixture working standard and drug product samples were analysed on second day to evaluate the inter-day precision.
- % Assay was calculated at each interval and stability of solutions were estimated.

Table no 7 result of intra day presicion

Intra Day precision			
Day 1	Sample ID	Vancomycin HCL	
		Area	Assay
Morning	WS	14119427	-
	DP	13985416	99.05
Evening	WS	14105641	-
	DP	13985412	99.15

Table no 8 Result of inter day presicion

Inter Day precision			
Day	Sample ID	Vancomycin HCL	
		Area	Assay
Day 2	WS	14119884	-
	DP	13999754	99.15

CONCLUSION

A novel RP-HPLC method was developed and successfully validated as per ICH guidelines for the estimation of Vancomycin HCL. All the results of various parameters were found to be within the acceptable limits. Hence the proposed RP-HPLC method for the analysis of Vancomycin HCLin bulk and its formulation was found to be specific, precise, accurate and fast.

ACKNOWLEDGEMENT

The authors are thankful toHetero Labs Limited Telangana,india for providing gift sample of Vancomycin HCL. The corresponding author gratefully acknowledges to Principal to D.S.T.S. Mandal's College of Pharmacy, Solapur, Department of Pharmaceutical Quality Assurance, Assistance Professor Dr. M.S. Kalshetti

REFERENCES:

1. Chauhan A, Mittu B, Chauhan P. Analytical method development and validation: a concise review. J. Anal. Bioanal. Tech. 2015;6(1):1-5
2. Pathuri R, Muthukumaran M, Krishnamoorthy B, Nishat A. A review on analytical method development and validation of pharmaceutical technology. Journal of Current Pharma Research. 2013;3(2):855.
3. Azim S, Mitra M, Bhain P. HPLC Method development and Validation. A Review. Int. Res. J. Pharm. 2013; 4(4):39-46
4. https://pubchem.ncbi.nlm.nih.gov/compound/Vancomycin
5. Butler-Laporte G, De L'Étoile-Morel S, Cheng MP, McDonald EG, Lee TC. MRSA colonization status as a predictor of clinical infection: A systematic review and meta-analysis. J Infect. 2018 Dec;77(6):489-495. [PubMed]
6. Koyama N, Inokoshi J, Tomoda H. Anti-infectious agents against MRSA. Molecules. 2012 Dec 24;18(1):204-24. [PMC freearticle] [PubMed]
7. Patel S, Preuss CV, Bernice F. Vancomycin.StatPearls. Last update Feb 2020.
8. CC Jhon. Clin Infect Dis., 1994, 18,188-193.
9. SC Jhon, HN Steven. Int. J of pharmaceutics, 1998,168, 41-48.
10. https://doseme-rx.com/vancomycin/articles/vancomycin-mechanisms-of-action
11. Alvino Rodrigues Júnior a, Marta M. D. C. Vila b & Matthieu Tubino, Green Spectrophotometric Method for the Quantitative Analysis of Vancomycin in Pharmaceuticals and Comparison with HPLC, Analytical Letters.2008;41:5, 822-836.
12. PatríciaAleixa do Nascimento , Ana Carolina Kogawa, Hérida Regina Nunes Salgado, A new and ecological miniaturized method by spectrophotometry for quantification of vancomycin in dosage form, Drug Analytical Research.2021;5(1): 39-45.

International e-Conference on Recent Trends in Nano-Materials and Its Applications-RTNA-2023

Organized By
Department of Physics
Sangola Taluka Shetkari Shikshan Prasarak Mandal Sangola's, Vidnyan Mahavidyalaya, Sangola
Tal-Sangola, Dist-Solapur, MH-413307, India
Collaboration with
Internal Quality Assurance Cell (IQAC)

Publisher

Technoscience Academy

Website : www.technoscienceacademy.com

Email : editor@ijsrst.com Website : http://ijsrst.com